| AD NUMBER | |
|---|---|
| **AD381334** | |
| CLASSIFICATION CHANGES | |
| TO: | **UNCLASSIFIED** |
| FROM: | **CONFIDENTIAL** |
| LIMITATION CHANGES | |
| TO: **Approved for public release; distribution is unlimited.** | |
| FROM: **Distribution: Further dissemination only as directed by Systems Engineering Group, Attn: SEAEA, Wright-Patterson AFB, OH 45433, OCT 1966, or higher DoD authority.** | |
| AUTHORITY | |
| **31 Oct 1978, DoDD 5200.10, per document marking; ASD/USAF ltr dtd 22 Apr 1974** | |

# SECURITY MARKING

**The classified or limited status of this report applies to each page, unless otherwise marked.**
**Separate page printouts MUST be marked accordingly.**

CONFIDENTIAL

# TECHNICAL REPORT

## ANALYSIS AND EVALUATION OF TACTICAL PENETRATION AIDS: A STUDY OF THE FLIGHT-PATH-CONTROL AND VEHICLE DESIGN FOR A SUBSONIC, LOW ALTITUDE, PENETRATION AID MISSILE (U)

**CAL No. UM-2176-E-SS4D**

**Prepared for:**
**Research and Technology Division**
**Air Force Systems Command**
**Wright-Patterson Air Force Base, Ohio**

**Contract No. AF 33(615)-1877**
**October 1966**



**CORNELL AERONAUTICAL LABORATORY, INC.**
OF CORNELL UNIVERSITY, BUFFALO, N. Y. 14221

CORNELL AERONAUTICAL LABORATORY, INC.
BUFFALO, NEW YORK 14221

CAL REPORT NO. UM-2176-E-SS4D

# ANALYSIS AND EVALUATION OF TACTICAL PENETRATION AIDS: A STUDY OF THE FLIGHT-PATH-CONTROL AND VEHICLE DESIGN FOR A SUBSONIC, LOW ALTITUDE, PENETRATION AID MISSILE (U)

CONTRACT NO. AF 33(615)-1877

OCTOBER 1966

PREPARED FOR
RESEARCH AND TECHNOLOGY DIVISION
AIR FORCE SYSTEMS COMMAND
WRIGHT-PATTERSON AIR FORCE BASE, OHIO



PREPARED BY: Chester D. Mayerson

*Chester D. Mayerson, Principal Aeronautical Engineer, Weapons Research Department*

APPROVED BY: H R Leland

*H.R. Leland, Assistant Head Weapons Research Department*

D B Dahm

*D.B. Dahm, Manager Penval Program*

## FOREWORD

The work reported on herein is part of the third phase of the 669A Analysis and Evaluation Program. This effort was performed by Cornell Aeronautical Laboratory, Inc., under Contract AF 33(615)-1877 for the Systems Engineering Group of the Research and Technology Division, Wright-Patterson Air Force Base, Ohio. The Air Force Technical Director for the Analysis is Mr. F. E. Pirie. Program Manager for Cornell Aeronautical Laboratory, Inc., is Mr. D. B. Dahm.

The work described herein was performed by various Cornell Aeronautical Laboratory (CAL) personnel assigned to the PENVAL program. Major technical contributions were made by:

| | |
|---|---|
| James A. Cadzow | Chapter 6 |
| Harry E. Criel | Chapter 3 |
| Stephen G. Foss | Chapter 3 |
| John Lew | Chapter 4, Appendix C |
| Chester D. Mayerson | Chapters 1, 2, 5, 8, 9, 10, Appendices B, C |
| Philip A. Reynolds | Chapters 6, 7, Appendix D |
| R. Paul Williamson | Chapter 7, Appendices A, D |

## PREFACE

This report is one of a series documenting the third-phase PENVAL* program work performed by Cornell Aeronautical Laboratory, Inc., (CAL) under Contract AF 33(615)-1877. This effort is being accomplished for the Systems Engineering Group of the Research and Technology Division, Wright-Patterson Air Force Base, as a portion of Program 669A.

The PENVAL program evaluates the effectiveness of penetration aids for enhancing the mission success of tactical aircraft in conventional (non-nuclear), limited-war situations. The first phase of the program emphasized evaluation of the effects of penetration aids on the survivability of a single penetrator (aircraft) using a single penetration aid against a single air-defense installation (threat). The second and current (third phase) and subsequent periods of effort add capabilities for evaluation in the context of multiple penetrators and threat complexes and include greater consideration of the effects, in addition to survivability, that penetration aids have on mission success.

The reports describing the first phase of the program (accomplished under Contract AF 33(657)-12058) were published as components or sections of a single, multivolume report, each part of which was issued as a single volume. During the second phase (accomplished under Contract AF 33(615)-1877), supplements were published to update the first-phase reports, and additional reports on new areas of investigation were issued. All reports issued in the first two phases of the program are listed in the table which follows. The table also lists the reports being issued for the third phase of the program and shows the approximate correspondence of all reports. In the third phase of effort, more emphasis is being placed on Flash Reports and Working Papers and, hence, the table does not fully reflect the increased scope and size of the effort in the third phase.

*Acronym conceived by Cornell Aeronautical Laboratory to facilitate reference to the present PENetration-aid eVALuation program.

## PENVAL PROGRAM FORMAL REPORT STRUCTURE

| ANALYSIS AND EVALUATION OF TACTICAL PENETRATION AIDS | | | | | |
|---|---|---|---|---|---|
| REPORT NO. SUFFIX | FIRST-PHASE REPORTS (UM-1801-E- ) | REPORT NO. SUFFIX | SECOND-PHASE REPORTS (UM-1968-E- ) | REPORT NO. SUFFIX | THIRD-PHASE REPORTS (UM-2176-E- ) |
| BACKGROUND AND SUPPORTING DATA | | | | | |
| - | DEFINITION OF THREAT SYSTEMS | -1 | SUPPLEMENTARY REPORT ON DEFINITION OF THREAT SYSTEMS | --- | |
| -2 | TACTICAL SITUATIONS AND MISSIONS FOR ANALYTICAL EVALUATION MODELS | -2 | SUPPLEMENTARY REPORT ON TACTICAL SITUATIONS AND MISSIONS FOR ANALYTICAL EVALUATION MODELS | --- | |
| -3 | IDENTIFICATION AND PRELIMINARY ANALYSIS OF PENETRATION AIDS | -3 | SUPPLEMENTARY REPORT ON IDENTIFICATION AND PRELIMINARY ANALYSIS OF PENETRATION AIDS | -MR5 | MEMORANDUM REPORT ON 57 mm AAA SYSTEM "THREAT" SUSCEPTIBILITY AND PENETRATION-AID ANALYSES |
| | | | | -MR8 | MEMORANDUM REPORT ON SAM TECHNIQUES |
| -4 | DEFINITION OF AIRCRAFT SYSTEMS | -4 | SUPPLEMENTARY REPORT ON DEFINITION OF AIRCRAFT SYSTEMS | -S/4 | SUPPLEMENTARY REPORT ON PENETRATION-AID AND AIRCRAFT SYSTEMS STUDY |
| --- | | -4A | SUPPLEMENTARY REPORT ON AIRCRAFT/PENETRATION AIDS SYSTEM ANALYSIS | --- | |
| ANALYSIS, RESULTS, AND METHODOLOGY | | | | | |
| -5 | EVALUATION METHODOLOGY AND MODEL DEVELOPMENT | -5 | SUPPLEMENTARY REPORT ON EVALUATION METHODOLOGY AND MODEL DEVELOPMENT | -5 | DESCRIPTION OF A SINGLE-PENETRATOR, MULTIPLE-PENETRATION-AID, MULTIPLE-THREAT MODEL FOR EVALUATING PENETRATION-AID EFFECTIVENESS |
| -5A | RESULTS OF ONE-ON-ONE EVALUATIONS | -5A | SUPPLEMENTARY REPORT ON RESULTS OF ONE-ON-ONE EVALUATIONS | -MR1 | FIRST MEMORANDUM REPORT ON MODEL DEVELOPMENT AND APPLICATION |
| | | | | -MR2 | SECOND MEMORANDUM REPORT ON MODEL DEVELOPMENT AND APPLICATION |
| | | | | -5A | FINAL THIRD-PHASE REPORT ON MODEL DEVELOPMENT AND APPLICATION |
| | | | | -MR7 | MEMORANDUM REPORT ON SMALL-ARMS MODEL |
| --- | | -9 | REPORT ON FEASIBILITY STUDY OF THE MULTI-SYSTEM PENETRATION SIMULATOR (MSPS) | -9 | DEVELOPMENT AND DEMONSTRATION OF A FEASIBILITY DEMONSTRATION MODEL OF A SYSTEMS PENETRATION ANALYZER |
| --- | | -SS1 | LAUNCH PROFILES OF ENEMY MANNED INTERCEPTORS | --- | |
| --- | | -SS2 | ANALYSIS OF FUNCTIONAL REQUIREMENTS AND CORRESPONDING WARNING - RECEIVER CAPABILITIES FOR ADAPTING COUNTERMEASURE ACTION TO THREAT ENVIRONMENT | --- | |
| --- | | -SS3 | AIRBORNE INTERCEPTOR COUNTERMEASURES ANALYSIS | --- | |
| --- | | -SS4 | DECOY AND TRACKBREAK ROCKET ANALYSIS | -MR3 | MEMORANDUM REPORT ON DECOY AND TRACKBREAK ROCKET ANALYSIS |
| | | | | -SS4B | REPORT ON DECOY AND TRACKBREAK ROCKET ANALYSIS |
| --- | | -SS4A | DECOY AND TRACKBREAK ROCKET ANALYSIS EVALUATION MODEL DEVELOPMENT | -MR4 | MEMORANDUM REPORT ON DECOY RADAR CROSS SECTION STUDY |
| | | | | -SS4C | FINAL REPORT ON DECOY RADAR CROSS SECTION STUDY |
| --- | | --- | | -SS4D | A STUDY OF THE FLIGHT-PATH-CONTROL AND VEHICLE DESIGN FOR A SUBSONIC, LOW ALTITUDE, PENETRATION AID MISSILE |
| --- | | --- | | -HFS | HUMAN FACTORS STUDY |
| TEST DATA DERIVATION | | | | | |
| -6 | FACILITIES SURVEY | -6 | SUPPLEMENTARY REPORT ON FACILITIES SURVEY | --- | |
| -7 | FLIGHT TESTS | -7/8 | SUPPLEMENTARY REPORT ON AN ASSESSMENT OF FLIGHT TEST DATA AND SIMULATOR TEST DATA | -7 | CAL FLIGHT-TEST ACTIVITIES AND DATA-REDUCTION EFFORTS |
| -8 | PHYSICAL SIMULATION TESTS | | | -8 | DESCRIPTION OF A SURFACE-TO-AIR MISSILE MODEL |
| SUMMARY, CONCLUSIONS, AND RECOMMENDATIONS | | | | | |
| -S | SUMMARY, CONCLUSIONS, AND RECOMMENDATIONS | -S | SUMMARY, CONCLUSIONS, AND RECOMMENDATIONS | -S | SUMMARY, CONCLUSIONS, AND RECOMMENDATIONS |

In this report, a Phase II investigation of a family of low altitude, subsonic-cruise penetration aid missiles is extended and expanded. The earlier study determined missile gross weight and range as a function of payload weight and missile diameter for a family of fixed length vehicles. No specific payloads, vehicle configurations, or control systems were examined in any detail (although more detailed studies were made on high altitude cruise missiles).

In this Phase III study, the requirements for a specific missile system are first defined. Then the aerodynamic, weight, inertial and control system characteristics of a selected number of candidate missile systems are determined and compared. Also investigated are the relative advantages and disadvantages of various kinds of storable/deployable lifting and control surfaces.

To help define some of the major problem areas and to illustrate the effect of the more sensitive of the system parameters, one of the candidate missile systems is "flown" in simulation under various conditions of launch, control and atmospheric disturbances. It is shown that, with the proper design precautions, a stable missile system is feasible. Recommendations are made for additional, more specific, Phase IV studies.

The PENVAL program is planned as an extensive analysis effort of approximately five years' duration with the development and application of a progressively more powerful methodology and the treatment of progressively more complex and changing situations. Reports covering areas of work similar to those discussed in this preface are being issued at approximately annual intervals; thus, the reader is cautioned to determine that he is using the latest applicable report or has all supplementary reports available in any particular area.

This report is classified Confidential because it contains information concerning penetration aids that may be employed by tactical aircraft in countering Sino-Soviet bloc surface-to-air missile (SAM), antiaircraft artillery (AAA), and interceptor defenses.

## TABLE OF CONTENTS

TABLE OF CONTENTS (Cont.)

## LIST OF FIGURES

## LIST OF SYMBOLS

### English Letters

| | | |
|---|---|---|
| A | Area (in rocket motor design) | $in^2$ |
| AR | Aspect ratio of wing = $b^2/S_w$ | no dim. |
| b | Wing span | feet |
| c | Wing chord | feet |
| $C_D$ | Drag coefficient = $D/\ q\ S_w$ | no dim. |
| $C_F$ | Thrust coefficient (rocket) = $F/\ P_c A_t$ | no dim. |
| $C_L$ | Lift coefficient = $L/\ q\ S_w$ | no dim. |
| $C_m$ | Moment coefficient = $M/\ q\ S_w\ d$ | no dim. |
| $C_N$ | Normal force coefficient = $N/\ q\ S_w$ | no dim. |
| $C_{Db}$ | Profile drag coefficient of body | no dim. |
| $C_{Di}$ | Induced drag coefficient (Eqn B 5) | no dim. |
| $C_{Dbw}$ | Profile drag coefficient of wing/body interference | no dim. |
| $C_{Dow}$ | Profile drag of wing | no dim. |
| $c_s$ | Velocity of sound in air | ft/sec |
| $C_L$ | Slope of lift curve = $dC_L/\ d\alpha$ (typical notation for all slopes) | per degree or per rad. |
| D | Drag | pounds |
| d | Missile body diameter | feet |
| E | Amplitude of control relay sinusoid input | rad. |
| e | Efficiency factor (Oswald's) for lift | no dim. |
| F | Engine thrust | pounds |
| g | Acceleration due to gravity = 32.17 | $ft/sec^2$ |
| G(s) | Roll system transfer function | |
| h | Altitude above sea level | feet |
| I | Moment of inertia (with subscript) | pound $in^2$ |
| $I_{sp}$ | Specific impulse of rocket propellant | sec |
| j | Complex number $\sqrt{-1}$ | no dim. |
| k | Control system constant (with subscript) (Eqns 6.3, 6.4 and 6.5) | |

## English Letters (Cont.)

| | | |
|---|---|---|
| K | Control system constant (with subscript) (Eqns 6.1, 6.2) | |
| L | Lift | pounds |
| M | Moment | ft lbs |
| M | Mach number = $V/c_s$ | no dim. |
| N | Normal force (normal to missile X-Y plane | pounds |
| N(E) | Control system describing function | |
| P | Pressure (in motor design) | $lb/in^2$ |
| q | Dynamic pressure = $1/2 \rho V^2$ | $lb/ft^2$ |
| r | radius | inch or feet |
| (s) | Laplace transform symbol | |
| S | Area (with subscript) | $ft^2$ |
| T | Relay repeat time | sec |
| t | time | sec |
| u | Projection of V vector in XX direction | ft/sec |
| V | Missile (or airplane) air velocity | ft/sec |
| v | Projection of V vector in YY direction | ft/sec |
| v' | Sidewash velocity divided by V | no dim. |
| W | Weight of missile or component (with subscript) | pounds |
| w | Projection of V vector in ZZ direction | ft/sec |
| w' | Upwash velocity divided by V | no dim. |
| X, Y, Z | Missile (or airplane) orthogonal axes (see Figure A.1) | |
| x, y, z | Distances along X, Y, or Z axis | feet |

## Greek Letters

| | | |
|---|---|---|
| $\alpha$ | Angle of attack = $\cos^{-1} w/V$ | degrees or radians |
| $\beta$ | Sideslip angle = $\cos^{-1} v/V$ | degrees or radians |
| $\Delta$ | Roll control system dead zone | radians |
| $\Delta$ | Finite increment (used as prefix) | |
| $\delta$ | Control surface deflection | degrees or radians |
| $\theta$ | Pitch angle, between horizon and XX axis | degrees or radians |

## Greek Letters (Cont.)

| | | |
|---|---|---|
| $\Lambda$ | Wing sweep angle | degrees |
| $\lambda$ | Wing taper ratio = tip chord/root chord | no dim. |
| $\pi$ | 3.1416 | |
| $\rho$ | Air density | slugs/ft$^3$ |
| $\tau$ | Time delay (Eqn 6.3a) | sec |
| $\phi$ | Roll angle | degrees or radians |
| $\psi$ | Yaw angle | degrees or radians |
| $\omega$ | Circular frequency | rad/sec |

## Subscripts

| | |
|---|---|
| a | Pertaining to the aileron |
| b | Pertaining to the body |
| c | Rocket chamber conditions |
| c.g. | Conditions at the center of gravity |
| c.p. | Conditions at the center of pressure |
| e | Pertaining to the elevator |
| e | Rocket exhaust conditions |
| $\ell$ | Pertaining to roll |
| p | Angular velocity in roll |
| q | Angular velocity in pitch |
| r | Angular velocity in yaw |
| r | Pertaining to the rudder |
| t | Pertaining to the tail |
| t | Rocket throat conditions |

## Superscripts

| | |
|---|---|
| ' (prime) | Refers to coefficients that use the body cross section area, $S_b$, as a reference |
| $\cdot$ (dot) | Refers to nondimensional wash velocity components time derivative of a variable, e.g. $\dot{w} = dw/dt$ |

# 1. SUMMARY

An investigation is made of various vehicle configurations and flight-path-control systems suitable for use with a low altitude, subsonic penetration aid missile system. System requirements are defined in terms of: launch altitude (500 feet), launch velocity (Mach 0.7), ECM payload (about 16 pounds), flight path (near-horizontal cruise or constant climb), and flight time (about 70 or more seconds). Various vehicle configurations, differing primarily in their method for generating lift, are defined and compared. They include vehicles with: a single-pivot wing, a double-pivot split wing, a reamer wing, a wingless body, and a Rogallo wing. All configurations are so configured that they can be launched from a 2.75 inch tube housed below the wing of a tactical airplane.

Roll, pitch, and yaw flight-path-control systems are also configured to provide the missile with on-board control and some degree of artificial aerodynamic damping.

A missile system is synthesized using the wingless vehicle configuration and various combinations of roll, pitch, and yaw control. This synthesized system is then "flown" on a simulator and its actions under dynamic conditions (including a disturbance from the flow field of the launch aircraft and from a gusty atmosphere) are examined.

It is concluded that an air launched, penetration aid missile meeting the above requirements is both aerodynamically and mechanically feasible. For the 2.75 inch diameter pod-launched missile, gross weight will be about 28 pounds, and length about 70 inches. Both the wingless missile and a winged configuration merit further, more detailed, investigation. Also, a control system that senses a linear combination of roll displacement and roll rate merits further consideration even though "hardware" may not now exist for such a system.

It is recommended that further, more detailed, analyses and studies be made of the more promising systems and that additional flight simulations

be made which will include the effects of: system errors, manufacturing tolerances, alternate flight paths, alternate launch conditions, "random" propulsion schedules, etc.

# 2. INTRODUCTION

## 2.1 STUDY OBJECTIVES

One of the penetration aid concepts under investigation in the PENVAL program is the use of a low altitude, subsonic, aerodynamic cruise vehicle capable of serving as a decoy (to radar) or as a trackbreaker of radar. It is the purpose of this study to investigate the flight performance and the relative merits of a number of selected vehicle configurations.

In particular, emphasis is given to the investigation of:

a. the aerodynamic performance of the vehicle (launch aerodynamics, cruise efficiency, static balance),

b. the configuration of the vehicle (lifting surface design, propulsion requirements),

c. the flight-path-control system (sensor characteristics, vehicle dynamics, system configuration).

## 2.2 BACKGROUND AND DISCUSSION

### 2.2.1 Background

In the PENVAL Interim Progress Report of July 1965 (Ref. 1), analyses were made of decoy and trackbreak rockets. In concept, these rockets were to be mounted on a penetrating aircraft and launched, when needed, to simulate (at radar frequencies) the launch aircraft. With one exception (Section VI, Appendix VI-A-1 of Ref. 1) all of the vehicles examined were intended to operate at high altitudes.

Since the completion of the Ref. 1 study, interest has been renewed in a low altitude, subsonic, aerodynamic cruise vehicle capable of defeating the SA-3 (or similar) missile system. Also, since the publication of Ref. 1, it has been shown that problems associated with missile flight-path-control, especially during the initial launch and during cruise, require more thorough investigation. Some of these problems originate because of the need for

storing and deploying the missile's aerodynamic surfaces. Others originate because of the peculiar inertial characteristics of the vehicle and the disturbances produced by the air flow field adjacent to the launching aircraft.

Because of the solution of these flight-path-control problems are intimately associated with the aerodynamic design (and, hence, configuration) of the vehicle, studies relating low altitude cruise efficiency to missile control and stability were initiated. The work reported herein is a record of these studies.

### 2.2.2 Discussion

The launching of a missile from a moving airborne vehicle is a well established concept; many missile systems have been designed, built and operated successfully. However, because each missile/aircraft/control system combination incorporates unique requirements and restrictions, each system becomes unique--with unique operational characteristics and unique problems.

For the low altitude, high speed, missile system under consideration here, unique problems also exist which require solutions. The manner in which some of these problems arise from the imposed requirements (described more fully in Chapter 5) is diagrammed below.

| Requirement | Effect on Design | Problem Areas |
|---|---|---|
| 2.75 inch diameter<br>14 to 16 pound payload<br>70 second cruise time | Missile will be long and thin | Roll moment of inertia is small.<br>Body volume is restricted, hence, critical. |
| Launch at low altitude and high subsonic speed (high "q") | Lifting surfaccs will be small | Aerodynamic damping will be small, especially in roll.<br>Aerodynamic forces can be high. |
| Tube launch | Body must be "smooth" and cylindrical. Tails and wings must be storable and deployable. | Storage problem. Complex mechanisms may be needed.<br>Deployment problem (time, geometry). |

| Requirement | Effect on Design | Problem Areas |
|---|---|---|
| Launch from carrier aircraft | Ejector or booster required | Flow field will disturb launch. |
| Aerodynamic cruise at relatively constant velocity | Sustainer motor required | Efficient cruise configuration is needed. |
| | Lifting surface required | Static and dynamic stability is required. |

Most of the effort described in this report was directed towards the solution, or better definition, of the problems noted above.

## 2.3 METHOD OF APPROACH

This study was conducted in three phases.

In Phase I, system requirements and limitations were identified. In particular, the following system characteristics were defined: payload size and volume, aircraft conditions at time of missile launch (velocity, altitude, launch direction), missile flight path history (velocity and altitude vs time), missile size and shape (approximate). The results of this work are recorded in Chapter 3 of this report.

In Phase II, preliminary screening investigations were made of various candidate vehicles. The candidates varied primarily in the kind of lifting surface employed and the method of storing and deploying these surfaces. Preliminary investigations were made of steady-state aerodynamics and methods of deployment. The results of this work are recorded in Chapter 4 of this report.

In Phase III, more detailed analyses were made of the more promising missile candidates. Three major areas were investigated: vehicle detail design (i.e. aerodynamics, structures and mechanisms)--reported on in Chapter 5, control system analysis--reported on in Chapter 6, and flight path simulation--reported on in Chapter 7. For the latter, the flight of a missile (defined in Chapter 5 and using a control system similar to that discussed in Chapter 6) was generated by a six-degree of freedom analog simulator.

Using the results of the study, conclusions were then drawn concerning the practibility and feasibility of designing a low altitude, high speed, aerodynamic cruise missile as a penetration aid.

Finally, because many problems have remained unresolved, recommendations were made for further study and a brief program was outlined for such a study.

# 3. DEFINITION OF SYSTEM REQUIREMENTS

## 3.1 GENERAL REQUIREMENTS

The missile, to act as an efficient decoy or trackbreak rocket, should simulate the flight characteristics of the carrier aircraft and should be sufficiently separated from the carrier as to be identified (by radar) as a separate flying object.

To accomplish this, the missile must:

1. fly at speeds and altitudes approximating those of the carrier aircraft,
2. fly within a given zone relative to the carrier aircraft,
3. perform only those maneuvers and flight path changes that approximate those of the carrier aircraft,
4. carry payloads (ECM equipment) of sufficient size and weight to accomplish its decoy, trackbreak or jamming mission,
5. have sufficient randomness incorporated into its design to cause the missile to fly ahead, behind, above, below or to the side of the carrier aircraft (the exact position varying with each launch).

In addition to the above general requirements and limitations, the missile should also have the following characteristics:

6. be of sufficiently small size and weight to permit a number (unspecified) to be stored on one carrier aircraft,
7. be synthesized from components and systems representing state-of-the-art technology (but not necessarily off-the-shelf items).

## 3.2 DETAILED REQUIREMENTS

### 3.2.1 General Discussion

Noted below are specific estimates of vehicle flight profiles, payload weights and volumes, and control requirements for a low altitude, subsonic cruise, decoy/trackbreak rocket. This information, while preliminary in nature, is felt to be sufficiently well defined to permit fulfillment of the study objectives given to Section 2.1.

The values selected are taken to be indicative of the family of existing tactical aircraft (the F-4C, F-105, and F-111). Because none of these craft normally fly supersonically with external stores (at least not for any extended periods of time), the study is limited to subsonic flight.

### 3.2.2 Flight Profiles

- Velocity $\cong$ 770 ft/sec - This value is approximately Mach 0.7 at sea level and represents a compromise between efficient subsonic cruise and the maximum speed capability of the aircraft with external stores.
- Launch altitude - An altitude of 5000 ft was arbitrarily selected as the upper bound on the low altitude decoy flight envelope. For most cases, a launch altitude of 500 ft should be used.
- Flight time > 70 sec (from launch to sustainer burnout) - This value corresponds to a minimum flight range of about 10 miles which is the approximate radial dimension of the SA-3 intercept zone (from the maximum range intercept to the missile dead zone).
- Nominal flight profiles - The following two flight profiles are postulated for the penetration aid missile:

  1. Constant climb angle
  2. Constant altitude or a climb and level-off.

- Direction of launch - forward with respect to the carrier airplane.

3.2.3 Payload Weight and Volume Requirements

Payload weight and volume requirements are defined for two kinds of ECM payloads:

A. S-band spot noise generator with a 6 MHz bandwidth and a two-minute operating time,

B. S-band repeater with capability to simulate a 10 $m^2$ target to a range of 10,000 feet without saturating.

| Item | System A | | System B | |
|---|---|---|---|---|
| | Weight pounds | Volume cu. in. | Weight pounds | Volume cu. in. |
| ECM Payload (including power supply, battery, and assoc. wiring) | 11.0 | 175 | 8.0 | 105 |
| Control System (including sensor, electronics, and actuators) | 3.5 | 50 | 3.5 | 50 |
| Reserve for contingencies | 1.5 | 10 | 1.5 | 10 |
| TOTAL | 16.0 | 235 | 13.0 | 165 |

Notes: Information on spot noise generator was obtained from Reference 1, Sect VII B.

Estimates for repeater was based on the repeater used on the low altitude version of the Raytheon RCU-1 designs.

3.2.4 Minimum Control Requirements

The low altitude penetration aid missile, which utilizes aerodynamic lift to balance vehicle weight in its cruise mode, requires minimal flight path control. The prime consideration in designing the vehicle control system should be to obtain well damped lateral and longitudinal dynamics, maintain the vehicle wings level, and follow approximately the flight paths prescribed in 3.2.2. Specifically, the decoy control system should be able to achieve the following flight path requirements:

- Cross range - Maintain the decoy wings approximately level and constrain the decoy heading with respect to the penetrator so that cross range dispersions remain at a reasonable percentage (tentatively set at 10 percent) of the range.
- Down range - Follow the flight path prescribed in 3.2.2. Accurate velocity control is not necessary. The flight path angle should be maintained positive and controlled to within an average of 1 degree from the nominal.

### 3.2.5 Vehicle Geometry and Mounting

Vehicle sizing will be determined on the basis of required ECM payload, propulsion and control system component weights and volume, and structural weight. Emphasis will be given to the 2.75 inch diameter vehicle, but larger body diameters may be studied, as required.

The vehicle shall be designed so that it can be mounted in existing (or modified) external pods which are, in turn, mounted to the wings or fuselage of the penetrating tactical aircraft.

# 4. ANALYSES OF MISSILE CONFIGURATIONS

## 4.1 INTRODUCTION

As stated in Section 2.1, the primary objective of this study is to investigate the relative merits and flight characteristics of a number of different missile configurations. In this section a selected number of missile configurations which could be used for the low altitude penetration aid role are defined--geometrically and aerodynamically. The relative advantages and disadvantages of each design are discussed, and some conclusions are drawn concerning "preferred" vehicle configurations.

Because the information generated here is to be used only for screening purposes, only typical values of vehicle characteristics are given. In Chapter 5, more detailed data are presented for the "preferred" candidate designs.

## 4.2 CONFIGURATION ANALYSES AND EVALUATIONS

### 4.2.1 Vehicle Design Considerations

In Section 2.2.2 the effects of various system requirements on the vehicle design are briefly noted. A more detailed explanation of those requirement/design relationships and their effects on the choice of configuration is given below.

- The missile will be long and thin. For the payload weights and volumes required (Section 3.2.3) and the small diameters needed (Section 3.2.5), the body fineness ratio (length/diameter) will range from about 20 to 30. The most likely shape for the body is a circular cylinder with an ogival nose.
- The lifting surfaces will be small. For the velocities (770 ft/s) and altitudes (500 to 5000 ft) noted in Section 3.2.2, dynamic pressure, $q$, will be about 700 $lb/ft^2$. Preliminary estimates (Chapter 5) place the missile weight at 25 to 30 pounds.

$$\text{Lift} = \text{Weight} \approx q\, C_L\, S$$
$$\text{or } S\, C_L = W/q = 30/700 \cong 0.04\ \text{ft}^2$$

Cruise lift coefficient, $C_L$, usually ranges from about 0.5 to 1.0 (based on wing area). Therefore, required wing area, $S$, will vary from about 0.04 to 0.08 $\text{ft}^2$.

- The body must be smooth. Because the missile is to be launched from a cylindrical tube, it must be of such shape that it can be stored within the tube. Hence, any aerodynamic surfaces needed for lift or control must be designed for storage.

- Boost and sustainer motors are required. To insure a proper launch from the carrier aircraft, the missile should be forceably ejected from its storage tube and, by accelerating, separate itself from the vicinity of the aircraft. While a boost engine is not the only way to accomplish this acceleration, it is a very efficient method--especially when another, cruise, motor is required. The requirement for near-constant velocity cruise can best be satisfied by a sustainer motor. Because of the small size of the vehicle and its relatively short flight time, a solid propellent rocket motor is recommended for both the booster and the sustainer.

- Control and balance surfaces are required. If the missile is to fly a controlled flight path, it must have some means of generating a control force. Two kinds of devices are possible for such a vehicle: movable aerodynamic surfaces and controlled deflection of the sustainer motor thrust vector. Both are feasible for a missile of this size; however, because thrust vector control does not lend itself very easily to a roll control system (which is needed for this missile) (see Chapter 6), the movable surfaces are recommended. For static balance, and to provide some aerodynamic damping, "fixed" aerodynamic tails or canards are recommended.

A number of configurations, each satisfying the design considerations noted above, have been postulated. Each is described in some detail in the sections that follow. The designs differ from one another primarily in the scheme used for generating lift or in deploying the lifting surface.

4.2.2 Single-Pivot Wing Configuration

(1) Description (See Figure 4.1a.)

In this design, aerodynamic lift is supplied by the wing and the horizontal tail. Prior to launch, the wing is stored in the fore-aft position. Because of its small size, the wing can be stored either within or external to the body. A 90 degree rotation about its geometric center will deploy the wing. For external wing storage, the missile body must be notched; when the wing is stored within the body, slots must be made on each side of the body. If the body angle of attack is to be maintained near-zero during cruise, the wing must be installed with a fixed angle of attack.

(2) Advantages

(a) Deployment mechanisms are relatively simple.

(b) The wing can be fabricated as a single unit with a single pivot.

(3) Disadvantages

(a) During wing deployment, one half of the wing moves into the wind, the other half away from the wind. This helicopter-like motion produces unsymmetrical lift across the wing and induces a rolling moment on the missile. It can be shown that wing tip velocities as low as $\pm 1.5$ ft/s can induce rolling accelerations the order of 30 rad/s$^2$.

(4) Comments

(a) See Section 4.2.7 for discussion of tails.

(b) Raytheon has built and tested an early version of the XADR-7A having a configuration similar to the one described above.

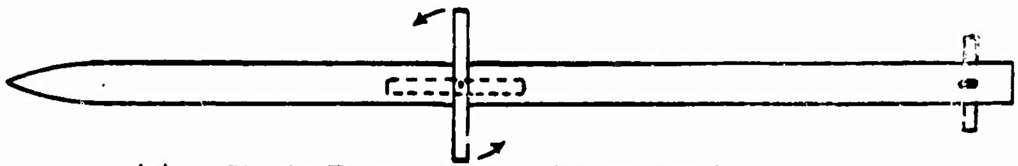

(a) Single Pivot Wing (Plan View)

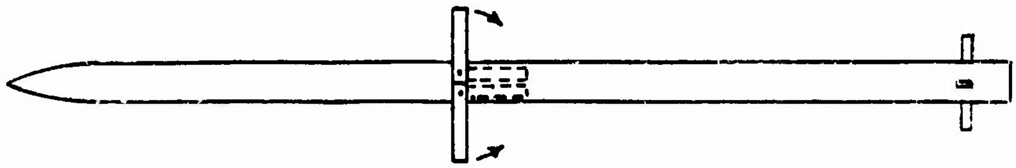

(b) Double-Pivot Split Wing (Plan View)

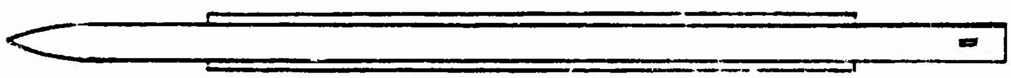

(c) Reamer Wing (Plan View)

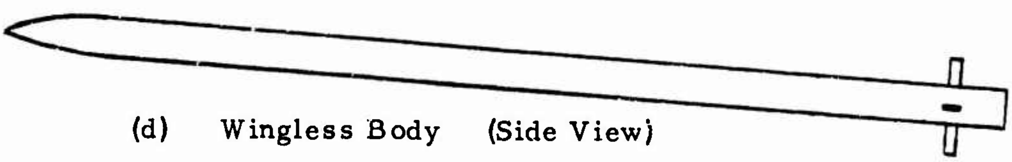

(d) Wingless Body (Side View)

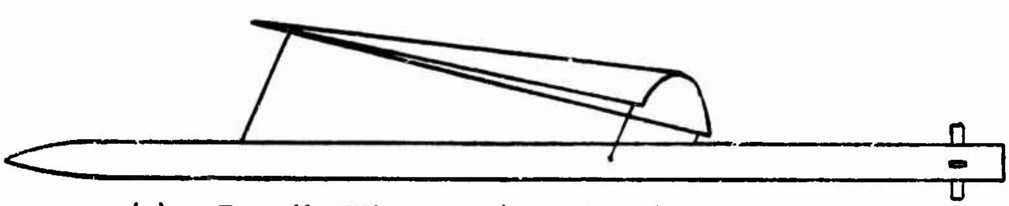

(e) Rogallo Wing (Side View)

Figure 4.1 MISSILE CONFIGURATIONS

4.2.3 Double-Pivot Split Wing Configuration

(1) Description (See Figure 4.1b.)

In this design, aerodynamic lift is supplied by the wing and the horizontal tail. Prior to launch, the two-sectioned wing is swept forward (or aft). Because of their small size, the wing halves can be stored either within the missile body or external to it. Both wing halves are deployed simultaneously by rotating 90 degrees about their inboard pivot. If external wing storage is used, the missile body must be notched to accommodate the wing. If internal wing storage is used, the missile body must be slotted. If the body angle of attack is to be maintained near-zero during cruise, the wing halves must be installed with a fixed angle of attack.

(2) Advantages

(a) Wings are deployed in a symmetrical manner, minimizing the tendency of the missile to roll during launch.

(3) Disadvantages

(a) Mechanisms for deployment can be somewhat more complex than those required for configuration of Figure 1a.

(b) A small center of pressure shift accompanies wing deployment.

(c) Angles of attack on left and right half wings may differ due to manufacturing tolerances.

(4) Comments

(a) See Section 4.2.7 for discussion of tails.

(b) Raytheon's new version of the XADR-7A has a wing similar to that described above.

### 4.2.4 Reamer Wing Configuration

(1) Description (See Figure 4.1c.)

"Reamer" is a name often given to a missile configuration having a cylindrical body and two or more attached wings of very low aspect ratio (on the order of .20 or less). For this configuration, aerodynamic lift is supplied by the wing-body combination and the horizontal tail. Although reamers have been shown to be effective lift producers at supersonic flight speeds, little data are available to indicate their effectiveness at subsonic speeds. Reference 2, however, contains test results of a low aspect ratio tapered wing (AR = 0.17) that may be considered as similar to a reamer wing. These data indicate that the low aspect ratio wing has a very much lower lift curve slope ($dC_L/d\alpha$) than a more conventional wing of aspect ratio 5.36 (slopes were 0.009 per degree compared to 0.066 per degree).

(2) Advantages

(a) Wings are fixed to body, hence no deployment is required.

(3) Disadvantages

(a) Volume allocated to the wings must be bought at the expense of body shell diameter. Hence, for a given payload and body weight, the reamer body length must be longer than a non reamer body. Lengths become excessive for small diameter (2.75 inch) vehicles.

(b) The small chord wings may be completely enveloped in the body boundary layer flow, and hence be made relatively ineffective as wings. At angles of attack, some of the wings will lie in the "shadow" of the body and hence may not be effective.

(4) Comments

(a) See Section 4.2.7 for discussion of tails.

(b) As indicated above, little data are available on the effectiveness of reamer wings at subsonic speeds. Such data would have to be obtained before any accurate flight performance predictions could be made.

4.2.5 Wingless Body Configuration

(1) Description (See Figure 4.1d.)

In this design, aerodynamic lift is supplied by the body and the horizontal tail. During cruise, body attitude is held at the proper value by tail (or canard) control surfaces. Sufficient aerodynamic data exist to indicate that, for the flight conditions under investigation, the body can achieve lift at modest angles of attack (less than 10 degrees).

(2) Advantages

(a) Wings are eliminated. Hence, mechanical and aerodynamic deployment problems are eliminated.

(3) Disadvantages

(a) Roll damping (usually provided by wings) is less on this configuration than on the winged ones.

(b) The drag of this configuration is higher than the winged ones. Hence, more fuel is required for cruise flight.

(4) Comments

(a) See Section 4.2.7 for discussion of tails.

4.2.6 Rogallo Wing Configuration

(1) Description (See Figure 4.1e.)

During the last six years, Rogallo (and others) at NASA has designed and tested a number of deployable, flexible wing like structures that have come to bear his name (e.g. see Reference 3). The wings, which are usually cone-like in form, are often attached by shroud lines to a rigid body. For this configuration, aerodynamic lift is supplied by the wing.

(2) Advantages

(a) The wing is simple in form, light in weight, and relatively easy to store.

(b) By proper design, the wing can be made aerodynamically stable and at the same time be used for control.

(3) Disadvantages

(a) The drag of the wing-body combination will be relatively high.

(b) The wing-body has inherent dutch roll instability. Other kinds of wing vs body oscillations might also occur, especially during boost or in rough air.

(4) Comments

(a) If tails are required on the body, then the discussion in Section 4.2.7 should be consulted.

### 4.2.7 Tails and Canard Surfaces

(1) General Discussion

It is anticipated that all of the configurations depicted in Figure 1 will require tail or canard surfaces. These aerodynamic surfaces are required to provide

(a) static stability during steady flight and/or

(b) control forces during steady flight or maneuvers and/or

(c) aerodynamic damping when the missile has been perturbed.

Because the missile must be stored within a tube, the surfaces must be capable of being stored and then deployed.

The exact size of the surface and the magnitude of the control motions required are dependent upon the details of the particular configuration chosen. Missile weight, center of gravity position(s), body diameter and length, shape of body nose, size, position and shape of wing(s), all dictate, to some degree, the size and positions of the balancing surfaces.

As most of the proposed configurations are very nearly symmetrical in pitch and yaw, and the missile must be stabilized in both these

directions, it is anticipated that vertical and horizontal surfaces of near equal size will be required. Because the flight path m$\imath$ ʰe controlled in pitch (see Section 3.2.2), all or a portion of the horizontal tail surfaces must be movable. In this preliminary analysis, the need for yaw control surfaces cannot be established. (As is indicated later, in Chapter 7, one particular missile configuration--the wingless missile--will require movable vertical surfaces.)

(2) Tail/C- ·r Comparison

Forwa' ounted canard surfaces operate (aerodynamically) in relatively undisturbed air and tend to remain effective as the missile angle of pitch, or yaw, is altered. On the other hand, aft mounted tail surfaces (especially those of small size), may, at certain body angles of pitch or yaw, lie in the wash of the wing or body. Under these conditions the variation of tail lift with body angle may be non linear.

Under body pitch or yaw conditions, canard surfaces generate forces that tend to increase the original motion (i.e., they are destabilizing). Tail surfaces, on the other hand, tend to be stabilizing under the same disturbing conditions.

## 4.3 GENERAL REMARKS AND CONCLUSIONS

Of the five configurations examined in this chapter, two are less well suited than the others for use as a low altitude, subsonic cruise vehicle.

- The Reamer Wing is not considered further because of its excessive length and of its uncertain aerodynamic characteristics. If, however, the missile were not required to be launched from a pod, and no restrictions were placed on missile diameter, such a configuration might merit further investigation.
- The Rogallo Wing is not considered further because of its small size, relatively high drag and its inherent Dutch roll (and other) instability.

Except for the very short time it takes to deploy the wing (from about .15 to .30 seconds), the Single-Pivot wing and the Double-Pivot Split wing configurations will behave nearly identically aerodynamically. Hence, in the remaining chapters of this report only two configurations are examined in detail:

- A winged configuration
- The wingless body configuration.

# 5. DETAILED ANALYSES OF SELECTED CONFIGURATIONS

## 5.1 INTRODUCTION

### 5.1.1 Objectives of Detailed Analyses

In Chapter 4, five missile configurations were screened as possible candidates for a low altitude decoy/trackbreak penetration aid for tactical aircraft. In this chapter, the preceding work is amplified and extended.

Specifically, three of the more promising candidate vehicles are defined in sufficient detail (a) to ensure design feasibility of each class of vehicle, (b) to permit definition of critical aerodynamic and inertial parameters (such information to be used as inputs to the six degree of freedom flight simulation discussed in Chapter 7), and (c) to permit a more intimate investigation to be made of various methods for storing and deploying aerodynamic surfaces (wings, tails, canards). Because the 2.75 inch rocket body is the smallest to be considered (see Section 3.2.5), and hence, the most difficult in (or on) which to store surfaces, it is the only body diameter investigated here.

### 5.1.2 Choice of Vehicle Configurations

As noted in Section 4.3 of the preceeding chapter, two generic vehicle designs are chosen for more detailed analyses:

- A winged configuration, and
- A wingless configuration.

For the winged configuration, the double-pivot split wing is chosen, rather than the single-pivot wing, because the former is somewhat more complicated mechanically and, hence, presents a greater design problem.

As will be explained later (Section 5.4.1), two versions of the wingless body are investigated; the first has only tails; the second has both tails and canard surfaces.

Hence, three configurations are examined in this chapter:

- The double-pivot, split wing
- The wingless body with tails, and
- The wingless body with both tails and canards.

A description and discussion of each of these designs is given in Sections 5.2, 5.3, and 5.4 following.

## 5.2 WINGED MISSILE WITH TAIL

### 5.2.1 Configuration

The geometric, weight and inertial characteristics of one particular winged missile satisfying the criteria and limitations of Chapter 3 are depicted in Figure 5.1. For this design, three aerodynamic surfaces are employed: (a) a wing, near mid-length, to provide most of the lift and some roll damping, (b) a vertical tail, near the aft end, to provide lateral stability and damping and some roll damping, and (c) an adjustable (in "lift") horizontal tail, near the aft end, to provide longitudinal stability and damping, pitch and roll control, and some roll damping. As indicated in Figure 5.1, all of the surfaces are relatively small and can be stored (during prelaunch) within the cylindrical body.

In Figures 5.2 and 5.3, two possible schemes for wing or tail storage are shown. As indicated in Figure 5.3, provision is made both to deploy each half of the horizontal tail and to change the pitch angle of each semi-tail. The primary advantage of the stowed-surface design is that the missile, in its pre-launch configuration, will have a "clean", smooth outside surface. Hence, the aerodynamic surfaces are protected from damage or maladjustment during handling, shipment, storage, loading, etc. The primary disadvantages of stowed-surface designs are that the mechanisms for deployment and control are somewhat complicated, and that slots must be cut in the body side. The latter need not penalize the structural integrity of the design if the slots are small (relative to the missile diameter) and if the slots can be adequately reinforced (e.g., by the molding of beads around the slot).

NOTE: All weights are in pounds, all dimensions are in inches.

| | | At Launch | | | | At Burnout | | |
|---|---|---|---|---|---|---|---|---|
| | | $W$ | $x_{base}$ | $W\,x$ | $W\,x^2$ | $W$ | $W\,x$ | $W\,x^2$ |
| Payload | - fwd | 13.0 | 53 | 689 | 36 520 | 13.0 | 689 | 36 520 |
| | - center | 1.0 | 33 | 33 | 1 090 | 1.0 | 33 | 1 090 |
| | - aft | 2.0 | 12 | 24 | 290 | 2.0 | 24 | 290 |
| Sustainer | - Propel. | 4.0 | 24 | 96 | 2 300 | - | - | - |
| | - Motor | .5 | 22 | 11 | 240 | .5 | 11 | 240 |
| Booster | - Propel. | .4 | 3 | 1 | 0 | - | - | - |
| | - Motor | .2 | 2 | 0 | 0 | - | - | - |
| Body | | 2.1 | 35 | 74 | 2 590 | 2.1 | 74 | 2 590 |
| Wing | | .6 | 34 | 20 | 680 | .6 | 20 | 680 |
| Horiz. Tail | | .6 | 14 | 8 | 110 | .6 | 8 | 110 |
| Vert. Tail | | .6 | 7 | 4 | 30 | .6 | 4 | 30 |
| Miscel. | | 1.0 | 35 | 35 | 1 220 | 1.0 | 35 | 1 220 |
| | SUM | 26.0 lb. | | 995 | 45 070 | 21.4 lb. | 898 | 42 770 |

$\bar{x} = 995/26.0 = 38.3$ in. $\qquad \bar{x} = 898/21.4 = 41.9$ in

$I_{oo\ payload} = \Delta w\, h^2/12 = 1\ 200$, $I_{oo\ body} = 860$, $I_{oo\ propel.} = 50$

At Launch : $I_{pitch\ c.g.} = 1200 + 860 + 50 + 45\ 070 - 26.0 \times (38.3)^2 = 9\ 060$ lb. in$^2$

At Burnout : $I_{pitch,\ yaw} = 1200 + 860 + 42\ 770 - 21.4\ (41.9)^2 = 7\ 250$ lb. in$^2$

$I_{roll} = 29.4$ lb. in$^2$ (at launch) , $27.5$ lb. in$^2$ (at burnout)

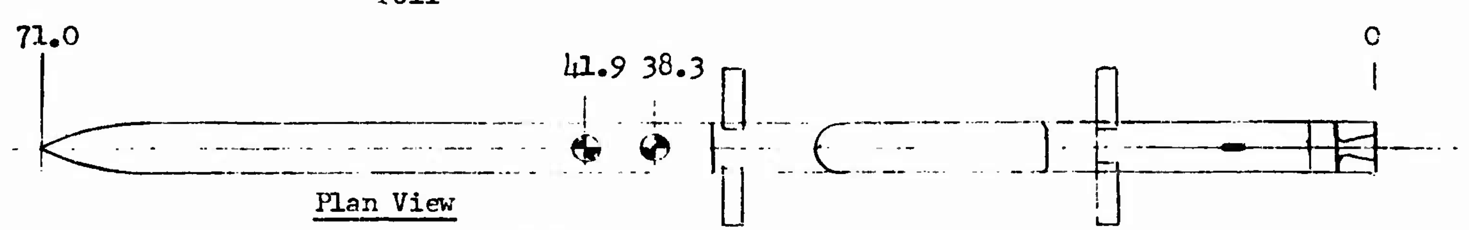


Plan View

Scale: 1 in = 10 in

Figure 5.1 WINGED MISSILE, WEIGHTS AND INERTIAS

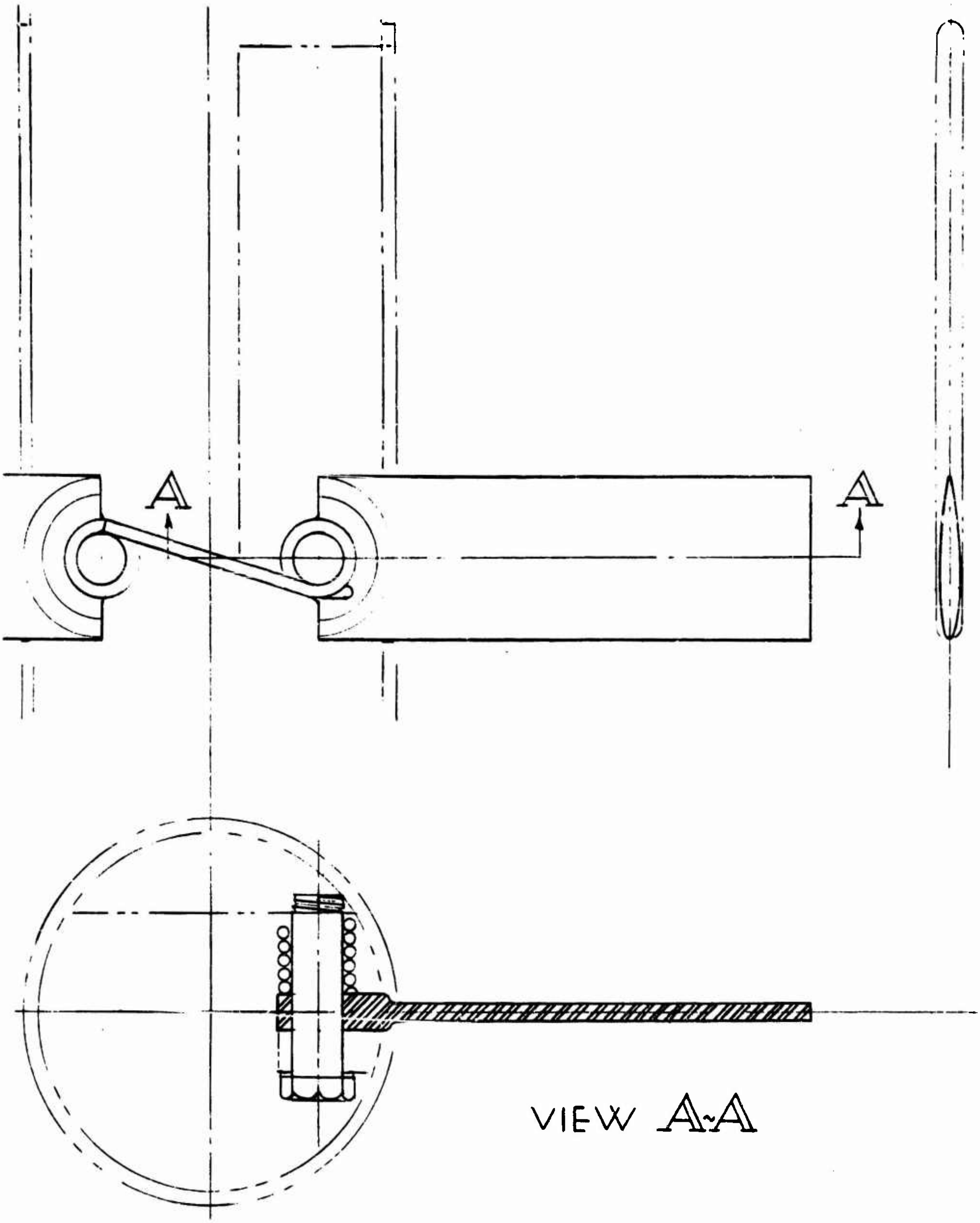


Figure 5.2 AIRFOIL TAIL (WING) INSTALLATION FIXED PITCH

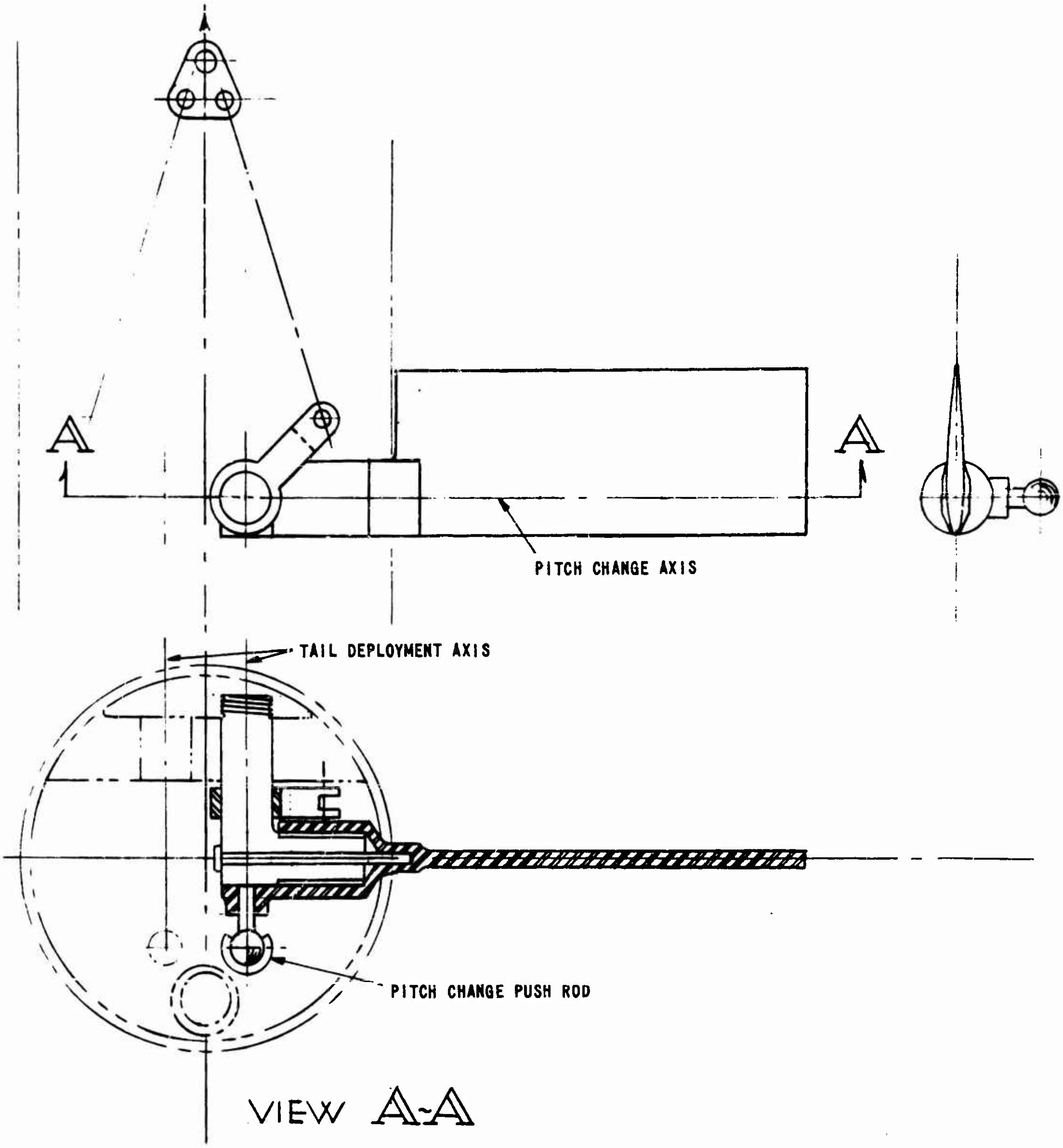


Figure 5.3 AIRFOIL TAIL INSTALLATION - ADJUSTABLE PITCH

Figure 5.4 illustrates an alternate scheme for wing or tail deployment or control. Here a hinged external surface is operated by a push rod. Surface lift is varied by increasing or decreasing the "flapping" angle of the surface. The prime advantage of this design lies in its mechanical simplicity. Its major disadvantages are that the air loads are difficult to determine and that cross coupling between pitch, roll, and yaw will probably occur.

Figure 5.5 is a half-scale sketch of the aft end of a possible missile design. The sketch indicates that it is possible to store a vertical tail, a horizontal tail, a booster and a sustainer transfer tube all within the confines of a 2.75 inch diameter cylinder. The booster shown here (details are given in Appendix B) is assumed to be ejected after burnout.

NOTE: The missiles described in Figure 5.1 (and subsequent figures) and the deployment schemes sketched in Figures 5.2, 5.3, and 5.4 should be considered only as feasibility studies. Design details of any specific penetration aid missile can be determined only after exact flight and performance requirements have been established.

### 5.2.2 Aerodynamics

(1) Definition of Flight Conditions

Flight conditions for this missile are given in Section 3.2.

Namely:

| | | |
|---|---|---|
| Velocity of carrier aircraft, V | | = 770 f.p.s. = Mach 0.7 (approx.) |
| Altitude at launch | | = 500 to 5000 ft |
| Direction of launch | | = forward |
| Total flight time | | > 70 sec. |
| Time of cruise flight | | = not specified = 70 sec. |
| Time of boost flight | | = not specified = 1.25 sec. |
| Dynamic pressure at launch | | $= 1/2\,\rho V^2$<br>$= 0.5\,(.00238)\,(770)^2$ (at sea level)<br>= 705 lb./psf |
| Payload: | Weight | = 16.0 lb. |
| | Volume | $= 235\ in^3$ |

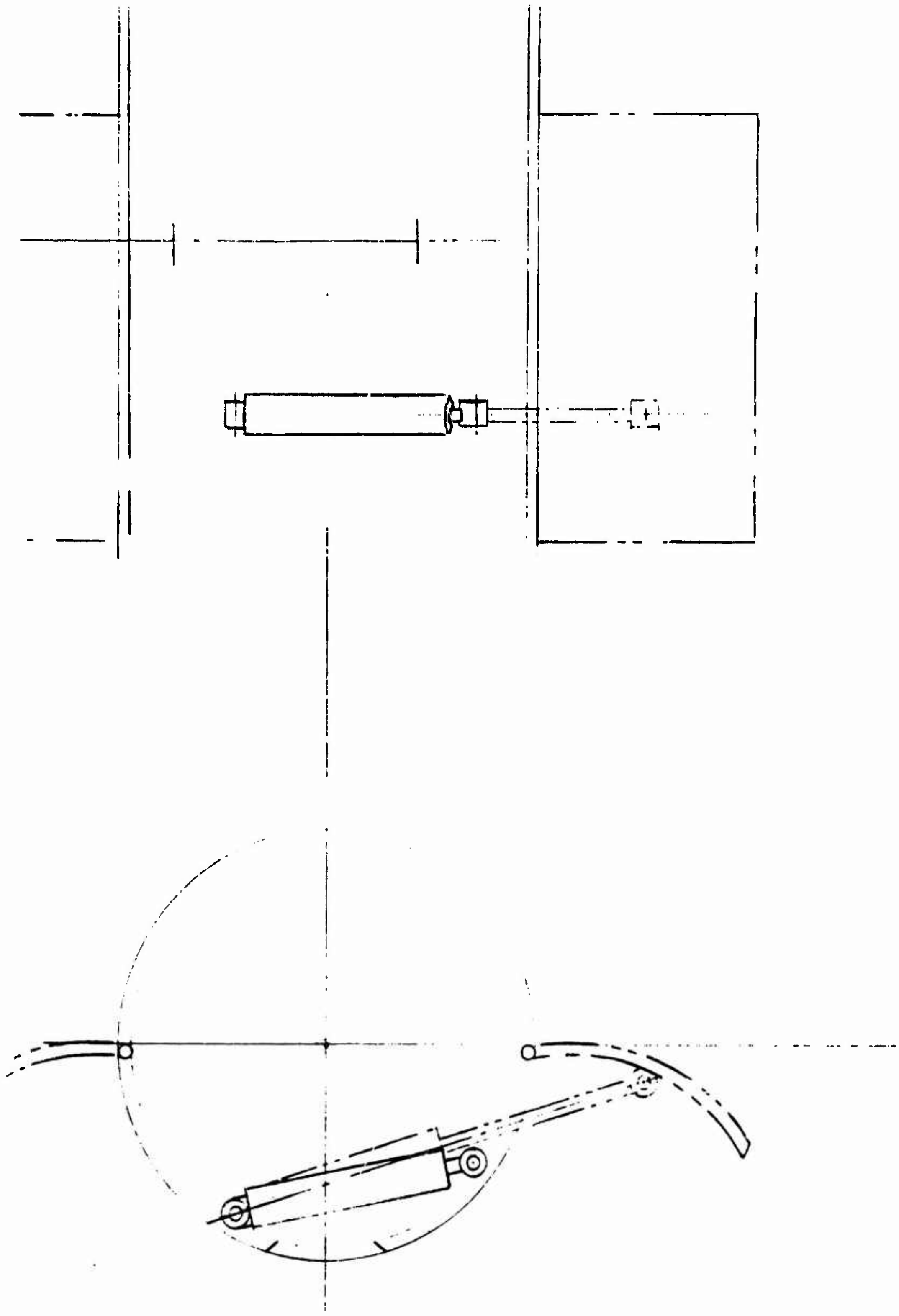

Figure 5.4 HINGED TAIL (OR WING) INSTALLATION - ADJUSTABLE ANGLE

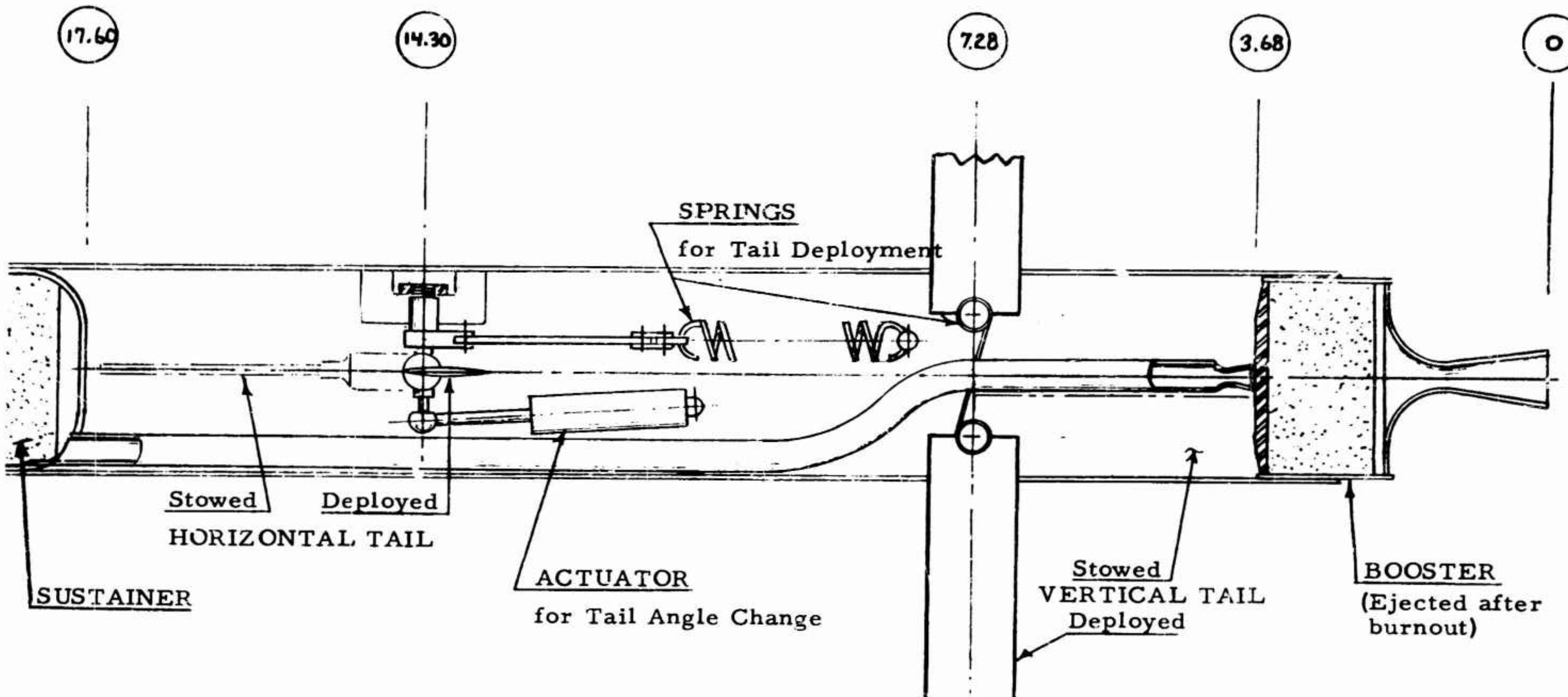


Drawn to Half Scale

Figure 5.5 MISSILE AFT END (TYP.)

(2) Determination of Optimum Wing Area

For aerodynamic cruising vehicles, maximum range (for minimum vehicle weight) is obtained when the ratio of lift to drag (L/D) is a maximum. For high drag bodies best L/D occurs when the induced drag of the wing, $C_{D_{iw}}$, is equal to the profile drag of the wing, $C_{D_{ow}}$ (see Appendix B). The wing for this missile is sized to accomplish this.

From Eq. 9 of Appendix B, max. L/D occurs when

$$D/L = \frac{(C_{Db}' + C_{Dbw}')}{W/S_b} q + 2 \left( C_{D_{ow}} / \pi \ AR \ e \right)^{1/2}$$

For the missile shown in Figure 5. 1,

| | | | |
|---|---|---|---|
| W | = average weight in cruise | = 21.4 + 4.0/2 | = 23.4 lb |
| $S_b$ | = body cross sectional area = | $(1.38)^2/144$ | = .0413 ft$^2$ |
| $C_{D_{ow}}$ | = profile drag of wing | = 0.020 (see Ref. 4) | |
| AR | = aspect ratio of wing | = 7.7 (assumed) | |
| e | = efficiency factor | = 0.8 for big body/small wing | |

$(C_{Db}' + C_{Dbw}')$ = Profile drag of body plus wing/body interference drag
= 0.375 (based on body cross sect. area) (see Appendix A)

If the above values are substituted into the D/L formula, then D/L min. = 0.528 and L/D max. = 1/.528 = 1.90

The 1.90 value is for the untrimmed condition. Trimmed L/D is computed in part (d) below.

In Appendix B, Equation 8, it is shown that the lift coefficient for maximum L/D occurs when

$$C_{L\ opt} = (C_{Dow} \pi \ AR \ e)^{1/2} = (0.020 \pi \ 7.7 \times 0.8)^{1/2} = 0.623$$

As indicated in Figure 5.1, the wing lies aft of the c.g. Hence a down tail load is required to balance the missile and wing lift exceeds the missile weight ( $L_w > W$). It can be shown that

$$L_w = \frac{(x_{cg} - 14.3)}{34.0 - 14.3} W$$

if the wing were at station 34.0 and the tail at 14.3. Values of $L_w$ and $L_t$ (tail load) are computed for three cruise conditions. Results are summarized below.

| Condition | W | $x_{cg}$ | $L_w$ | $L_t$ |
|---|---|---|---|---|
| Start of Cruise | 25.4 lb | 39.0 in. | 31.8 lb. | -6.4 lb. |
| Mid-Cruise | 23.4 | 40.4 | 31.0 | -7.6 |
| End of Cruise | 21.4 | 41.9 | 30.0 | -8.6 |

The wing is sized for the mid-cruise condition.

Wing Area = $S_w = L_w/q\ C_L = 31.0/705 \times 0.623 = .0707\ ft^2$

or $S_w = 10.2\ in^2 = 1.15$ in. by 8.8 in.

The angle of attack of this wing, $\alpha = C_L/\ (dC_L/d\alpha)$

where $\frac{d\,C_L}{d\,\alpha} = \frac{0.1}{1 + 2/AR\,e}$ From Ref. 5, Sect. VII-2

$$\therefore\ d\,C_L/d\,\alpha = 0.075 \text{ per deg.}$$

and $\alpha = 0.623/0.075 = 8.3$ deg.

Summary:

Wing Area = $S_w = 10.2\ in^2$

Chord = 1.15 in. Span = 8.8 in.

Aspect Ratio = AR = 7.7

Fixed angle of attack = 8.3 deg.

L/D max. = 1.90 (untrimmed)

$d\,C_L/d\,\alpha$ = 0.075 per deg.

The above values have been optimized for the flight conditions at mid-cruise time = 1.25 + 70.0/2 = 36.25 sec.

(3) Determination of Horizontal Tail Area

The horizontal tail should be large enough to provide static balance, to provide static stability, and to provide some damping in pitch and roll. It should also be of sufficient size to provide sufficient forces for pitch and roll control.

Tail lift, $L_t$, is computed in Part (1) above. As indicated in the table, balancing tail loads will vary from 6.4 to 8.6 pounds.

Because in this preliminary analysis control loads and damping cannot be adequately evaluated, the best size for a tail cannot be determined. For a first estimate, the tail is assumed to be the same size and shape as the wing. Hence

$$\text{Tail area} = 10.2 \text{ in}^2$$

$$\text{chord} = 1.15 \text{ in. and span} = 8.8 \text{ in.}$$

The angle of attack required to produce the 7.6 pound balancing load, at the mid-cruise time,

$$\alpha_t = (7.6/31.0) \times 8.3^\circ = 2.0^\circ$$

For the wing/body/tail combination described above and depicted in Figure 5.1, it can be shown that the stability coefficient, $d\,C_M/d\alpha$, will have the following values:

| Condition | $dC_M/d\alpha$ | |
|---|---|---|
| Start of cruise | - 1.26 | Coefficients are referenced to |
| Mid Cruise | - 1.41 | body diameter and body |
| End of Cruise | - 1.58 | cross section area. |

Sufficient aerodynamic data were not available to permit a determination to be made of the proper shape and size of the hinged, circular arc, surface depicted in Figure 5.4.

(4) Determination of Vertical Tail Area

The proper size of the vertical tail for the missile of Figure 5.1 will probably be dictated by dynamic flight conditions. As a first estimate, the tail is assumed to have the same size as the wing and the horizontal tail.

(5) Determination of Drag and L/D Trimmed

As noted in (2) above, the L/D value of 1.90 is for the untrimmed flight condition at mid-cruise--it does not include the drag of the tails. Values of $C_L$, $C_D$, and L/D are recomputed for trimmed flight for each of three cruise times. Results are tabulated below.

For a wing and tail of the same size and shape and having the profile drags noted in part (2), it can be shown that the drag coefficient of the wing-body-tail combination is

$$C_D = 0.259 + (C_{Lw}^2 + C_{Lt}^2)/19.4$$

where the "w" and the "t" subscripts refer to the wing and tail respectively and the coefficients are referenced to wing area.

| | $C_{Lw}$ | $C_{Lt}$ | $C_D$ | Drag | W | L/D |
|---|---|---|---|---|---|---|
| Start of cruise | .638 | -.128 | .281 | 14.0 lb | 25.4 | 1.81 |
| Mid-cruise | .623 | -.152 | .280 | 13.9 | 23.4 | 1.68 |
| End of Cruise | .603 | -.172 | .279 | 13.9 | 21.4 | 1.54 |

Hence, the drag remains very nearly constant during the entire cruise period even though the weight varies from 25.4 to 21.4 pounds.

## 5.3 WINGLESS MISSILE WITH BODY LIFT

### 5.3.1 Configuration

The geometric, weight and inertial characteristics of a wingless missile satisfying the criteria and limitations of Section 5.3.1 are depicted in Figure 5.6. For this design, only two aerodynamic surfaces are employed: (a) a vertical tail, near the aft end, to provide lateral stability and damping and some roll damping, and (b) an adjustable (in "lift") horizontal tail, near the aft end, to provide longitudinal stability and damping, pitch and roll

NOTE: All weights are in pounds, all dimensions are in inches.

| | | At Launch | | | | At Burnout | | |
|---|---|---|---|---|---|---|---|---|
| | | W | $x_{base}$ | W x | W $x^2$ | W | W x | W $x^2$ |
| Payload | - fwd | 14.0 | 48 | 682 | 32 740 | 14.0 | 682 | 32 740 |
| | - aft | 2.0 | 12 | 24 | 290 | 2.0 | 24 | 290 |
| Sustainer | - Propel. | 4.4 | 27 | 119 | 3 200 | - | - | - |
| | - Motor | .5 | 22 | 11 | 240 | .5 | 11 | 240 |
| Booster | - Propel. | .4 | 3 | 1 | 0 | - | - | - |
| | - Motor | .2 | 2 | 0 | 0 | - | - | - |
| Body | | 2.0 | 33 | 66 | 2 180 | 2.0 | 66 | 2 180 |
| Horiz. Tail | | .6 | 14 | 9 | 130 | .6 | 9 | 130 |
| Vert. Tail | | .6 | 7 | 4 | 30 | .6 | 4 | 30 |
| Miscel. | | 1.0 | 28 | 28 | 790 | 1.0 | 28 | 790 |
| | SUM | 25.7 lb. | | 944 | 39 600 | 20.7 lb. | 824 | 36 400 |

$\bar{x} = 944/25.7 = 36.7$ in $\qquad \bar{x} = 824/20.7 = 39.7$ in

$I_{oo\ payload} = \Delta w\, h^2/12 = 1\ 200$, $I_{oo\ body} = 820$, $I_{oo\ propel.} = 50$

At Launch: $I_{pitch,yaw\ c.g.} = 1200 + 820 + 50 + 39\ 600 - 25.7\ (36.7)^2 = 7\ 730\ \text{lb in}^2$

At Burnout: $I_{pitch,yaw\ c.g.} = 1200 + 820 + 36\ 400 - 20.7\ (39.7)^2 = 5\ 760\ \text{lb in}^2$

$I_{roll} = 24.2\ \text{lb in}^2$ (at Launch), $22.3\ \text{lb in}^2$ (at burnout)

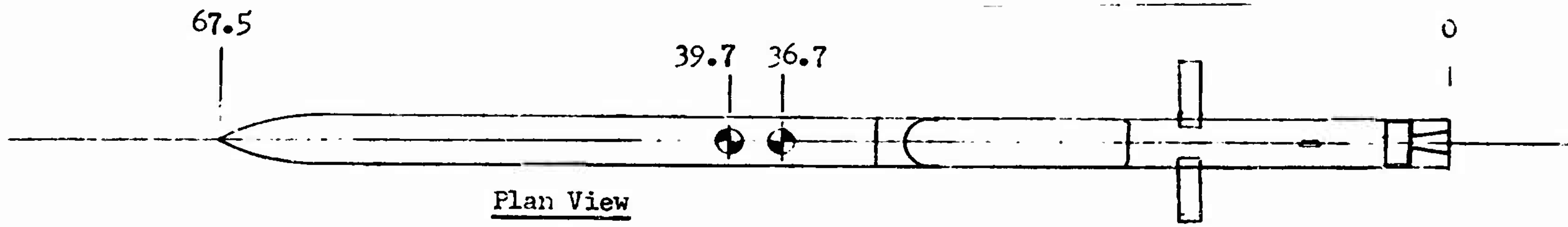


Plan View

Scale: 1 in. = 10 in.

Figure 5.6 WINGLESS MISSILE, WEIGHTS AND INERTIAS

control, and some roll damping. As indicated in Figure 5.6, all of the surfaces are relatively small and can be stored (during pre-launch) within the cylindrical body. The body, held at an angle of attack by the horizontal tail, provides most of the missile lift; the horizontal tail provides the remainder.

As with the winged missile (see Section 5.3.2.(1)), surfaces of the kind sketched in Figures 5.2, 5.3, and 5.4 could be used.

## 5.3.2 Aerodynamics

### (1) Determination of Body Lift Forces

While body lift forces can be computed theoretically, wind tunnel test data are available on bodies having shapes and fineness ratios similar to the missile under consideration. One such set of data is duplicated in Figure 5.7. It is reduced from the information on Figure 3 of Ref. 6. Using these data, body lift and angle of attack are computed for each of three flight conditions.

Taking moments about the c.g. in the pitch plane (please refer to Figure 5.5 and the sketch in Figure 5.6)

$$M_{c.g.} = 0 = L_b\,(x_{cpb} - x_{cg}) - L_t\,(x_{cg} - x_t)$$

where $L_b$ = body lift in pounds
$L_t$ = tail lift = $W - L_b$ in pounds
$x_{cpb}$ = distance of body center of pressure from aft end
$x_{cg}$ = distance of c.g. from aft end
$x_t$ = distance of horiz. tail from aft end

The data of Figure 5.7 are not sufficiently accurate to permit an accurate determination of body center of pressure (c.p.) position. Also, the c.p. position is very dependent upon the exact shape of the body-nose, especially at low angles of attack. For purposes of this analysis, the body c.p. position is assumed to be fixed at a position 30% of body length aft of the nose. Hence, for the 67.5 inch long body of Figure 5.6, $x_{cpb}$ = 67.5 (1.00 - 0.30) = 47.3 in. (measured from missile base).

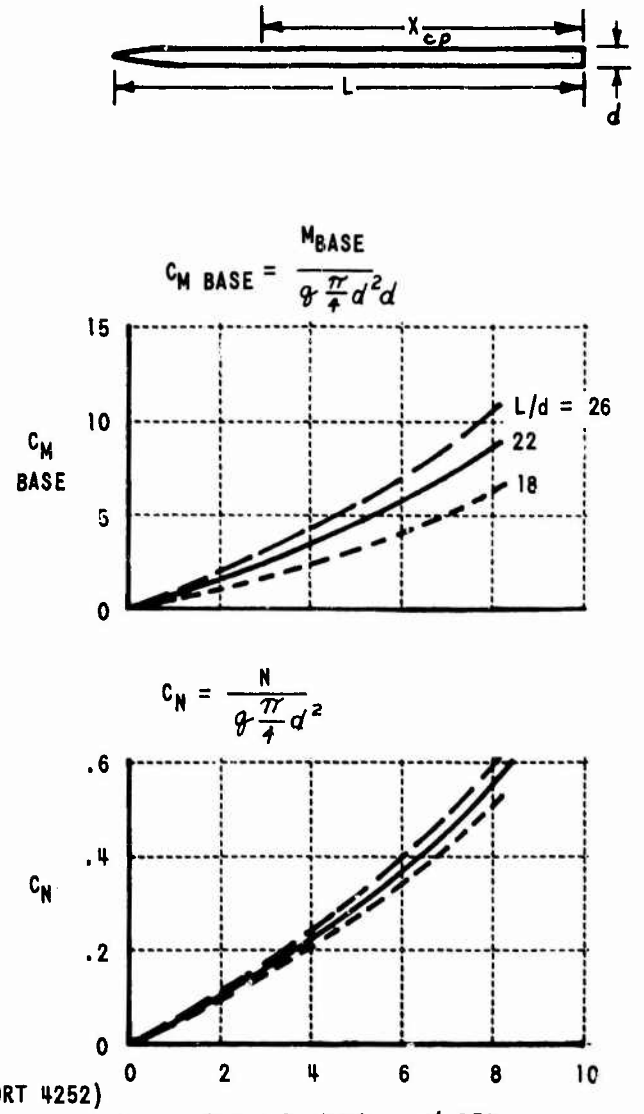


( FROM NAVORD REPORT 4252)
MACH 0.8 $R_e$/ ft. = $4.24 \times 10^6$

ANGLE OF ATTACK. $\alpha$ DEG.

Figure 5.7 BODY NORMAL FORCE AND MOMENT VARIATION WITH ANGLE OF ATTACK

From Figure 5.5, $x_t = 14.3$

$$\therefore M_{c.g.} = 0 = L_b (47.3 - x_{cg}) - (W - L_b)(x_{cg} - 14.3)$$

Body lift and tail lift are computed for three conditions: start of cruise, mid-cruise, and end of cruise. The weights and c.g. positions are derived from the information given in Figure 5.6. Also computed is the body angle of attack, $\alpha_b$. It is obtained in the following manner

$$L_b = q\, C'_{Nb}\, S_b$$

$$C'_{Nb} = L_b / 705 \times 0.0413 = 0.0344\, L_b$$

Using the above value of body normal force coefficient (equals body lift coefficient for small $\alpha_b$) a value of body angle of attack, $\alpha_b$, is read off of Figure 5.7 for a fineness ratio of 67.5/2.75 = 24.5.

Computed parameters are summarized below.

| Condition | W | $x_{cg}$ | $L_b$ | $L_t$ | $C'_{Nb}$ | $\alpha_b$ |
|---|---|---|---|---|---|---|
| Start of cruise | 25.1 lb | 37.4 in. | 17.6 lb. | 7.5 lb. | .60 | 8.1 deg |
| Mid-Cruise | 22.9 | 38.5 | 16.8 | 6.1 | .58 | 8.0 |
| End of Cruise | 20.7 | 39.7 | 16.0 | 4.7 | .55 | 7.9 |

Hence, during cruise the body angle of attack remains nearly constant at about eight degrees.

(2) Determination of Tail Areas

Because balancing tail loads and vehicle inertias are very nearly the same for the missiles shown in Figures 5.1 and 5.6, the tails for this wingless missile are, as a first estimate, made the same size as those of the winged missile.

Therefore: Tail area = $S_t$ = 10.2 in.$^2$
Tail chord = 1.15 in., span = 8.8 in.
Aspect ratio = AR = 7.7
Lift curve slope = $C_{L\alpha}$ = 0.075 per deg.

Using the above values for wing and tail characteristics, the static stability of the missile was computed for three cruise conditions. The resulting values of moment curve slope, $dC_M/d\alpha$ , are:

| | |
|---|---|
| Start of cruise | -0.68 |
| Mid-cruise | -0.80 |
| End of cruise | -0.89 |

Moments are taken about the missile c.g. and use the missile diameter (0.229 ft) as the reference length and the missile cross section area (0.0413 $ft^2$) as the reference area.

(3) Determination of Drag

The following are the major contributors to missile drag:

Body profile drag $= C'_{Db} = .375$ ( see Appendix B)
Tail profile drag $= .020$ per tail (based on tail area)
Body drag due to lift $= C'_{Nb} \sin\alpha$
Tail drag due to lift $= C_{Lt}^2 / \pi AR e$

Hence, $$C_D' = .375 + (.020 + .020)\frac{10.2}{5.95} + C_{Nb}' \sin\alpha + \frac{C_{Lt}^2}{\pi\ 7.7 \times .8}$$

$$= .375 + .068 + C_{Nb}' \sin\alpha + .002$$

$$= .445 + C_{Nb}' \sin\alpha$$

The primes refer to coefficients based on body cross section area.

For body angles of eight degrees (see preceding table), $C_{Nb}' = 0.58$ (from Figure 5.7). Hence, $C_D' = 0.526$

Drag $= C_D'\ q\ S_b = 0.526 \times 705 \times 0.0413 = 15.3$ lbs.

Because body angle remains at about eight degrees, drag will remain nearly constant during the entire cruise period.

To overcome this drag during cruise flight, the sustainer motor (see Appendix C) must supply a thrust of at least 15.3 pounds.

## 5.4 WINGLESS MISSILE WITH CANARDS

### 5.4.1 Configuration

The geometric, weight and inertial characteristics of a wingless, canard missile satisfying the criteria and limitations of Section 5.3.1 are depicted in Figure 5.8. For this design, four aerodynamic surfaces are employed: (a) a vertical tail, near the aft end, to provide lateral stability and damping and some roll damping, (b) an adjustable (in "lift") horizontal tail, near the aft end, to provide longitudinal stability and damping, pitch and roll control, and some roll damping, and (c) and (d) a set of orthogonal canard surfaces, near the nose, to provide additional pitch and yaw damping. (Additional damping may be required for certain dynamic flight conditions.) As indicated in Figure 5.8, all of these sur aces are relatively small and can be stored (during pre-launch) within the cylindrical body.

The methods of tail and canard storage can be similar to those depicted in Figures 5.2 through 5.5.

### 5.4.2 Aerodynamics

(1) Determination of Horizontal Surface Areas

Lift on this missile is obtained from the body, the horizontal canard and the horizontal tail surface. The missile must be so balanced that (a) the sum of the three lifts just equals the missile weight (for "level" flight), (b) the pitching moments about the missile center of gravity are zero, and (c) the missile is statically stable. Depending upon the degree of stability and pitch damping required, a number of combinations of canard and horizontal tail can satisfy the noted balance requirements. One such combination, shown in Figure 5.8, has surfaces and characteristics noted below.

| | Horiz. Canard | Horiz. Tail |
|---|---|---|
| Area in.$^2$ | 6.25 | 10.2 |
| Chord in. | 1.0 | 1.15 |
| $dC_L/d\alpha$ of surf. | .0715 | .075 |
| x dist. from base in. | 63.5 | 14.3 |
| Span in. | 6.25 | 8.8 |

NOTE: All weights are in pounds, all dimensions are in inches.

| | | At Launch | | | | At Burnout | | |
|---|---|---|---|---|---|---|---|---|
| | | W | $x_{base}$ | W x | W $x^2$ | W | W x | W $x^2$ |
| Payload | - fwd | 1.0 | 67 | 67 | 4 490 | 1.0 | 67 | 4 490 |
| | - center | 13.0 | 47 | 598 | 27 510 | 13.0 | 598 | 27 510 |
| | - aft | 2.0 | 12 | 24 | 290 | 2.0 | 24 | 290 |
| Sustainer | - Propel. | 4.2 | 25 | 105 | 2 730 | - | - | - |
| | - Motor | .5 | 22 | 11 | 240 | .5 | 11 | 240 |
| Booster | - Propel. | .4 | 3 | 1 | 0 | - | - | - |
| | - Motor | .2 | 2 | 0 | 0 | - | - | - |
| Body | | 2.1 | 35 | 74 | 2 590 | 2.1 | 74 | 2 590 |
| Canards | | 1.0 | 63 | 63 | 3 970 | 1.0 | 63 | 3 970 |
| Horiz. Tail | | .6 | 14 | 8 | 110 | .6 | 8 | 110 |
| Vert. Tail | | .6 | 7 | 5 | 40 | .6 | 5 | 40 |
| Miscel. | | 1.0 | 35 | 35 | 1 220 | 1.0 | 35 | 1 220 |
| | SUM | 26.6 lb. | | 991 | 43 890 | 21.8 lb. | 885 | 40 460 |

$\bar{x} = 991/26.6 = 37.2$ in $\qquad \bar{x} = 885/21.8 = 41.0$

$I_{oo\ payload} = \Delta w\, h^2/12 = 1200,\quad I_{oo\ body} = 860,\quad I_{oo\ propel.} = 50$

At Launch : $I_{pitch,yaw\ c.g.} = 1200 + 860 + 50 + 43\,890 - 26.4\,(37.2)^2 = 8\,820$ lb in$^2$

At Burnout : $I_{pitch,yaw\ c.g.} = 1200 + 860 + 40\,460 - 21.8\,(41.0)^2 = 5\,870$ lb in$^2$

$I_{roll}$ = 29.8 lb. in$^2$ (at launch), 27.9 . in$^2$ (at burnout)

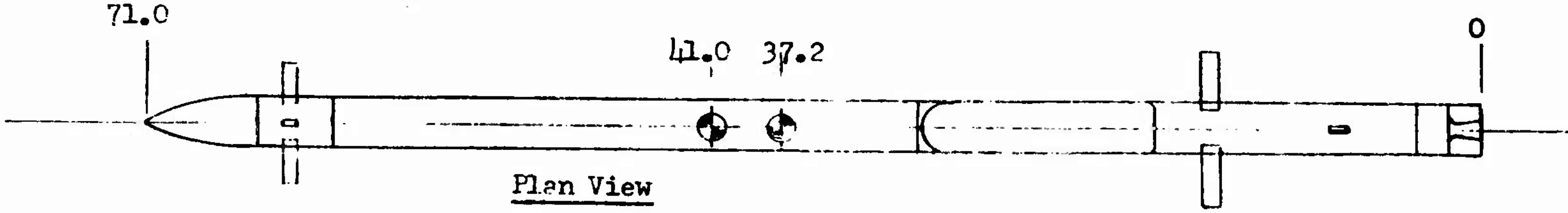


Plan View

Scale: 1 in. = 10 in.

Figure 5.8 WINGLESS/CANARD MISSILE, WEIGHTS AND INERTIAS

The missile has the following characteristics:

| Condition | Time | Weight | $x_{cg}$ | $\alpha_b$ | $\Delta\alpha_t$ | $dC_M/d\alpha$ |
|---|---|---|---|---|---|---|
| Start of cruise | 1.25 sec | 25.5 lb | 38.0 | $3.2^\circ$ | $-0.2^\circ$ | -.07 |
| End of cruise | 71.25 | 21.5 | 41.0 | 3.1 | -1.2 | -.38 |

where $\alpha_b$ = body angle of attack at balance

$\Delta\alpha_t$ = tail angle of attack, with respect to body center line, at balance conditions

$dC_M/d\alpha$ = slope of $C_M$ vs $\alpha$ curve at balance conditions

$C_M$ = pitching moment/ $(q\,S_b\,d)$

It can be seen from the above that the body angle of attack remains almost constant during the 70 sec. cruise. However, the c.g. moves forward 3.0 in. and the static stability increases almost six fold ($dC_M/d\alpha$).

(2) Determination of Drag

Drag is computed in a manner similar to the computation made for the wingless missile (see Section 5.3.2 (3)).

$$C_D' = .375 + (.020 + .020)\,\frac{6.25}{5.95} + (.020 + .020)\,\frac{10.2}{5.95}$$

$$+ \; C_{Nb}' \sin\alpha + \text{induced drag of canard and tail}$$

The induced drag is of the order of 0.002, therefore

$$C_D' = 0.487 + C_{N\,b}' \sin\alpha$$

From the table above, $\alpha_b = \alpha \cong 3$ deg (approx.)

From Figure 5.7, $C_{Nb}' = 0.16$ for $\alpha = 3^{o}$. Hence, $C_D' = 0.495$ (near constant)

$$\text{Drag} = q \; C_D' \; S_b = 705 \times 0.495 \times 0.0413 = 14.4 \text{ pounds}$$

Because the body angle remains at about 3° throughout the cruise, and the induced drag is so small, the drag on the missile remains near constant throughout cruise.

As shown in Appendix C, a constant thrust sustainer motor is needed to counteract this drag.

## 5.5 CONCLUSIONS

The following conclusions have been drawn as a result of this study:

(a) Missiles using a variety of methods for generating aerodynamic lift can be designed to satisfy the requirements of Section 3.2 and the objectives noted in Section 2.1.

(b) Missile weight, for the 2.75 inch diameter vehicle, will be about 25 to 30 pounds, missile length about 65 to 75 inches, (payload was taken to be 16 pounds).

(c) Wings, tails and canard surfaces (needed for lift, control and/or damping) are small enough to be stored within and deployed from a 2.75 inch diameter cylindrical body.

(d) The exact size and placement of lifting surfaces will depend upon the requirements for proper flight dynamics. These areas and positions can be better defined after missiles have been "flown" (in a six degree of freedom simulator, see Chapter 7).

# 6. CONTROL SYSTEM ANALYSES

## 6.1 INTRODUCTION

Because the penetration aid missile is not required to fly an exact flight path (see Section 3.1 (4)), it could conceivably be designed without a flight-path-control system. Such a missile, however, would have to be both statically and dynamically stable about all three axes of rotation. To some extent, static and dynamic stability can be incorporated into both pitch and yaw--if sufficient aerodynamic damping were available. However, because the missile has a very small roll moment of inertia (see Figure 5.1), it is very easily disturbed in roll. In fact, because of rotational cross-coupling (pitch/roll, yaw/roll) rotations occuring about any of the missile's three axes will induce roll.

It is important, therefore, that the missile have at least a roll control system. (It will be shown in Chapter 7 that a yaw control system is also desirable. Also, if altitude is to be maintained, a pitch control system is needed.)

In the technical discussions following, two kinds of roll control systems are examined. In the first, components are chosen that have been used or suggested for use in similar control situations. In the second, a simpler but less "available" system is described. Also described is an elementary yaw damping system and an altitude sensitive pitch system. In Chapter 7 following, various combinations of roll, pitch and yaw systems are synthesized for use in a complete missile system.

## 6.2 ROLL CONTROL SYSTEMS

### 6.2.1 State-of-the-art System

(1) Actuators

One of the more important components in the roll control system is the actuator that drives the control surface. Because the missile has extremely small time constants, the actuator response must be very rapid. In

addition, the actuator should function using only the onboard, unregulated, battery power supply; its size should be small enough to fit into the small confines of the missile body; and its weight should be small.

The direct current stepping motor appears to be one likely choice for satisfying the noted requirements. With such an actuator, the resultant control system will operate in a non-linear, sampled data manner.

(2) Overall Control System

A roll control system is postulated consisting of the following components: (a) the missile itself, (b) a roll deflection gyro (to act as a sensor), (c) a stepping motor (to produce aileron deflections), and (d) a compensator (to help stabilize the system). This system is depicted diagramatically in Figure 6. 1.

Each portion of the system is described below.

(a) The Missile Dynamics

The transfer function relating the missile's roll angle, $\Phi$, to the aileron deflection angle, $\delta_a$, is, for purposes of this analysis, approximated by:

$$\frac{\Phi(s)}{\delta_a(s)} = \frac{K_1}{s\,(s+\omega_1)} \tag{6.1}$$

| | |
|---|---|
| where $\Phi(s)$ | is the Laplace transform of the roll angle |
| $\Phi$ | is the roll angle, radians |
| $\delta_a(s)$ | is the Laplace transform of the aileron angle |
| $\delta_a$ | is the aileron angle, radians |
| $K_1$ | is a system constant, $(\text{rad/sec})^{-2}$ |
| $\omega_1$ | is a system constant, rad/sec |

$K_1$ and $\omega_1$ are parameters that characterize the roll dynamics of the missile.

The poles corresponding to the Dutch roll effect are neglected in Equation (6. 1).

(b) The Position Gyro

The transfer function for the gyro is taken to be $K_g$.

(c) The Stepping Motor

The block diagram for the stepping motor is contained within the broken line boundary of Figure 6.1. As indicated, the assembly contains a sampling switch. In its operation, the sampling switch closes periodically every T seconds and generates impulses of +1, 0, or -1, depending upon the value of C(t) that occurs at the sampling instant. An analysis of the stepping motor will show that $\delta_a$ changes by $+K_2$, 0, or $-K_2$ degrees each sampling instant and that its wave form is, therefore, of a staircase nature. Hence, the stepping motor is inherently non linear.

(d) The Compensator

A double lead compensator having the transfer function noted in Figure 6.1 is used to help stabilize the system.

(3) System Analysis

To determine the stability of the overall non linear system, the describing function technique is used. It is assumed that the sampling rate is sufficiently large to permit the stepping motor to be approximated by a continuous system (shown in Figure 6.2). In this technique, the linear portions of the system and the non linear portions are first treated separately.

(a) Linear Portion of System

The linear portion of the system can be described by a function G(s).

$$G(s) = \frac{C(s)}{\dot{\delta}_a(s)} = \frac{K_1 K_2 K_g (s + a\omega_2)^2}{s^2 (s + \omega_1)(s + \omega_2)^2} \tag{6.2}$$

In Figures 6.3 and 6.4, the function $\frac{G(j\omega)}{K_1 K_2 K_g}$ is plotted in the complex plane for various values of the factor $\omega$. For this plot the following values were assigned to system constants: $a = 0.1$, $\omega_1 = 3.1$ and $\omega_2 = 31.$, $K_1 = 1430$. The values of a and $\omega_2$ were chosen so as to indicate a stable system when the describing function technique is used.

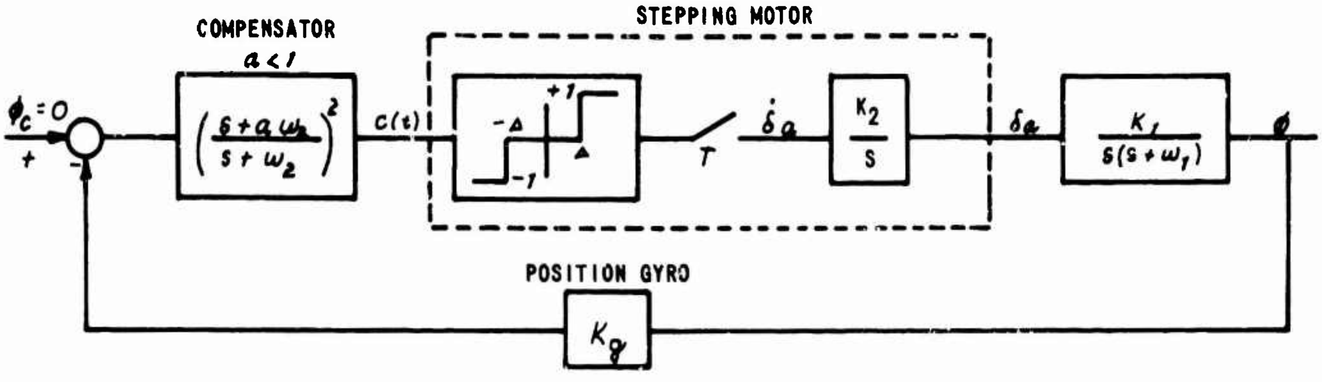


Figure 6.1 ROLL CONTROL SYSTEM CONFIGURATION

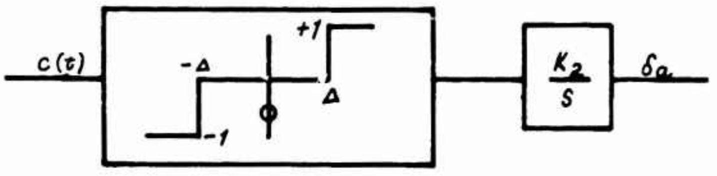


Figure 6.2 APPROXIMATION OF STEPPING MOTOR

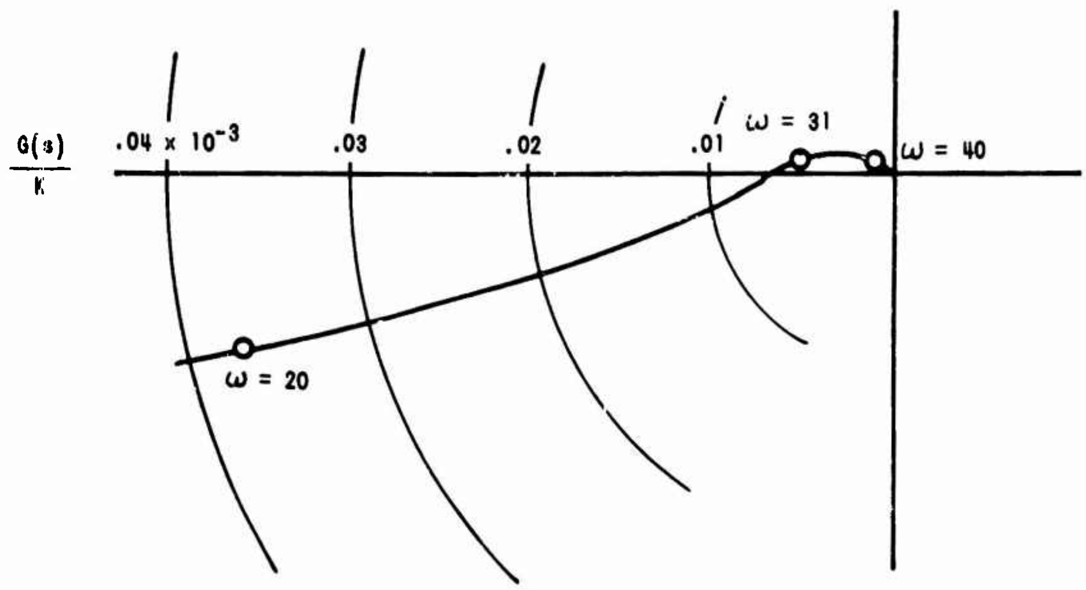


Figure 6.3 G(s) vs. ω FOR ω ≥ 20

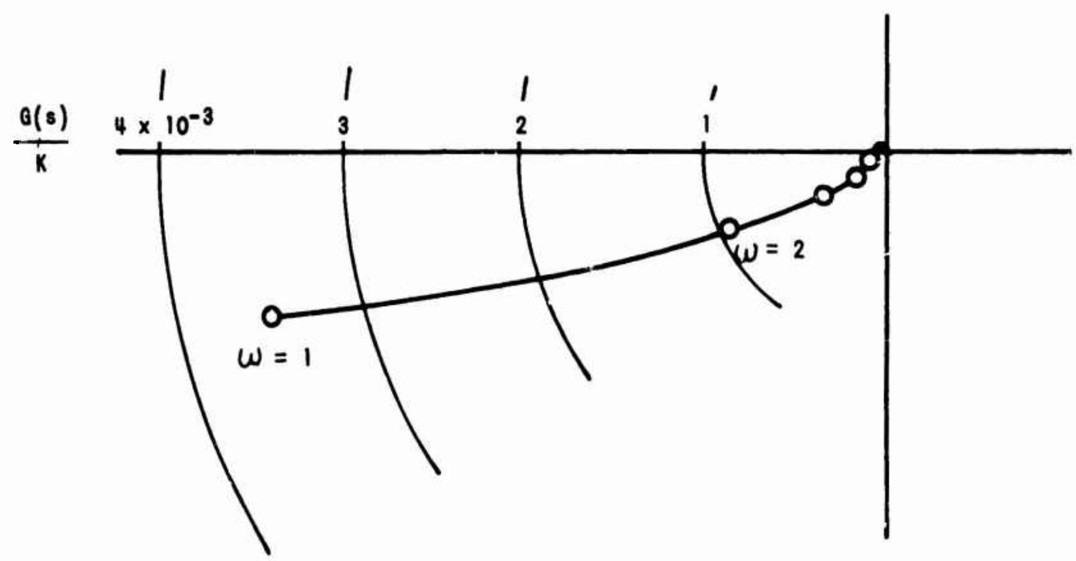


Figure 6.4 G(s) vs. ω FOR SMALL VALUES OF ω

(b) The Non Linear Portion of the System

This portion of the system (i. e., the relay with dead zone) is analyzed by a describing function. As indicated in Reference 8, the negative inverse describing function of a relay with a dead zone ($2\Delta$) is given by

$$-\frac{1}{N(E)} = -\frac{\pi}{4}\frac{\Delta}{\Delta/E}\frac{1}{\sqrt{1-(\Delta/E)^2}}$$

where E is the amplitude of the relay sinusoid input. For a given value of dead zone, $\Delta$ , the factor $-1/N(E)$ will depend upon E. For $\Delta/E \rightarrow 1$, $-1/N(E) \rightarrow -\infty$ , and as E is made greater than $\Delta$, $-1/N(E)$ moves towards the origin along the negative real axis. This continues until $E = \sqrt{2}\,\Delta$ , and then $-1/N(E)$ moves back towards $-\infty$ for all E exceeding this critical value. Figure 6.5 below illustrates this phenomenon.

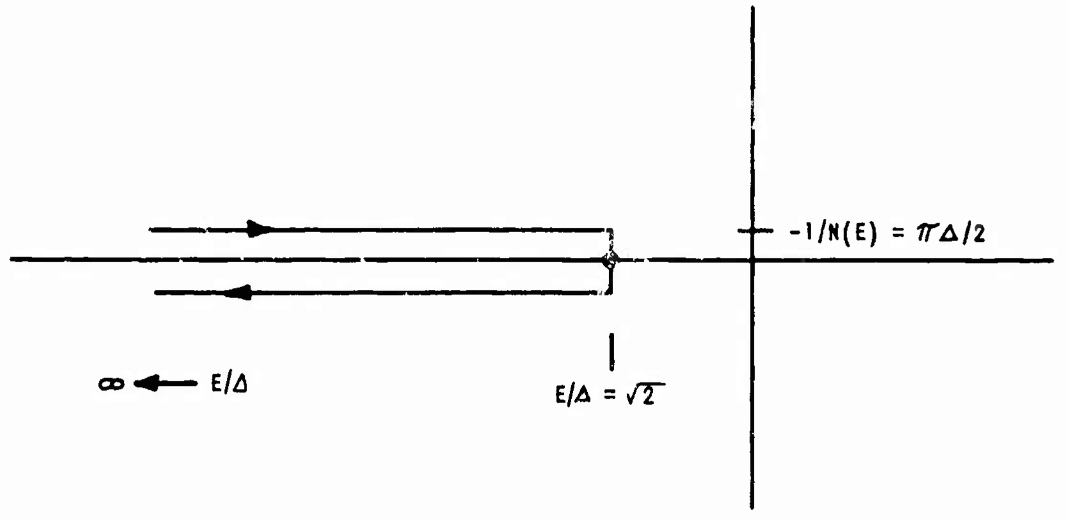


Figure 6.5 PLOT OF -1/N(E) vs. E/Δ

(c) Combined Linear and Non Linear Portions of the System

To determine whether a system with a relay that possesses a dead zone is stable, one plots $G(j\omega)$ and the describing function $-1/N(E)$ on the same graph. If they intersect (i.e., if they have a common operating point) then an oscillation is indicated. It can be either stable or unstable.

For the system under investigation, the value of $K_1 K_2 K_g$ was set equal to 14 and the dead zone was assumed to be $\Delta = 0.4$ degrees. A plot was made of the two functions, and, for the values noted, no steady state oscillation was indicated (i.e., no intersection of the curves was obtained).

NOTE: Although the above analysis indicates that the system under investigation will be stable in roll, other factors, not included in the above analysis must be taken into account. It can be shown that a sampled-data control system employing a relay may have the property that the origin (in its state space representation) is not the only equilibrium point. Hence, for the configuration shown in Figure 6.2, roll ange, $\phi$, might have a steady state value different from zero (even with $\Delta = 0$). The above roll system was checked on a simplified digital computer program (not that described in Appendix D). For the constants chosen, this system was found to settle out at a steady state roll angle of about three degrees with an oscillation of about one degree. Unfortunately, no time was available in this feasibility study to redo the system. However, the primary purpose of this analysis was to investigate the feasibility of a particular control system configuration, and to point out problem areas. A detail design of a system was not within the scope of this study.

(4) Conclusions

It is concluded that the stepping motor that serves as the actuator for the aileron control surface has many of the physical properties desired for the penetration aid missile roll control system. For the missile under study, it is shown that for a pseudo linear system having the proper control constants, a stable roll control system can be designed. Two precautionary notes must be made, however. (a) The "real" system has non linearities arising out of the stepping motor and the actual missile dynamics, and (b) a steady state roll error can be built into the system if the proper choice of system constants is not made.

6.2.2 Simplified Roll Control System

A roll control system is postulated in which the commanded control surface deflection, $\delta_a$, is made a simple linear function of the roll angle $\Phi$ and the roll rate $\dot{\Phi}$. For this arrangement,

$$\tau \dot{\delta}_a + \delta_a = k_1 \Phi + k_2 \dot{\Phi} \tag{6.3a}$$

where $\tau$ = system time lag in seconds

To obtain typical values for the constants $k_1$ and $k_2$, the missile/control-system dynamic equations (see Appendix D) were solved in an approximate manner. Values of $k_1$ and $k_2$ were then chosen (by use of a root locus plot) so that the resulting system motions were, in theory, both stable and properly damped. With these computed values of $k_1$ and $k_2$, Equation (6.3a) becomes,

$$\tau \dot{\delta}_a + \delta_a = 0.111 \Phi + 0.0112 \dot{\Phi} \tag{6.3b}$$

As is discussed in Section 7.3.1, two values of time constant, $\tau$, are examined in a flight simulation model. $\tau$ represents the difference in time between the sensing of the roll rate and deflection, and the initiation of the actuator motion.

## 6.3 YAW CONTROL SYSTEM

### 6.3.1 Simplified Yaw Control System

A yaw control system capable of producing damping as a linear function of yaw rate, r, was postulated for the penetration aid missile system. In such a system, rudder deflection, $\delta_r$, will vary as

$$\tau \dot{\delta}_r + \delta_r = k_3 r \qquad (6.4a)$$

As was done in Section 6.2.2, a computation was made, using typical missile dynamic characteristics, to determine a value for $k_3$ that will give proper yaw damping. With this computed value, the above equation becomes

$$\tau \dot{\delta}_r + \delta_r = -1.7 r \qquad (6.4b)$$

## 6.4 PITCH CONTROL SYSTEM

### 6.4.1 Simplified Pitch Control System

If missile flight path altitude is to be maintained (see Section 3.2.2), then a pitch control system (or pitch schedule) must be employed. A simple system programming elevator deflection, $\delta_e$, as a linear function of altitude change, $\Delta h$, is suggested. For this system,

$$\Delta \delta_e = k_4 \Delta h \qquad (6.5)$$

where $k_4$ is the constant of proportionality having values on the order of $10^{-4}$ to $10^{-5}$ radians/foot.

## 6.5 GENERAL REMARKS AND CONCLUSIONS

Because the missile has a very low roll moment of inertia (see Figure 5.1) and relatively poor aerodynamic damping in roll, the roll control system is expected to be the system posing the most problems and requiring the greatest degree of sophistication.

Two kinds of systems have been investigated here for roll. The major elements of the first system are: a d.c. stepping motor, a displacement gyro, and a compensator. The major advantage of such a system is that it uses

state-of-the-art hardware, i.e., equipment that exists and can be fitted within the 2.75 inch diameter cylinder that forms the missile body. The major disadvantages of this system are: it is relatively complicated in concept, it senses only roll displacement (roll rate is obtained indirectly by a compensating circuit), and it may tend to stabilize the missile at a steady state roll angle that is not necessarily zero (the desired value).

The second system proposed for roll control employs both a roll position and a roll rate sensor. Control surface deflection is made a simple linear function of these two values. The system's primary advantage is that it is relatively simple in concept. Its major disadvantage is that it requires hardware (a d.c. motor) that is not in production, i.e., existing on-the-shelf hardware is too large or heavy for this particular application.

In Chapter 7, both of the above roll systems are combined, in various combinations, with pitch and yaw systems (and with different aerodynamic configurations) to form a missile system. A more comprehensive evaluation is then made of the combined system.

# 7. MISSILE FLIGHT SIMULATION

## 7.1 INTRODUCTION

### 7.1.1 Objectives of Flight Simulation

The objectives of this portion of the analysis are:

(1) to synthesize one or more vehicle/control system combinations using the information of Chapters 6 and 7,

(2) to "fly" the synthesized system on a six-degree-of-freedom simulator under various conditions of launch, wind, etc., using the program described in Appendix D,

(3) to examine the results of the flight simulation to

(a) determine relationships between system characteristics and resulting flight path histories,

(b) identify the more sensitive system parameters,

(c) identify the major problem areas,

(d) select, if possible, a preferred vehicle/control system combination.

### 7.1.2 Definition of Missile System and Components

The penetration aid missile system has four major components: (1) the missile, (2) the control system, (3) the launch aircraft, and (4) the atmosphere. (See Figure 7.1.) Any valid flight simulation should incorporate each of these components and account for the relationships among them. For analysis purposes, each of these components can be expressed in terms of defining parameters.

A diagrametric representation of the missile system is shown in Figure 7.1 along with a notation of the interrelationships (arrows) and the pertinent parameters (symbols). Definition of symbols is given in the frontal pages of this report.

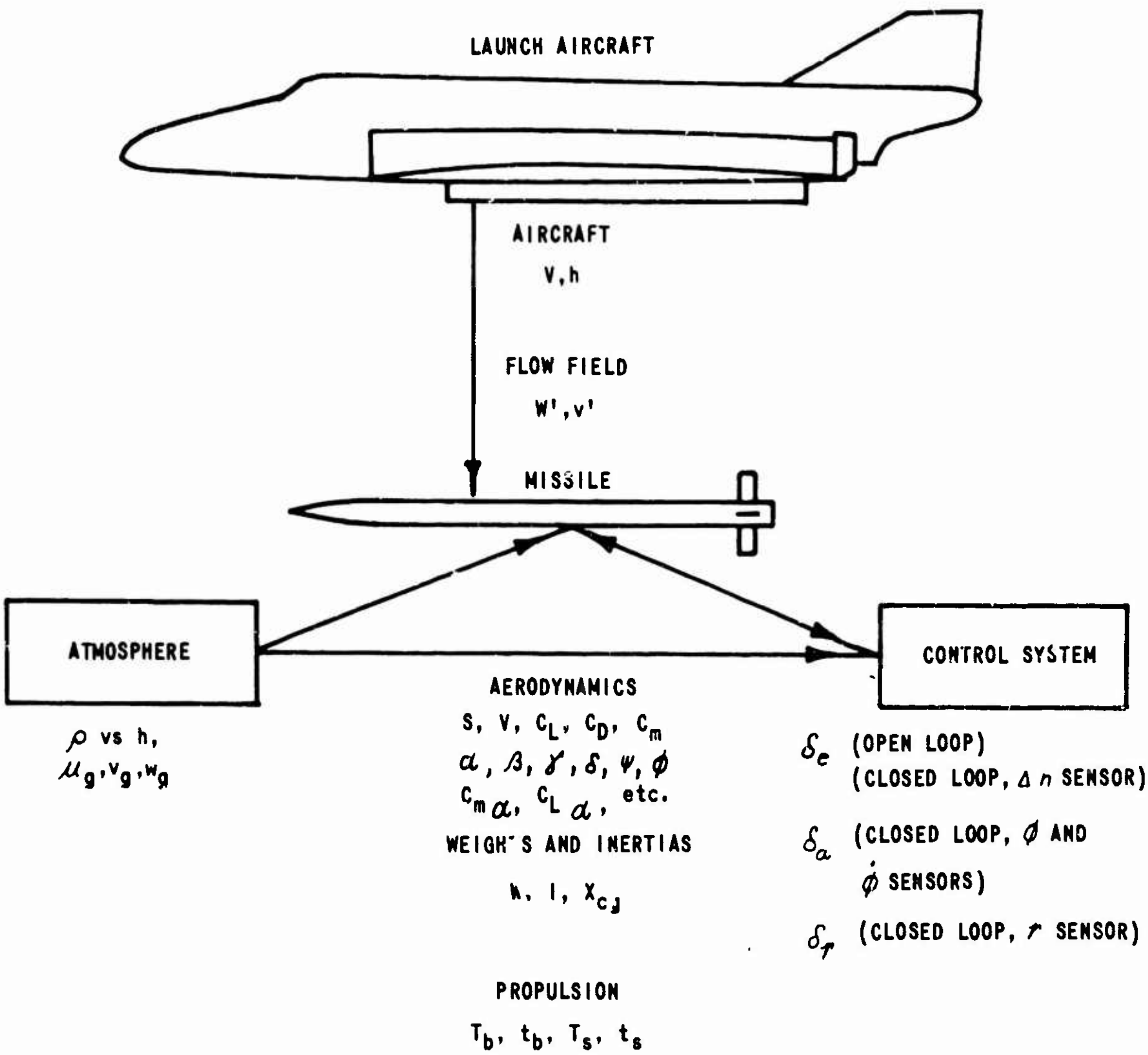


Figure 7.1 DECOY/TRACKBREAK MISSILE SYSTEM - MAJOR COMPONENTS AND PARAMETERS

It should be noted that the launch aircraft influences the missile system only during the first few seconds of flight; the missile-control system-atmosphere relationships continue throughout the flight.

In Section 7.2, following, typical numerical values for each of the system parameters are defined and their interrelationships are noted.

## 7.2 SYSTEM SYNTHESIS

### 7.2.1 The Missile

The wingless missile (Section 5.3) is chosen for this initial synthesized system because it appears to be the simplest of the three described in Chapter 5. Many of the characteristics of this missile are summarized in Figure 5.6; other needed parameters have been computed.

All major system characteristics required as inputs to the simulation program (Appendix D) are summarized in Table 7.1; two flight conditions are given. (See fore part of this report for definition of symbols and units.)

### 7.2.2 The Control Systems

The control systems used here are assembled from the roll, yaw and pitch subsystems described in Sections 6.2, 6.3, and 6.4 respectively. Four different systems are investigated. For simplicity, they are designated Number I, Number II, etc.

Control System Matrix

| Subsystem | Ref. Section | System Number | | | |
|---|---|---|---|---|---|
| | | I | II | III | IV |
| Roll - simplified | 6.2.2 | x | x | x | |
| - state-of-art | 6.2.1 | | | | x |
| Yaw - simplified | 6.3.1 | x | x | | x |
| Pitch - simplified | 6.4.1 | | x | x | x |

TABLE 7.1
Missile System Characteristics and Constraints

| Item | At $\alpha_{trim} = 0°$ time = 0 | At $\alpha_{trim} = 8.1°$ time = 2.5 | Item | At $\alpha_{trim} = 0°$ time = 0 | At $\alpha_{trim} = 8.1°$ time = 2.5 |
|---|---|---|---|---|---|
| W | 25.6 | 25.1 | $C_{\ell_p}$ | -18.3 | -17.3 |
| $I_{xx}$ | .0052 | .0052 | $C_{\ell_{\delta a}}$ | -148 | -148 |
| $I_{yy}$ | 1.67 | 1.66 | $C_{\ell_\beta}$ | 0 | .30 |
| $I_{zz}$ | 1.67 | 1.66 | $C_{\ell_r}$ | 0 | -5.03 |
| $I_{xz}$ | 0 | 0 | $C_{n_p}$ | 0 | -38.5 |
| $C'_L$ | 0 | .861 | $C_{n_{\delta a}}$ | 0 | 0 |
| $C'_D$ | .445 | .526 | $C_{n_{\delta r}}$ | -148 | -148 |
| $C_{L_\alpha}$ | 9.66 | 13.08 | $C_{n_\beta}$ | 71.0 | 63.5 |
| $C_{L_{\delta e}}$ | 7.36 | 7.36 | $C_{n_r}$ | -1310 | -1285 |
| $C_{m_\alpha}$ | -51.6 | -37.2 | $C_{Y_\beta}$ | -9.66 | -8.93 |
| $C_{m_q}$ | -1330 | -1390 | $C_{D_\alpha}$ | 0 | .605 |
| $C_{m_{\dot\alpha}}$ | 0 | 0 | | | |
| $C_{m_{\delta e}}$ | -60.1 | -61.9 | | | |

Note: All of the above coefficients are based upon body cross section area of 0.0413 $ft^2$, on body diameter of 0.229 ft and on radian measure. Moments of inertias have been converted to slug-feet$^2$.

### 7.2.3 The Launch Aircraft

Aircraft flight conditions at the instant of launch are given in Section 3.2.2. As noted there, launch velocity is 770 ft/s and launch altitude is 500 ft.

The flow field velocities, v' and w', into which the missile is launched are defined in Appendix A. As noted there, the field strength and direction vary as a function of x, y, and z displacement from the aircraft. Because the simulation program of Appendix D is time-dependent (i.e., all variables are expressed or computed as a function of time), an approximation was made to the flow field to convert it from space dependency to time dependency. This converted flow field is used as an input to the computer program.

### 7.2.4 The Atmosphere

The atmosphere has two major effects on the missile system: atmospheric density, $\rho$, varies with altitude, and random atmospheric gusts are applied to the missile. The first is accounted for by storage of density vs altitude equations in the simulation program (Appendix D). Gust velocity increments, $u_g$, $v_g$, and $w_g$, are imposed by a band-limited white noise generator; the noise is taken to be homogeneous. Noise strength is specified by a root mean square, r.m.s., value (in feet/second).

## 7.3 FLIGHT PATH RUNS

### 7.3.1 Description of Simulation Assumptions and Runs

The missile system described in Section 7.2 was "flown" under various conditions of launch, wind, control, etc., on the simulation program described in Appendix D. In all, six runs were made. Certain parameters and flight conditions were common to all six runs; these are described below.

At instant of launch,* time = $t = 0$

| | | |
|---|---|---|
| Launch velocity, $V$ | = | 770 ft/s |
| Delta velocity, $\Delta V$ | = | 25 ft/s |
| Altitude, $h$ | = | 500 ft |
| Pitch rate, $\dot{\theta}$ | = | -1.96 deg/sec |
| Launch direction | = | forward (x direction) |

Trim angle of attack, $\alpha_{trim}$, history:

| | |
|---|---|
| $0 \leq t < 2.5$ sec | $\alpha_{trim} = 0°$ |
| $t = 2.5$ sec | $\alpha_{trim} = 8.1°$ |
| $t > 2.5$ sec | $\alpha_{trim} = 8.1° \pm \Delta\alpha$ due to c.g. change |

Elevator angle, $\delta_e$, history:

| | |
|---|---|
| $0 \leq t \leq 2.0$ sec | $\delta_e = 0°$ (open loop system) |
| $2.0 < t \leq 3.0$ sec | $\delta_e = -5.84° \ (t - 2.0)$ (open loop) |
| $3.0 < t$ | $\delta_e = -5.84°$ + control (closed loop) |

For times zero thru 2.5 seconds, all dynamic stability derivatives are evaluated at $\alpha_{trim} = 0$. At time = 2.5 seconds, the trim angle of attack is suddenly changed to 8.1 degrees and all dynamic stability derivatives are evaluated at this new angle. In addition, the missile dynamic equations are now linearized about the new $\alpha_{trim}$. The quantities $\Delta\alpha$ and $\Delta\theta$ are now (at 2.5 seconds) measured with respect to the new $\alpha_{trim} = \theta_{trim} = 8.1°$. In effect, then, a completely new set of differential equations are used to describe the motion of the vehicle after 2.5 seconds. This change was made to permit use of linear equations of motion in a system that is essentially non linear.

The variation of center of gravity position ($x_{cg}$) was accounted for in all six runs by varying each of the following with time:

---

*Zero time is taken to be that instant when the missile is a free body in the air stream, i.e., when it has fully emerged from the launch tube after having traveled its own length (about 5 feet).

Missile mass, m ; Moments of Inertia, $I_{xx}$, $I_{yy}$, $I_{zz}$ ;

Dynamic derivatives, $C_{m_\alpha}$, $C_{n_\beta}$, $C_{m_{\delta e}}$, $C_{m_q}$, $C_{l_r}$, $C_{n_p}$, $C_{n_r}$

Lift force (due to weight loss); pitching moment (due to $x_{cg}$ change).

All of the above quantities are assumed to vary linearly with time during each of the following two intervals: Boost phase $0 \leq t < 1.25$ sec
Sustainer $1.25 \leq t < 71.25$ sec

Each of the six runs simulated on the computer are described below. Because each run has the above factors in common, the description given includes only those factors that make the run distinct.

Run 1 — The missile is launched into the flow field of the aircraft. The atmosphere is calm (r.m.s. value of roughness = zero). The control system used is Number I (see Section 7.2.2). Time lag for roll and yaw, $\tau = 0$ (Equations (6.3b) and 6.4b)).

Run 2 — Run 1 is repeated but with rough air (r.m.s. = 3 ft/s).

Run 3 — Run 1 is repeated but with very rough air (r.m.s. = 9 ft/s) and with the flow field strength increased to three times its nominal predicted value (from Appendix A). This is done to simulate launch during aircraft maneuvers.

Run 4 — The missile is launched into the flow field of the aircraft. The atmosphere is rough (r.m.s. = 3 ft/s). The control system used is Number II; pitch constant, $k_4 = 1.7 \times 10^{-5}$ rad/ft (Equation (6.4)). Time lag for roll and yaw, $\tau = 0.0333$ sec (Equations (6.3b) and (6.4b)).

Run 5 — Run 4 is repeated but with control system Number III (no yaw damper).

Run 6 — Run 4 is repeated but with control system Number IV (state-of-the-art roll control). Sampling time is taken as .05 sec., dead zone $\Delta = \pm 1.7°$ of $\Phi$, and stepping motor increment = 1.5° of $\delta_a$.

7.3.2 Discussion of Run Results

Time histories of a number of flight parameters are presented in Figures 7.2 through 7.7 for all six runs.* A discussion of these runs, based upon information obtained from these figures and from other flight path data,** is given below. Because certain time-dependent phenomena are common to many of the six runs, these time repeating patterns are discussed first.

(1) The aircraft flow field acts almost instantaneously on the missile causing it to oscillate in both pitch and yaw. The frequency of oscillation is about 2 cps. Angle variation is about ±3° in pitch and ±1° in yaw.

(2) The velocity increment (missile velocity minus airplane velocity) builds up to a maximum at 1.25 seconds (end of boost), decays slowly to a minimum at about 40 seconds, then increases again. This phugoid undulation has a period of about 80 seconds for the missile under investigation.

(3) In runs where no altitude control system is used (Runs 1, 2, and 3), the missile climbs slowly as it loses weight. Altitude gained is about 4500 feet.

(4) When lateral control is used (Runs 1, 2, 3, and 4), lateral dispersion is relatively small being less than 100 feet after a 68 second flight time. (Gyro and system errors assumed zero).

(5) During the 68 second flight period, the missile moves ahead of the launch aircraft by about 3500 to 5000 feet. (The latter value corresponds to paths in which altitude control is used, Run 4.)

---

*Figures start on page 7-14.

**As noted in Appendix D, the computer program generates and prints out information on the time-variation of 12 flight parameters. These data are presented in both graphical (Figures 7.2, etc.) and tabular form. The latter are not presented here because of their bulk and because they are peculiar only to the specific missile system synthesized in Section 7.2.

(6) The roll control system used in the first four runs is very effective in maintaining low values of roll angle and roll rate.

(7) The control surface displacements required for roll, pitch, and yaw control are very small--on the order of 0.10 degree.

Discussed below are the time histories of each of the six runs. As noted above, only those phenomena that are peculiar to each run are singled out for discussion.

Run 1 Initial disturbances due to the aircraft flow field (Appendix A) are completely damped out in about eight seconds. After this time, the roll and yaw rates are zero (no disturbance is supplied by the calm atmosphere). The very small pitch rate is caused by the changing missile weight and c. g. position, and the phugoid oscillation.

Run 2 The addition of a rough-air atmosphere imposes a continuous jitter about all three missile axes. The pitch oscillation (in rate and displacement) occurs at about two cps, yaw and roll oscillations occur at about three cps. All oscillations appear to be adequately damped. Maximum pitch rate during cruise is about ±10 degrees per second.

Run 3 The imposition of a strong initial disturbance and a strong gust field produces missile oscillations about all three axes that are similar to those of Run 2--only larger in magnitude. Maximum pitch rates in Run 3 are about ±25 degrees per second and oscillate at a frequency of about two cps. The mean pitch angle variation with time remains very close to that of Run 1. Roll and yaw oscillations also increased in magnitude two to three fold over those of Run 2. Frequencies were unchanged.

Run 4 The altitude control system (which is first used in this run) causes the missile to undulate about a mean altitude position (about 1000 feet) at a phugoid frequency of 1/80 cps. Maximum and minimum heights above the ground

were 1600 and 280 feet respectively. The inclusion of a "realistic" time lag (0.033 sec) in the roll (yaw) system appears to have affected neither the roll (yaw) rate nor displacement. As noted in (5) above, the range of the missile is increased over that of the preceding three runs. This range extension is probably bought with the energy that was formerly used (in Runs 1, 2, and 3) to lift the missile up to 5000 foot altitude.

Run 5 — With the yaw control eliminated, the roll rate and roll angle motions damp out to zero in about 0.5 seconds and remain at zero until about 2.5 seconds. During this period, pitch and side slip angle oscillate at about two cps about a zero degree mean. At 2.5 seconds, when the body angle of attack is increased to provide lift during cruise, an umdamped two cps oscillation is induced in the roll rate, roll angle, yaw rate, and azimuth angle. All these oscillations continue to build up in amplitude until at about 4.5 seconds the run is terminated because the missile has become uncontrollable.

Run 6 — With the d.c. step motor employed as a control device, the missile immediately enters into an undamped, but stable, six cps oscillation in roll. Roll amplitude is maintained at a constant $\pm 5°$ until 2.5 seconds; at this time, the missile is pitched up to produce body lift. This motion induces an uncontrollable roll oscillation causing the run to be terminated at about five seconds. Roll rate and angle oscillations occur at about six cps. Pitch angle and rate, which appeared to be damping out at the end of the run, oscillated at about two cps.

## 7.4 GENERAL REMARKS AND CONCLUSIONS

### 7.4.1 Precautionary Note

In the preceding sections, only a single missile configuration and a selected number of control systems were investigated. Also, only a few flight paths were traced at near identical launch conditions. Caution, therefore, must be exercised in extending the results of these limited studies to configurations and control systems having substantially different characteristics. However, certain general truths have been revealed in these simulated flights; it is these that are reported on in the discussion that follows.

### 7.4.2 General Remarks and Discussion

(1) Flight path disturbances caused by missile roll appear to be the major trouble source for the missile system under study.

With the missile at near-zero angle of attack (during the first 2.0 seconds for the runs made here, missile rotation about all three axes can be controlled to reasonably small angles. Both of the roll control systems investigated (see Section 6.2) appeared to accomplish this task.

With the missile body angle of attack increased (for the wingless missile, this increase is mandatory for the production of lift), rolling accelerations tend to become very large, and if not properly kept under control can cause large flight path deviations. These large accelerations result from a combination of low $I_{xx}$ and induced rolling moments caused by yaw/roll coupling (pitch/roll coupling also can occur, but the simulation program of Appendix D does not quite include these terms). The control system that sensed both roll rate and displacement was able to cope with these large roll accelerations, provided that a yaw damping system was also employed. The state-of-the-art system that sensed only roll displacement lost control of the situation. This latter might be made to work if (a) the sampling rate (for roll error) were increased beyond the 20 per sec used, (b) the incremental aileron angle were made smaller than the $\pm 1.7°$ used, and (c) a roll rate gyro were used.

It appears, therefore, that if the missile is to fly at any appreciable body-angle of attack ( > 6°), some kind of roll rate sensor is needed plus some kind of yaw rate sensor and yaw producing aerodynamic surface. Although it was not simulated, a yaw rate sensor (or a lateral acceleration sensor) operating on the aileron surfaces may reduce roll at high body angles.

(2) For the "large" movable surfaces used in the proposed designs, aileron deflections required for control are very small--on the order of 0.1 degrees. While minutely small deflections ( $< 10^{-2}$ degrees) were possible in the hypothetical linear system used in the simulation, in a "real" system, real limits and tolerances exist. It is possible that a less sensitive system will work. This should be checked out in future runs. If such systems do not work, then smaller aerodynamic surfaces, having larger angular motions, may be required. Such small aerodynamic surfaces (of about one square inch in area) may pose a mechanical design problem. Larger, fixed surfaces will still be needed for static stability and for aerodynamic damping.

(3) The missile flight paths flown in Runs 1 through 4 appear to be satisfactory for the penetration aid task. The missile moves away from the carrier aircraft at a reasonable rate and keeps ahead and below or above it. With the sustainer motor/drag balance used, the missile remained ahead of the aircraft all the time (i.e., for 71 seconds). It is possible, by the proper choice of sustainer thrust to missile drag ratio, to make the missile fall behind--or to make a select number of missiles in a "volley" to fall behind, or pull ahead, of the launch aircraft.

The missile also dispersed to the side in a random manner; as noted in Section 3.4 (Item (4)) this is a desirable characteristic.

(4) The simple altitude-sensing pitch control system (see Section 6.4.1) appears to work very well. Although exact altitude is not maintained (see Figure 7.5), the near-eighty second phugoid oscillation might be cancelled out by a timed elevator deflection. As with roll surface deflections (see comment (1) above), elevator surface deflections required to maintain a given altitude will probably be very small.

(5) Although not readily evident in the chosen missile designs of Chapter 5, a small static margin has to be specified in pitch in order to provide high short period damping ratios. (The canard configuration of Section 5.4 was proposed as a possible solution to this modest-damping/low-static-margin problem.) Such a combination produces a low short period pitch frequency and makes the pitch and yaw moment/angle derivatives ($C_{m_\alpha}$ and $C_{n_\beta}$) very sensative functions of body aerodynamics and body c.g. position. Hence, slight "manufacturing" variations in either missile shape or weight could cause the missile to become unstable in the short period or Dutch Roll modes. The runs made here did not illustrate this phenomenon because the proper static margins were maintained throughout the flight.

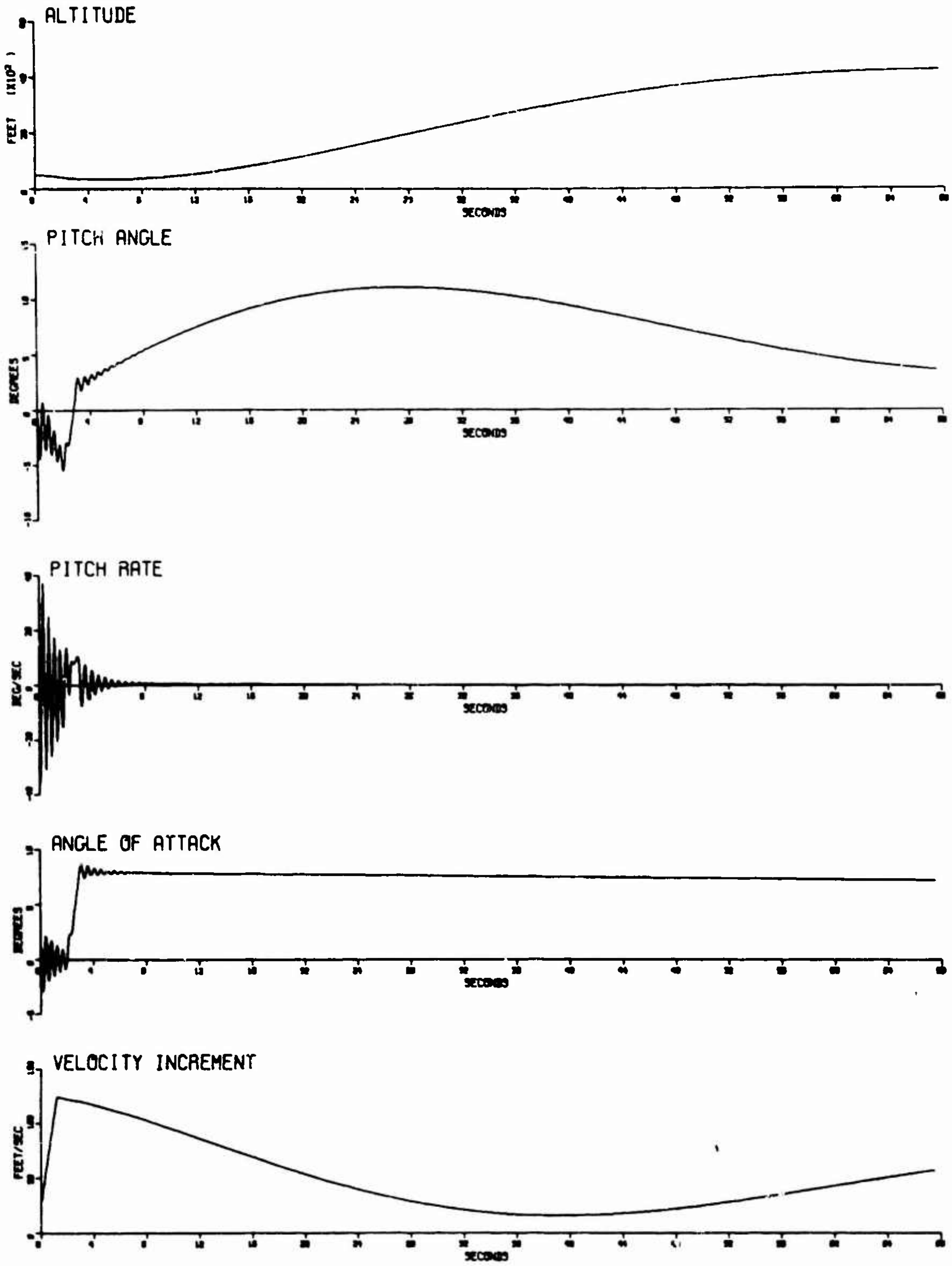


Figure 7.2a RUN 1, TIME HISTORY OF PARAMETERS

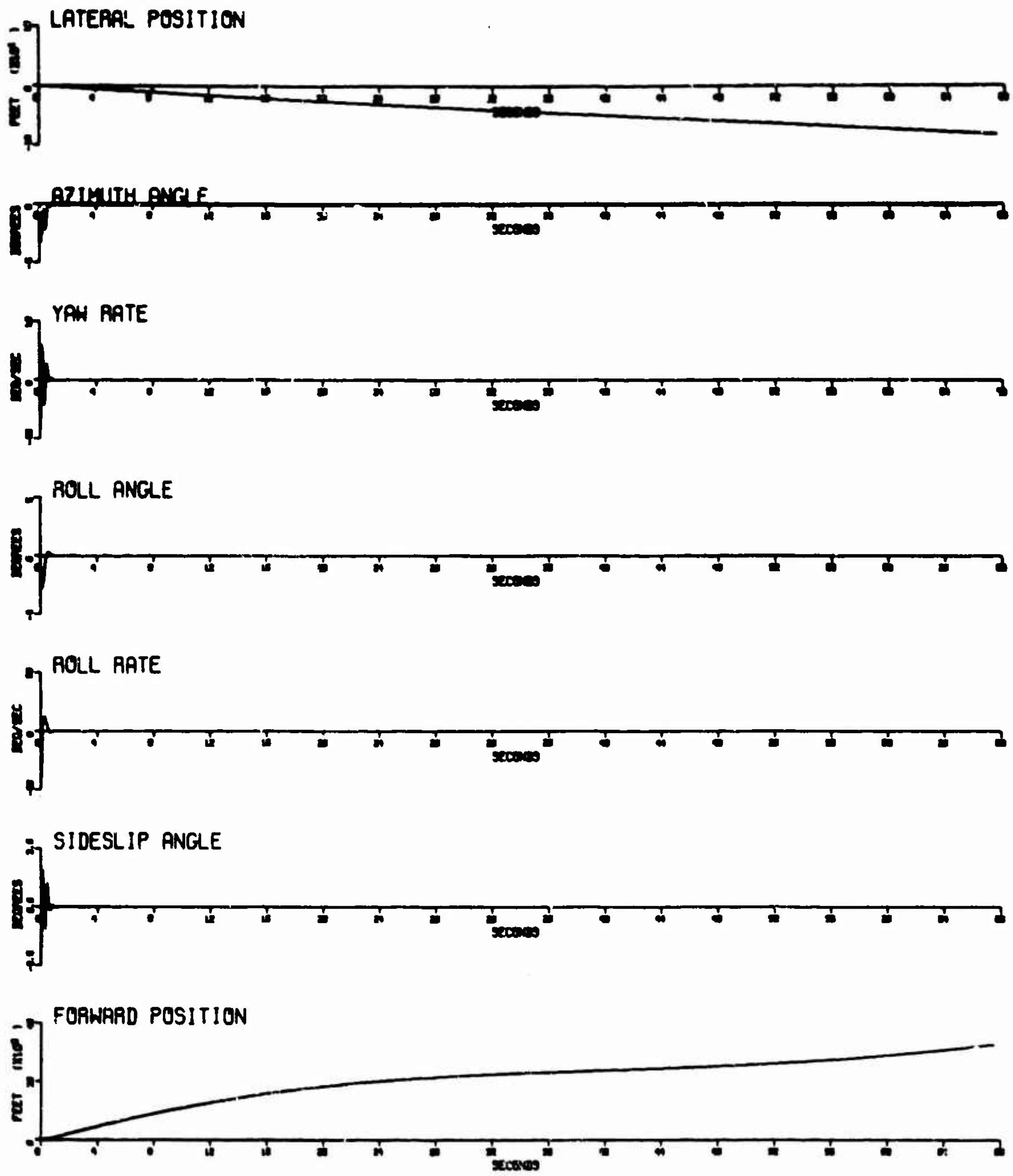


Figure 7.2b RUN 1, TIME HISTORY OF PARAMETERS (Cont.)

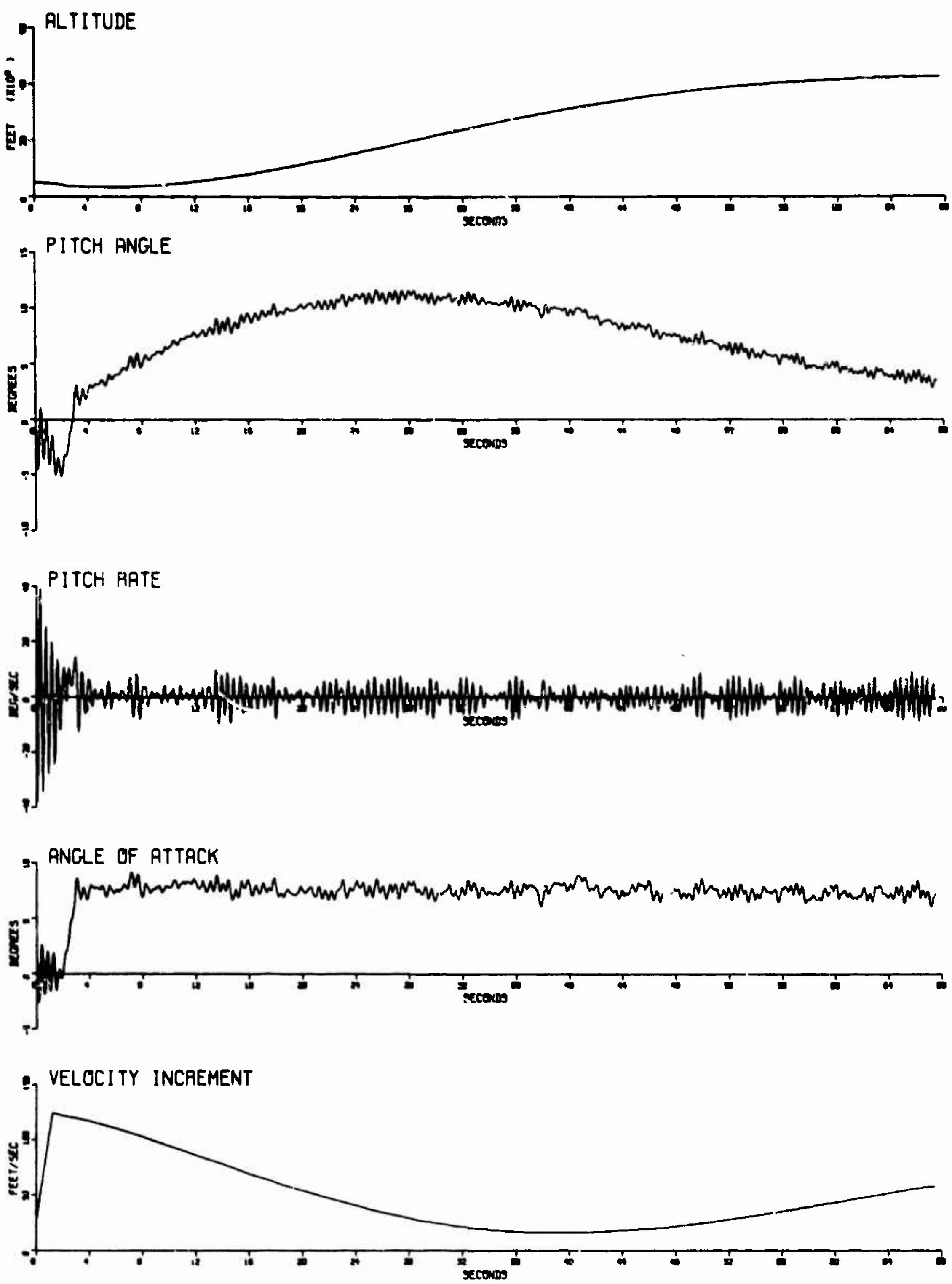


Figure 7.3a RUN 2, TIME HISTORY OF PARAMETERS

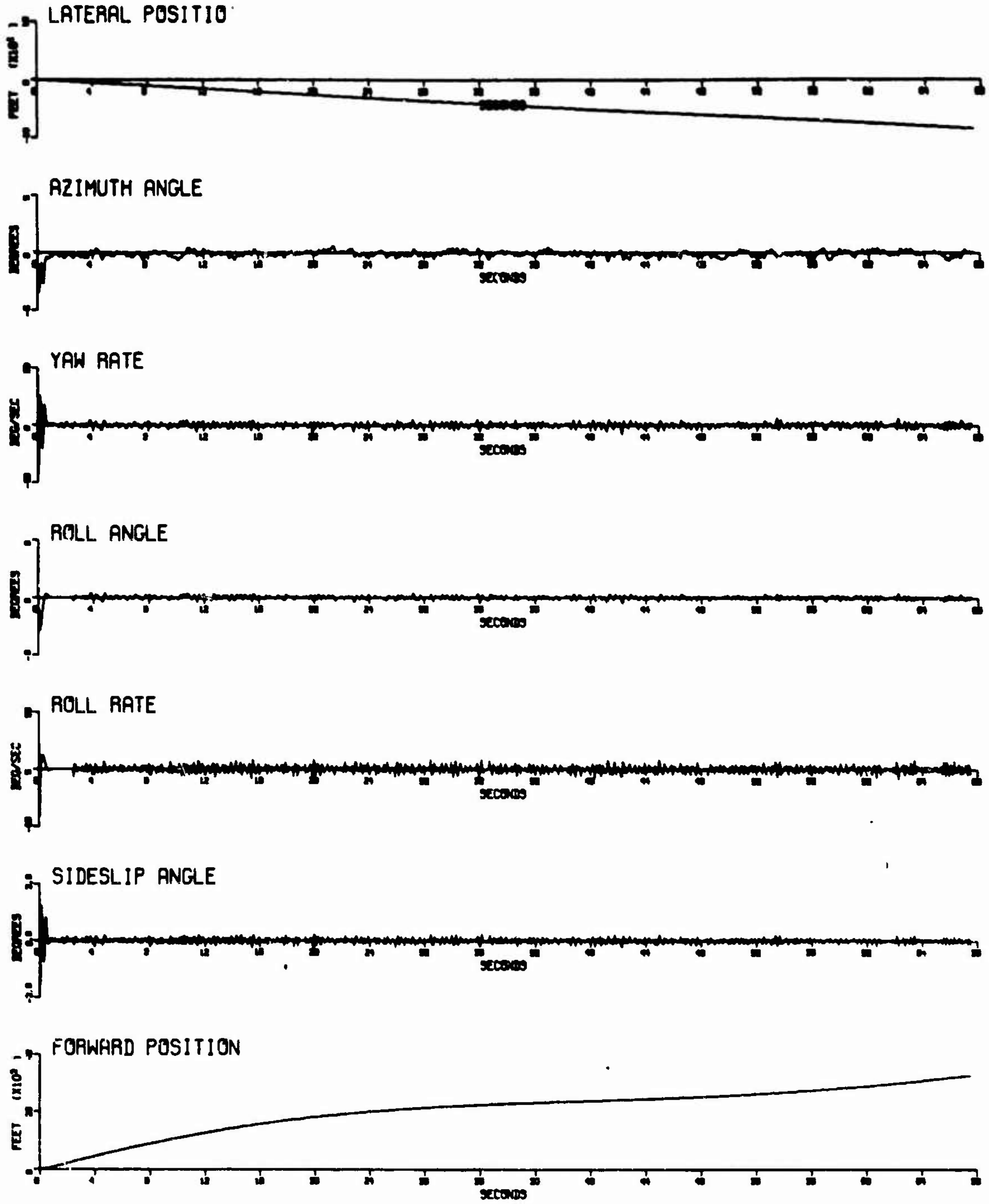


Figure 7.3b RUN 2, TIME HISTORY OF PARAMETERS (Cont.)

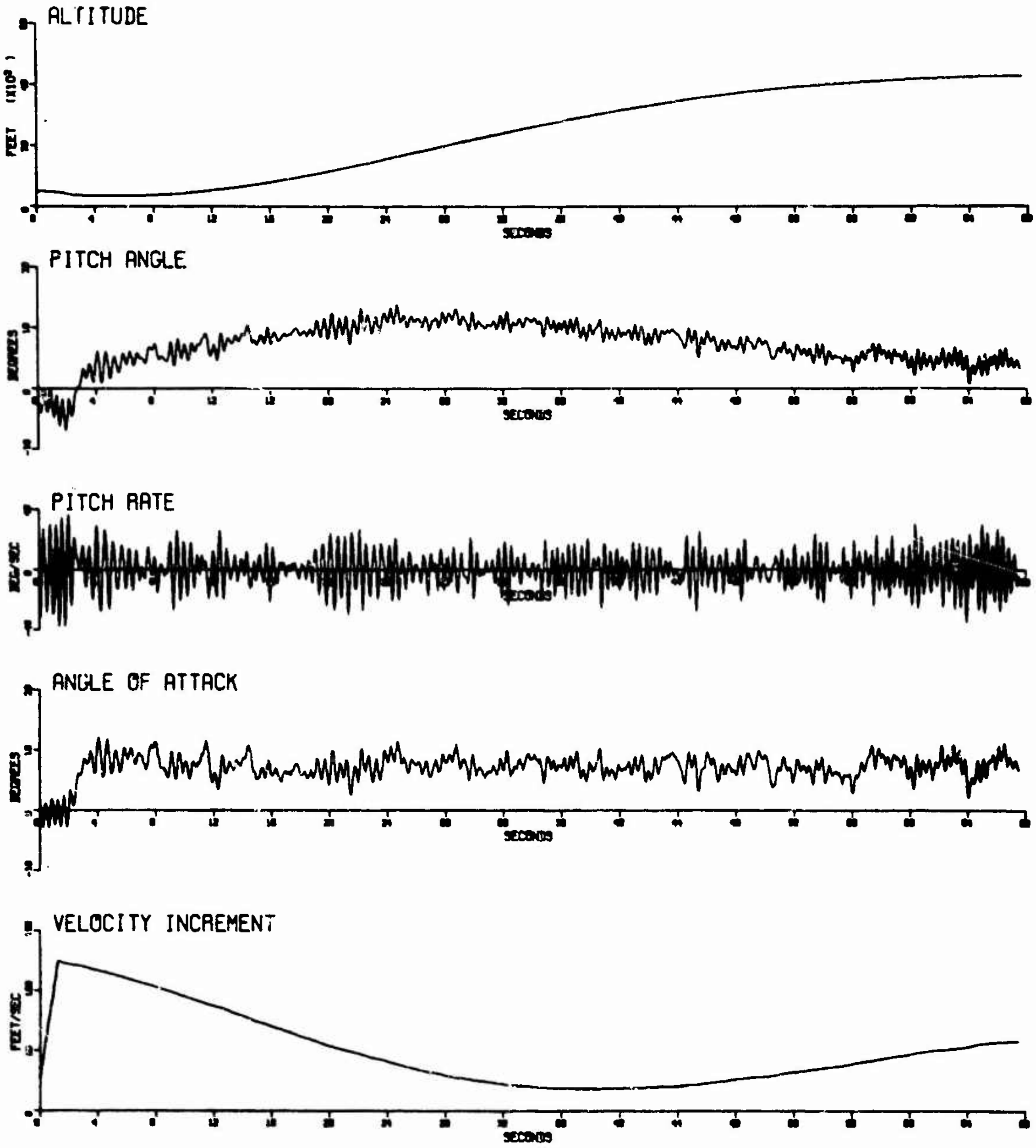


Figure 7.4a RUN 3, TIME HISTORY OF PARAMETERS

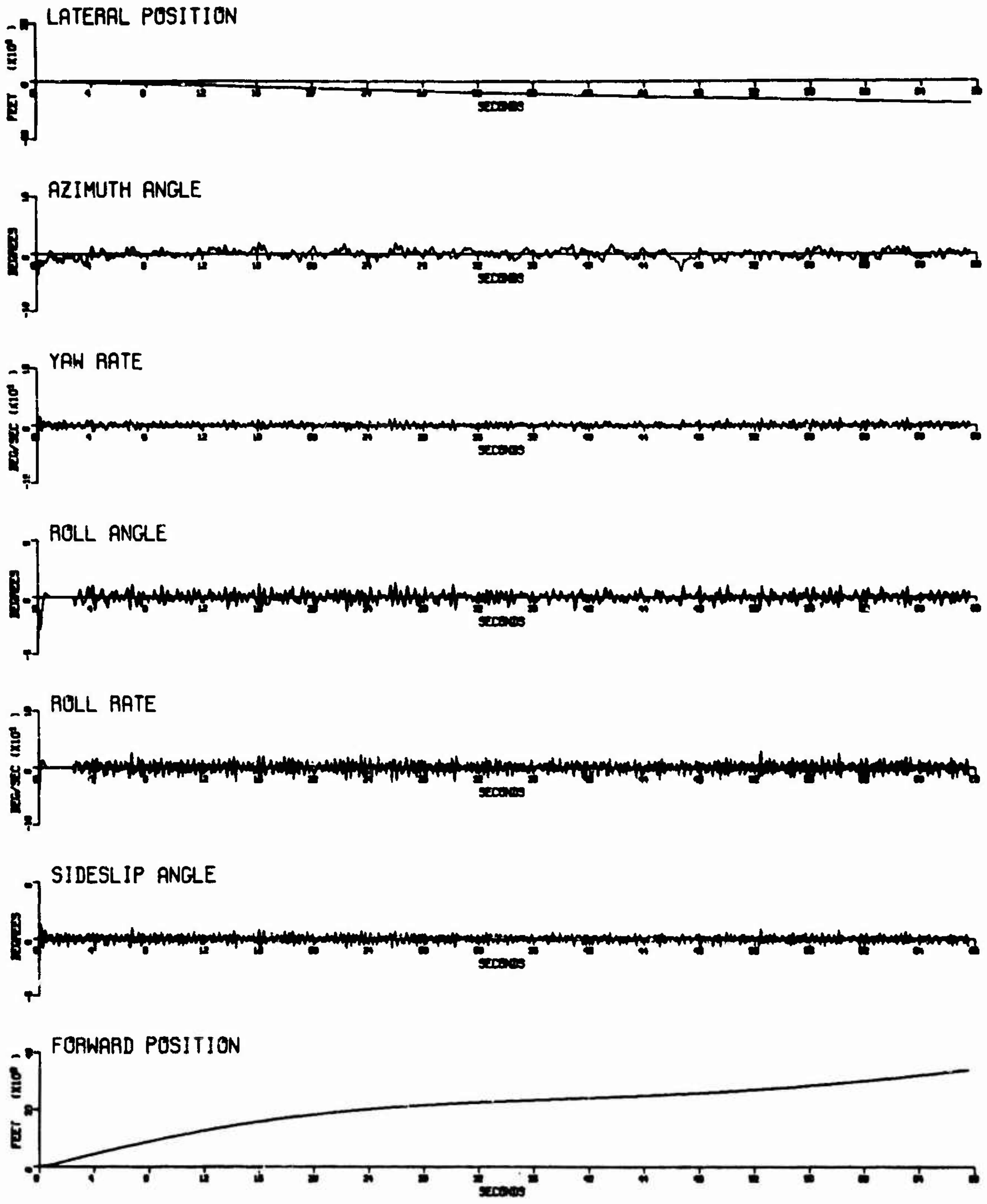


Figure 7.4b RUN 3, TIME HISTORY OF PARAMETERS (Cont.)

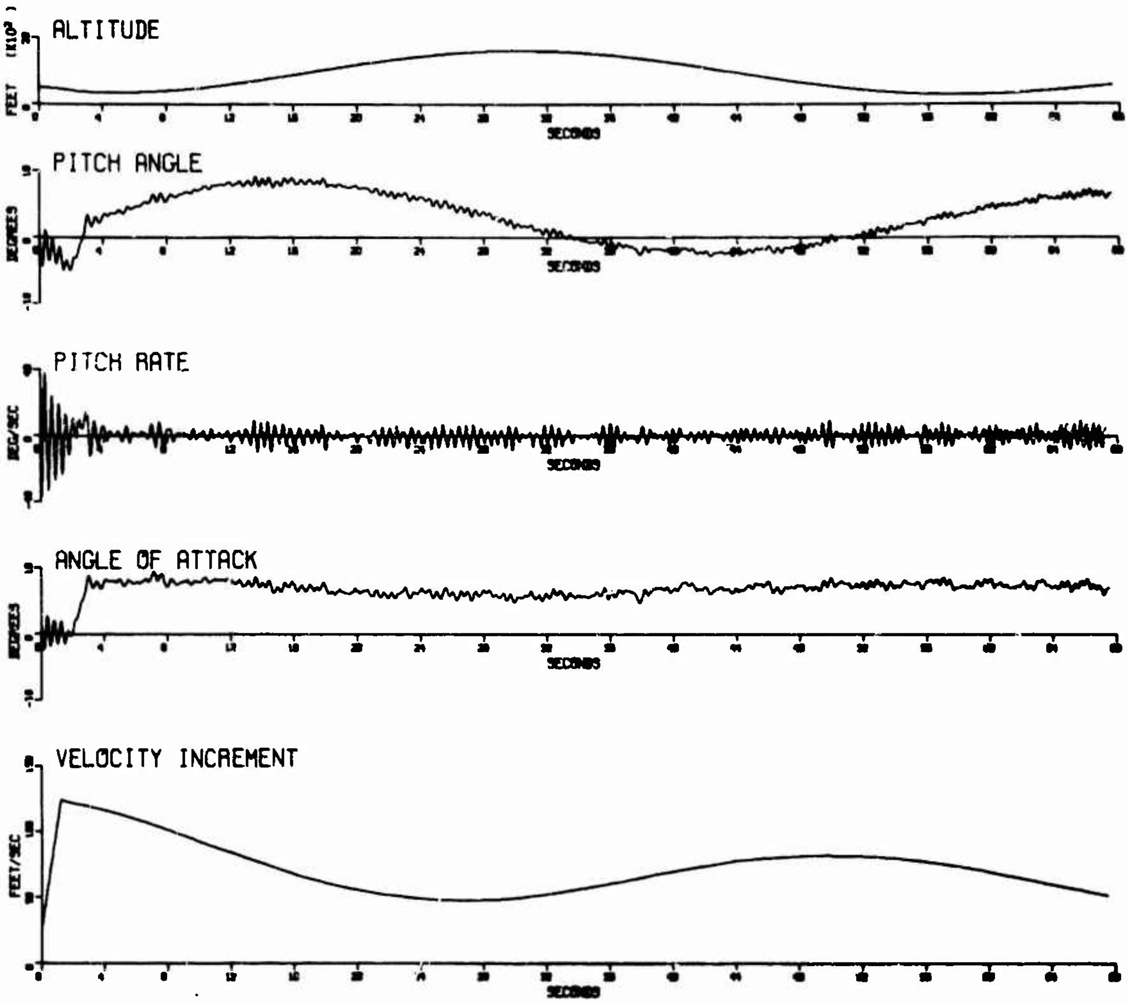


Figure 7.5a RUN 4, TIME HISTORY OF PARAMETERS

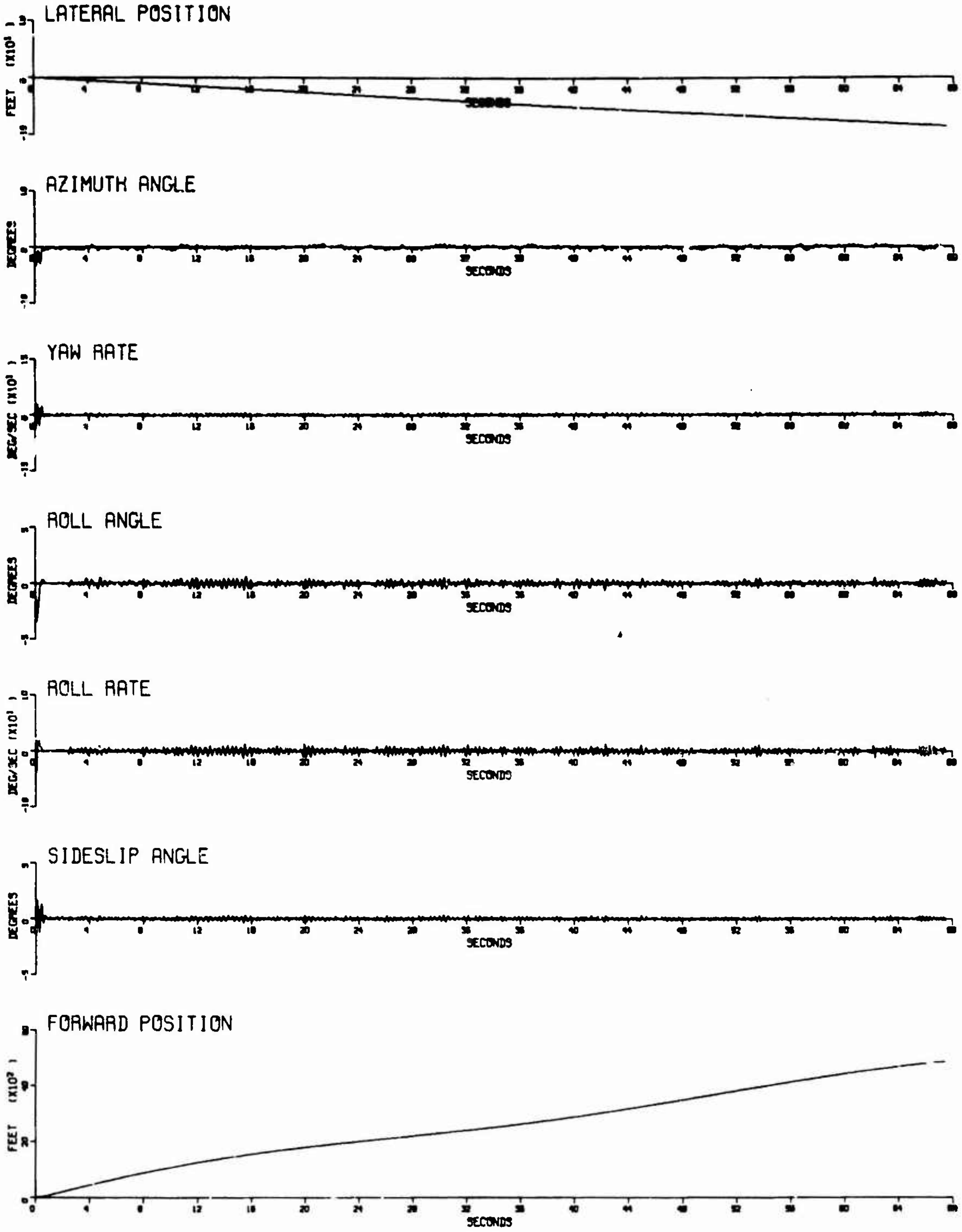


Figure 7.5b RUN 4, TIME HISTORY OF PARAMETERS (Cont.)

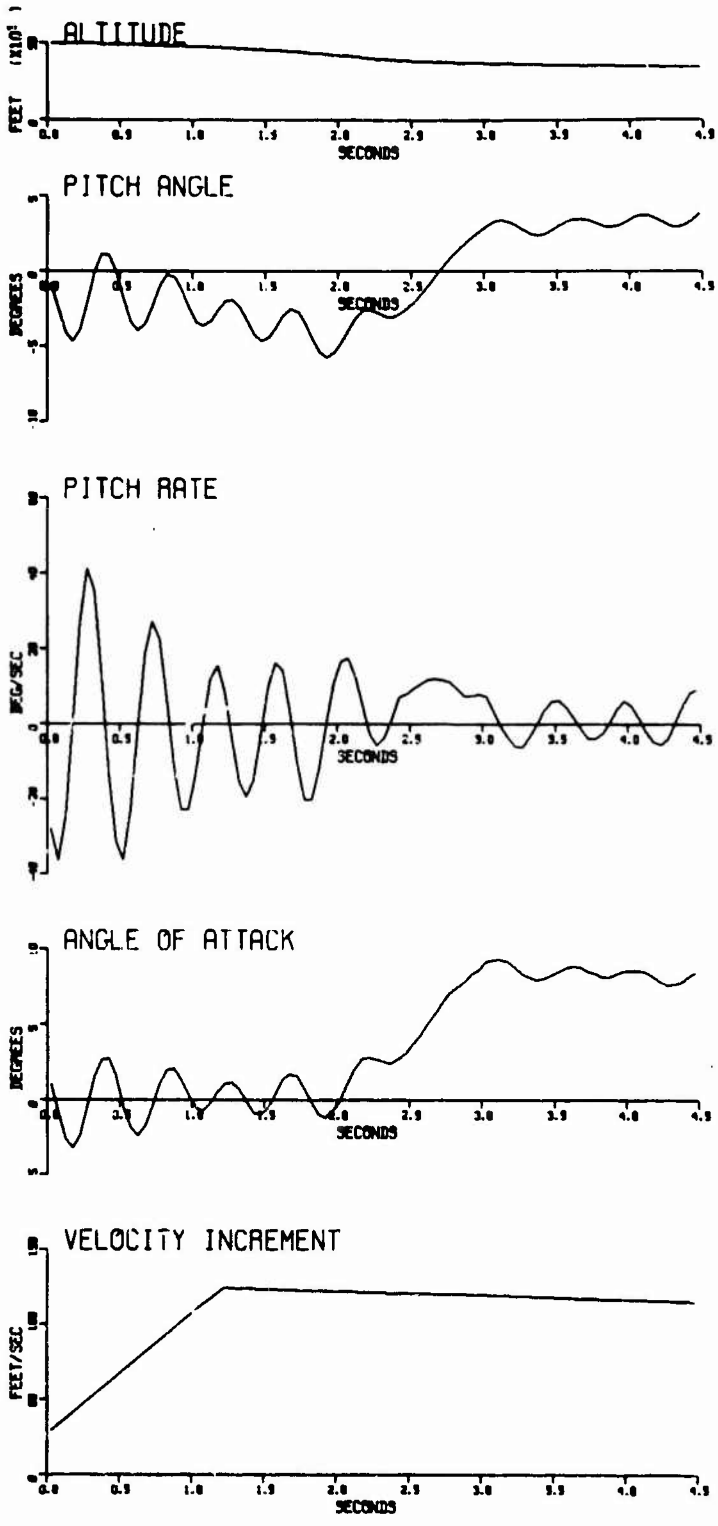


Figure 7.6a RUN 5, TIME HISTORY OF PARAMETERS

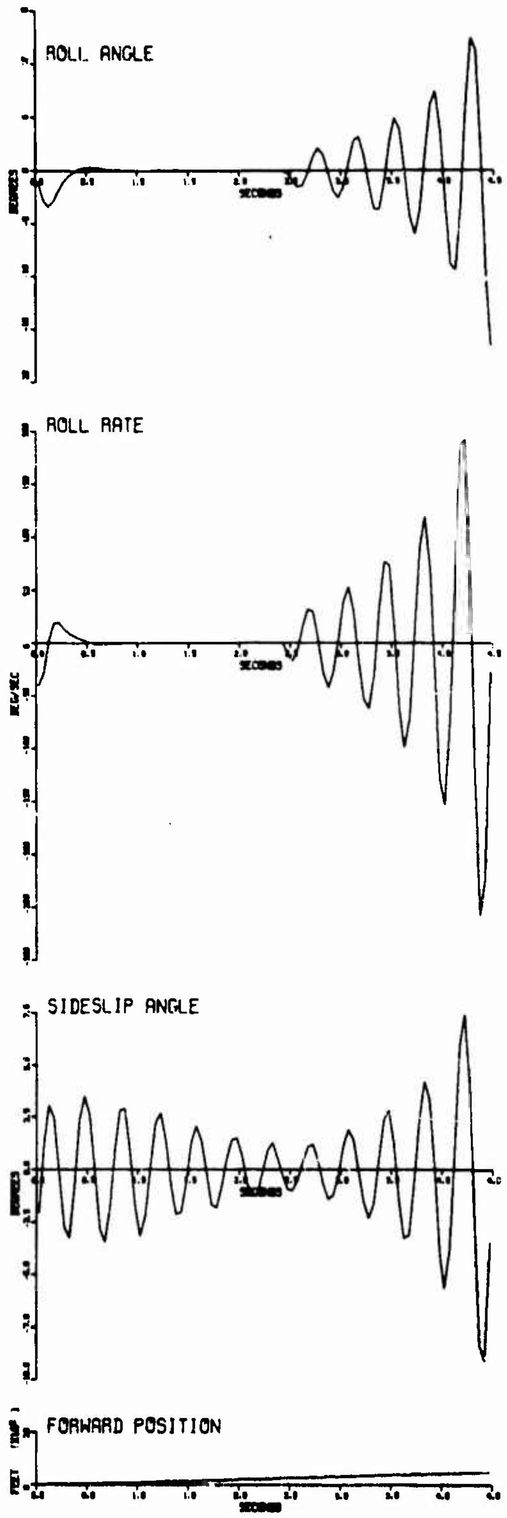


Figure 7.6b RUN 5, TIME HISTORY OF PARAMETERS (Cont.)

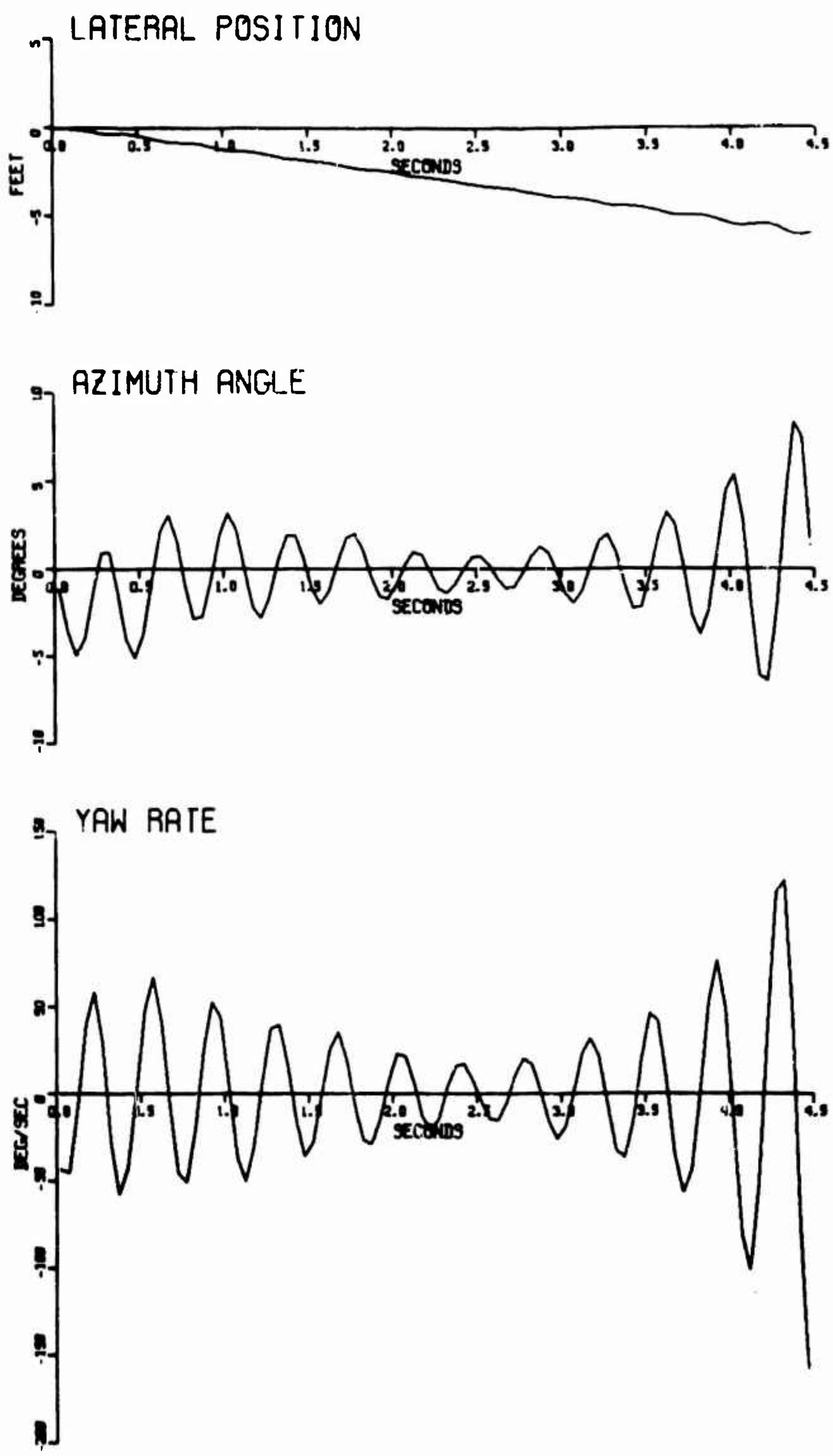


Figure 7.6c RUN 5, TIME HISTORY OF PARAMETERS (Cont.)

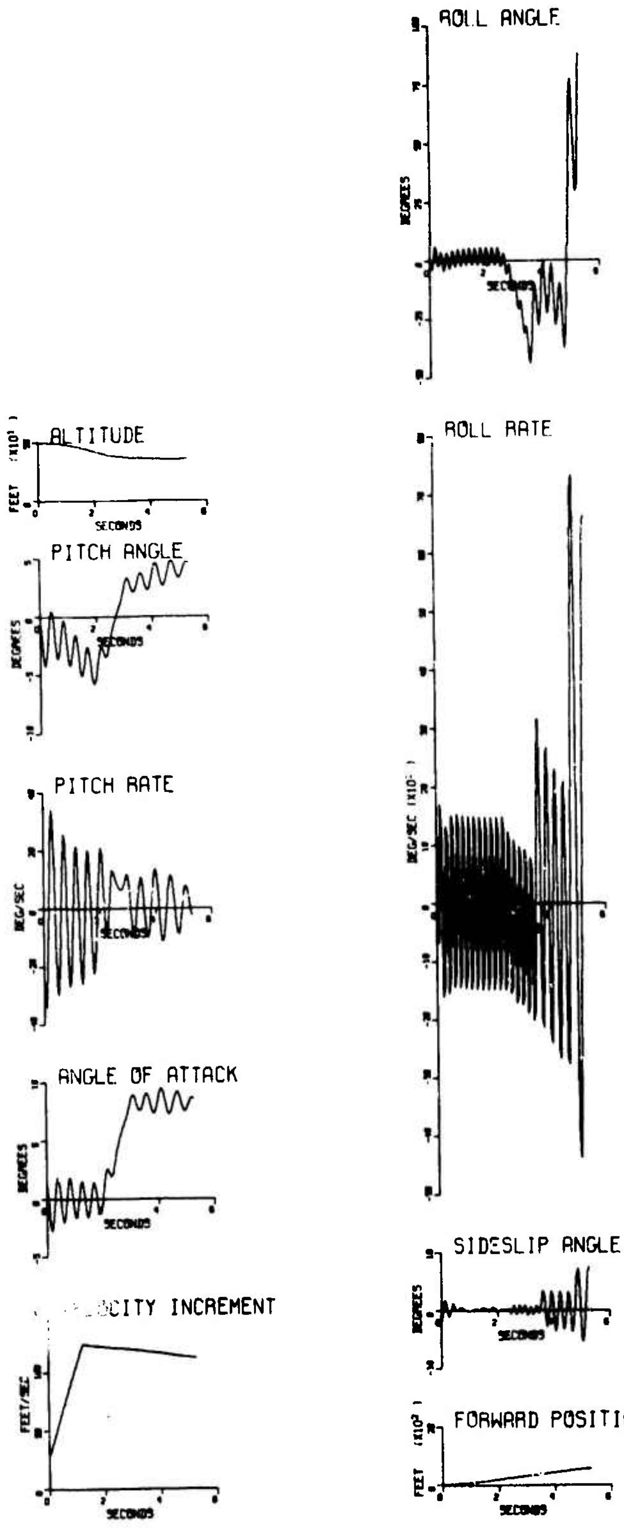


**Figure 7.7a RUN 6, TIME HISTORY OF PARAMETERS**

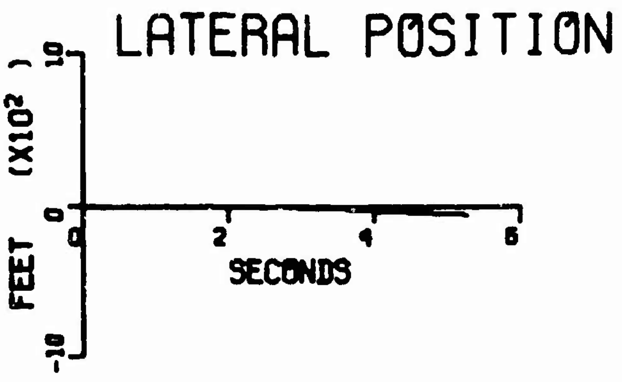


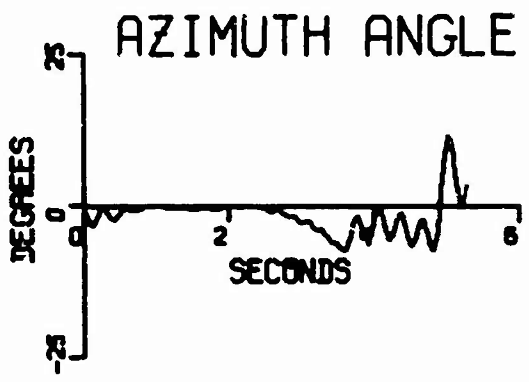


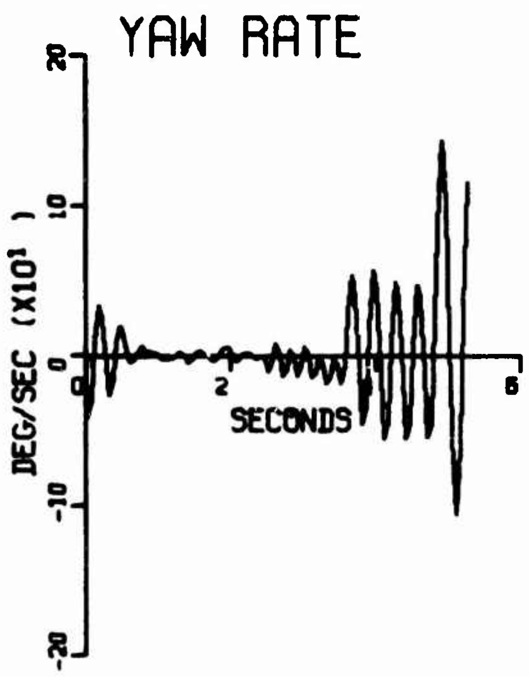


Figure 7.7b RUN 6, TIME HISTORY OF PARAMETERS (Cont.)

# 8. RESULTS AND CONCLUSIONS

## 8.1 GENERAL RESULTS AND CONCLUSIONS

It is concluded that an air-launched, low altitude, subsonic cruise missile capable of being launched from a tactical aircraft and capable of carrying a modest ECM payload (about 16 pounds) is both aerodynamically and mechanically feasible.

For a near-seventy second flight time, a 2.75 inch diameter configuration will weigh about 28 pounds and will be about 70 inches long. It will require both a booster motor, to separate it from the launch aircraft, and a sustainer motor, to maintain near-constant velocity.

An on-board roll control system is mandatory; pitch and yaw control may be needed depending upon the kind of configuration chosen and the shape of the flight path required.

If the missile is to be launched from a pod, then deployable aerodynamic surfaces are required. It is desirable that these surfaces be arranged symmetrically and that they be deployed in a symmetrical manner. Two symmetrical (in cruise) vehicle configurations that appear to merit further consideration are: the wingless missile (with all-movable horizontal and vertical tail surfaces), and the winged missile configuration (with all-movable horizontal tails and fixed vertical stabilizers).

More detailed results and conclusions are given in the two sections that follow.

## 8.2 MISSILE FLIGHT PATH CONTROL SYSTEM

(1) Missile roll, caused by low roll moment of inertia, $I_{xx}$, is the source of most of the problems in control system design. Even small disturbing forces tend to produce large rolling accelerations.

(2) The largest external disturbance to the missile is produced by the flow field surrounding the launch aircraft. Disturbances

caused by a gusty atmosphere are relatively moderate--for the wingless missile configuration examined here.

(3) Where body angles of attack exceeding about six degrees are required (as, for example, on a wingless missile in cruise), yaw/roll and pitch/roll cross coupling will induce large rolling moments. These moments place added demands upon the roll control system and, unless a yaw damping system is employed, cause the missile to go out of control.

(4) A roll control system that deflects ailerons as a linear function of both roll rate and roll deflection can control the missile throughout its entire launch-cruise history. However, if the missile body is elevated to modest angles of attack (see comment (3) above), a yaw damper will be required. If all-movable tail surfaces are used, the required control surface deflections become very small (about 0.1 degree). Such small deflections may pose design problems.

(5) A roll control system that employs a d.c. stepping motor and senses only roll displacement may work at near-zero body angles of attack; however, such a system provides little roll damping. For the one run made here, this kind of a system was not able to control the missile when body angles exceeded a few degrees. It is possible, however, that if a faster error sampling rate, a smaller aileron step, and a rate sensing gyro were used, this system could be made to work.

(6) A pitch control system utilizing an altitude-change sensor appears to be capable of maintaining a near-constant altitude flight path. Only the phugoid undulation remains--and this might be cancelled by programming pitch control as a function of time. For the all-movable elevators used in this study, very small surface deflections were needed for control.

(7) A yaw control system employing yaw rate and yaw displacement sensors is capable of stabilizing the missile laterally when combined with the roll control system described in (4) above. This yaw system requires movable vertical tail surfaces. Although not investigated, a system employing a yaw rate sensor (or a lateral acceleration sensor) coupled to the aileron surfaces might also provide the proper amount of yaw damping.

## 8.3 CONFIGURATION

(1) The wingless missile appears to be the simplest configuration concept. However, because it requires that the body be set at an angle of attack in cruise, a yaw damping system may be required (see comment 8.2 (4) above).

(2) A winged configuration (either single-pivot, or double-pivot split wing) deserves further consideration. Although somewhat more complicated than the wingless missile, the winged configuration might be able to operate with only elevator/aileron control (i.e., with a fixed vertical tail surface). Whether the wing should be constructed in one or two sections--and deployed unsymmetrically or symmetrically deserves more detailed study.

(3) Because only tube launched missiles were considered here, no conclusions can be drawn concerning configurations with non-deployable aerodynamic surfaces. Such configurations are inherently more simple, mechanically, then ones requiring deployable surfaces.

# 9. RECOMMENDATIONS FOR FUTURE WORK

## 9.1 GENERAL RECOMMENDATIONS

Investigations should be continued, both analytically and on the flight path simulator, on both the wingless body and a winged configuration. Flight path control systems, especially the roll system, should be more precisely defined and the effect of system errors should be explored. In addition, launches at other than optimum conditions should be made.

## 9.2 DETAILED RECOMMENDATIONS

(1) The two roll control systems defined in this study should be further explored.

(a) With the rate/deflection sensing system, larger gains should be examined to obtain more reasonable (i.e., larger) control surface deflections. A more thorough investigation into available "hardware", real system effects (e.g., noise, threshold cutoffs, etc.) should be made.

(b) With the d.c. stepping motor system, the effect of using smaller sampling times, and smaller aileron deflection steps, should be examined. Also, a system using a roll deflection plus a roll rate sensor should be explored.

(2) The yaw system should be checked to determine if it is needed on a winged missile. Also, the system employing yaw rate (or lateral acceleration) feedback to the aileron control should be examined.

(3) The use of a time dependent pitch control (to cancel the phugoid) should be checked in conjunction with the altitude error sensing pitch system.

(4) The effects of manufacturing tolerances and system errors on control surface deflections, and the effects of missile weight and center of gravity position variations should be investigated. Flight path perturbations due to these variables should be determined.

(5) The randomness required of flight paths (to deceive the aircraft-tracking radar) and the randomness obtained by system errors, tolerances, gusts, etc. should be obtained and compared.

(6) The effects of adjustable propulsion thrust schedules on flight path and missile/airplane separation should be examined. Techniques for varying thrust schedules in a "random" (but predictable) manner should be explored.

(7) The relative advantages of a one piece wing (with a single pivot) and a split wing (with a double pivot) should be explored in more detail.

## 10. REFERENCES


1. Dahm, D. B., "Analysis and Evaluation of Tactical Penetration Aids: Decoy Rocket and Trackbreak Rocket Analysis (U)," Interim Progress Report, CAL Report No. UM-1963-E-SS 4, July 1965, SECRET.

2. Tosti, L. P., "Low-Speed Static Stability and Damping-In-Roll Characteristics of Some Swept and Unswept Low-Aspect-Ratio Wings," NACA TN 1468, October 1947.

3. Rogallo, F. M., Lowry, J. G., Croom, D. R., and Taylor, R. T., "Preliminary Investigation of a Paraglider," NASA TN D443, August 1960.

4. Abbott, J. H. and Von Doenhoff, A. E., "Theory of Wing Sections," Dover Publications, Inc., New York, New York, 1959.

5. Von Mises, R., "Theory of Flight," Dover Publications, Inc., New York, New York, 1959.

6. Gauzza, H. J., "Static Stability Test of 18, 22, and 26 Caliber Ogive Bodies of Revolution at Mach Numbers from 0.49 to 3.22 (U)," NAVORD Report 4242, Aeroballistic Research Report 335, 23 July 1956, Confidential.

7. Zucrow, M. J., "Aircraft and Missile Propulsion," Vol. II, John Wiley and Sons, Inc., New York, London, 1958.

8. Kuo, B. C., "Automatic Control Systems," Prentice Hall, 1962.

9. Thielen, J. A., "Aerodynamic Study of Missile-Aircraft Compatibility, Report 4, Induced Flow Field Around a Subsonic Wing-Body," Sperry Report No. 4283-1507-4I.

10. Alford, W. J. and King, T. J., "Experimental Investigation of Flow Fields at Zero Sideslip near Swept and Unswept Wing-Fuselage Combinations at Low Speed," NACA RM L56J19.

11. Anon, "Solid Propellant Manual," CPIA/M2 (U) Solid Propellant Information Agency, Applied Physics Lab., The Johns Hopkins University, Confidential.

12. Etkin, B., "Dynamics of Flight," John Wiley & Sons, Inc., New York, 1959.

# APPENDIX A
# DEFINITION OF FLOW FIELD ABOUT CARRIER AIRCRAFT

## A.1 INTRODUCTION

### A.1.1 Statement of the Problem

Because the penetration aid missile will be launched from beneath the wing of a lifting (and possibly maneuvering) airplane, it will be immersed in the flow field induced by that airplane. Such a flow field generates forces and moments on the missile that tend to perturb its motion. If the missile does not have adequate dynamic stability characteristics (either inherent or artificial), its flight path may be so altered by these perturbations as to make the missile useless as a decoy or trackbreaker. It is necessary, therefore, to obtain a correct definition of the flow field surrounding the carrier aircraft.

### A.1.2 Method of Approach

This appendix presents a method for computing the geometry of a non-uniform flow field induced by the wing-fuselage of a typical fighter aircraft. The aircraft is assumed to be in constant-velocity flight (i.e., non maneuvering), to be right side up, and to be travelling on an essentially level path.

The missile is assumed to be launched in a vertical plane a distance $y$ outboard of and parallel to the airplane's plane of symmetry. Mathematical expressions are determined for upwash and sidewash velocities as a function of fore-aft position, $x$. To account for lateral dispersion of the missile, expressions are also derived for variation of upwash and sidewash with displacement, $\Delta y$, to the left or right of the initial $y$ position.

An additional analysis is made to account for the spatial (and time) variation of flow along the length and width of the missile--the missile being "large" relative to the dimensions of the non uniform flow field.

## A.2 FLOW FIELD DEFINITION

The velocity perturbation field in the region in front of the leading edge of the wing of a subsonic launch aircraft has been investigated both analytically and experimentally. Reference 9 details a method for computing this field, given the geometry of the wing and information on the fuselage. Reference 10 gives results of wind tunnel tests at low subsonic speeds with a swept-wing-fuselage combination. The geometry of this model, as well as the geometries of two prospective launch aircraft, the F-105 and the F-4C, are presented in Table A.1 below. Note that the model characteristics resemble the F-105 more closely than the F-4C. In the following discussion, primary attention is given to the F-105 rather than the F-4C, but the results apply in a qualitative form to the F-4C as well.

TABLE A.1

COMPARISON OF GEOMETRY OF MODEL TO ACTUAL LAUNCH AIRCRAFT

| Aircraft | Wing Aspect Ratio, $AR$ | Wing Taper Ratio, $\lambda$ | Sweep Angle $\Lambda$ at Quarter-Chord |
|---|---|---|---|
| Wind Tunnel Test Model Ref. (10) | 4.00 | 0.300 | 45° |
| F-105 | 3.18 | 0.467 | 45° |
| F-4C | 2.82 | 0.167 | 45° |

In this study, the experimental data rather than the analytic method of computing the flow field has been used. The latter method, outlined in Ref. 9, is cumbersome at best, requiring a large digital program. Further, it gives results which are believed to be less accurate than the experimental data.

For the wind-tunnel tests, the model tested had no pylons or pods underneath the wings, and since probes were used, the disturbance of the induced flow field by the missile itself was not considered. These secondary effects are not important, however, except in the region directly in front of

the launch tube. In this region the missile is constrained by the launch tube, so neglect of these secondary interactions should cause negligible error in the calculated trajectory (see Figure A. 1).

In Ref. 10, the induced flow field is investigated for zero sideslip and for various angles of attack of the launch vehicle. Because it is assumed the missile will be launched when the aircraft is in straight and level flight ($\beta = 0$), the nominal angle of attack ($\alpha_{nom} = \alpha_{trim} - \alpha_{zero\ lift}$) $\cong 3.32°$ for the F-105. The inboard pylon on the F-105 is 10 ft, 9 in. outboard from the aircraft's centerline, and the forward tip of the uncapped pod is 22 inches ahead of the wing's leading edge and 30 inches below the mean chord (see Figure A. 1).

Because loading conditions on the missile are more severe at the inboard pylon, it, rather than the outboard pylon, has been used for the calculations.

By appropriate normalization and interpolation, the above dimensions specify the field locations to be used in Ref. 10. In that reference, these upwash and sidewash distributions are expressed as $\alpha_e(x)$, $\beta_e(x)$, the local angles of attack and sideslip. It can be shown that

$$w'(x) = \frac{w(\ )}{Vo} = \sin(\alpha_e(x) - \alpha_{nom}) \approx \alpha_e(x) - \alpha_{nom} \qquad v'(x) = \frac{v(x)}{Vo} = \sin \beta_e(x) \approx \beta_e(x)$$

for small $\alpha_e$, $\beta_e$. $w'(x)$ is the upwash velocity, $w(x)$, normalized by Vo, the free stream velocity. Similarly $v'(x)$ is the normalized sidewash velocity.

In general, $w' = w'(x, y, z)$ and $v' = v'(x, y, z)$ where the x-y-z coordinate system is given in Figure A. 1, with the origin at the pod tip. These are body axes of the launch aircraft, with the x- and y- axes in the horizon plane, and the z- axis aligned with the gravitational field. The y-axis is perpendicular to the aircraft's plane of symmetry. The coordinate system is assumed to be inertial because of the uniform motion of the aircraft. Because the missile travels primarily along the x- axis and suffers very

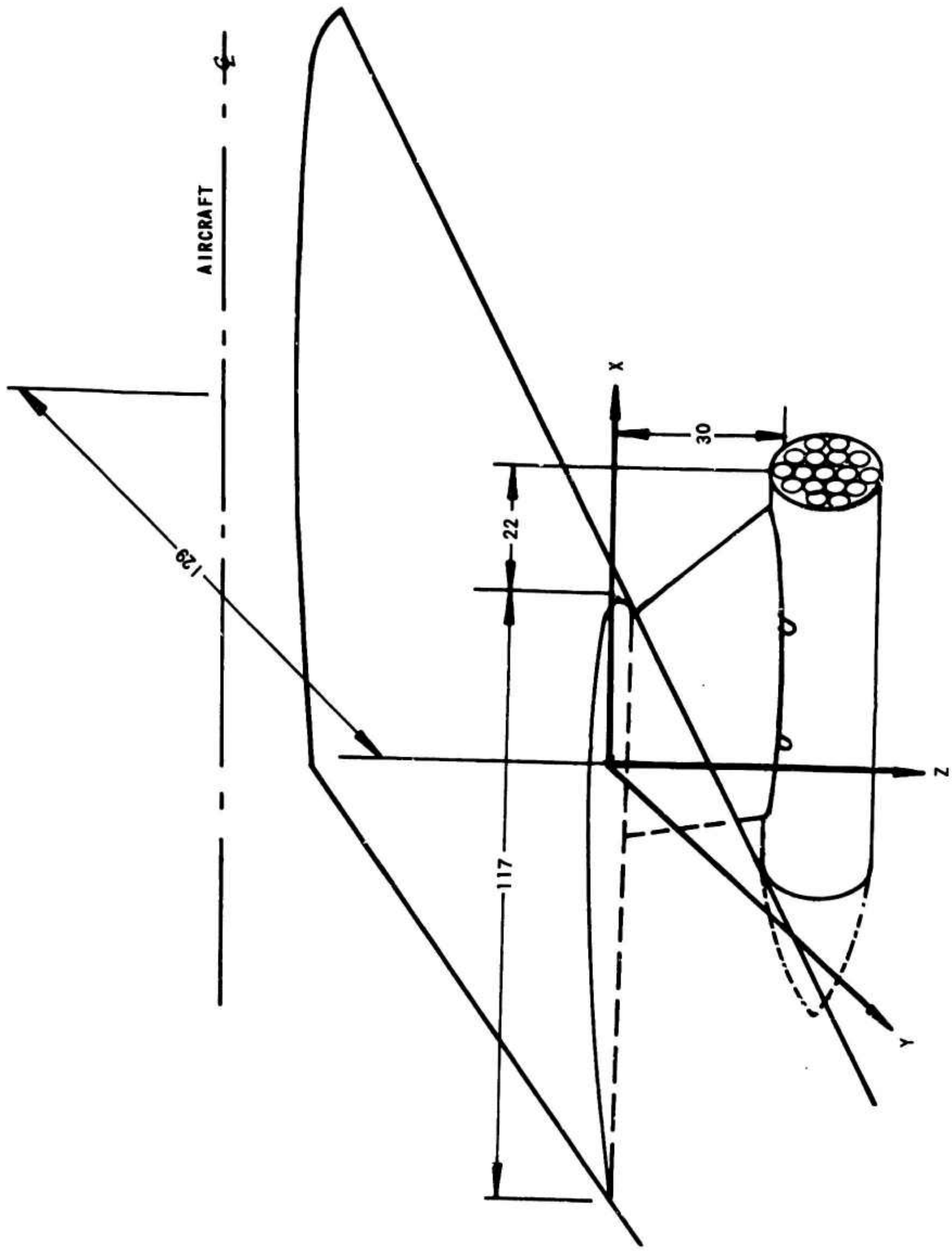


Figure A.1 MISSILE POD LOCATION ON F-105 (SCHEMATIC)

little displacement in the y- and z- directions during the time it is in the vicinity of the launch aircraft, it is the x- variation of $w'$ and $v'$ that is of principal interest. For the F-105 airplane, the wing span $b = 35.0$ ft and the mean aerodynamic chord $c = 9.8$ ft. Hence for the launch pod position ( $y = 10.8$ ft, $z = 2.5$ ft), the non-dimensional location is:
$y/(b/2) = .616$, $z/c = .255$.

Upwash and sidewash distributions were obtained from Ref. 10 (by interpolation) at the above locations. These distributions are plotted as the solid curves in Figures A.2 and A.3. Note that the sidewash perturbation exists for large distances upstream due to the presence of the fuselage.

Also noted on these Figures are analytical approximations to the experimental curves (broken lines). For the sidewash, the expressions are:

$$\left.\begin{aligned} v' &= 0.24 + 0.040\, e^{-0.458\, x} + 0.006 \sin(0.483\, x + .896) && \text{for } x \leq 21.5 \\ v' &= 0.0183\, e^{-0.110\,(x-21.5)} && \text{for } x > 21.5 \end{aligned}\right\} \qquad (A.1)$$

For upwash the expression is

$$w' = 0.036\, e^{-0.110\, x} \qquad \text{for all } x \qquad (A.2)$$

It is the above expressions that are used as inputs to the computer program.

The expressions given in Equations (A. 1) and (A. 2) hold true only at wing station $y/(b/2) = .616$ and at height $z/c = .255$. If the missile moves inboard or outboard of this sstation, or above or below this level, the above equations should be modified. Because the missile is expected to be perturbed only slightly from its original line of flight, small corrections are made to the above equations to account for these motions.

The spanwise (y direction) variation of upwash given in Ref. 10 is sufficiently detailed to permit calculations to be made in the change of $w'$ with y. Values of $w'/\Delta y$ were computed using span station $y/(b/2) = .616$ as a reference. Results are plotted in Figure A.4.

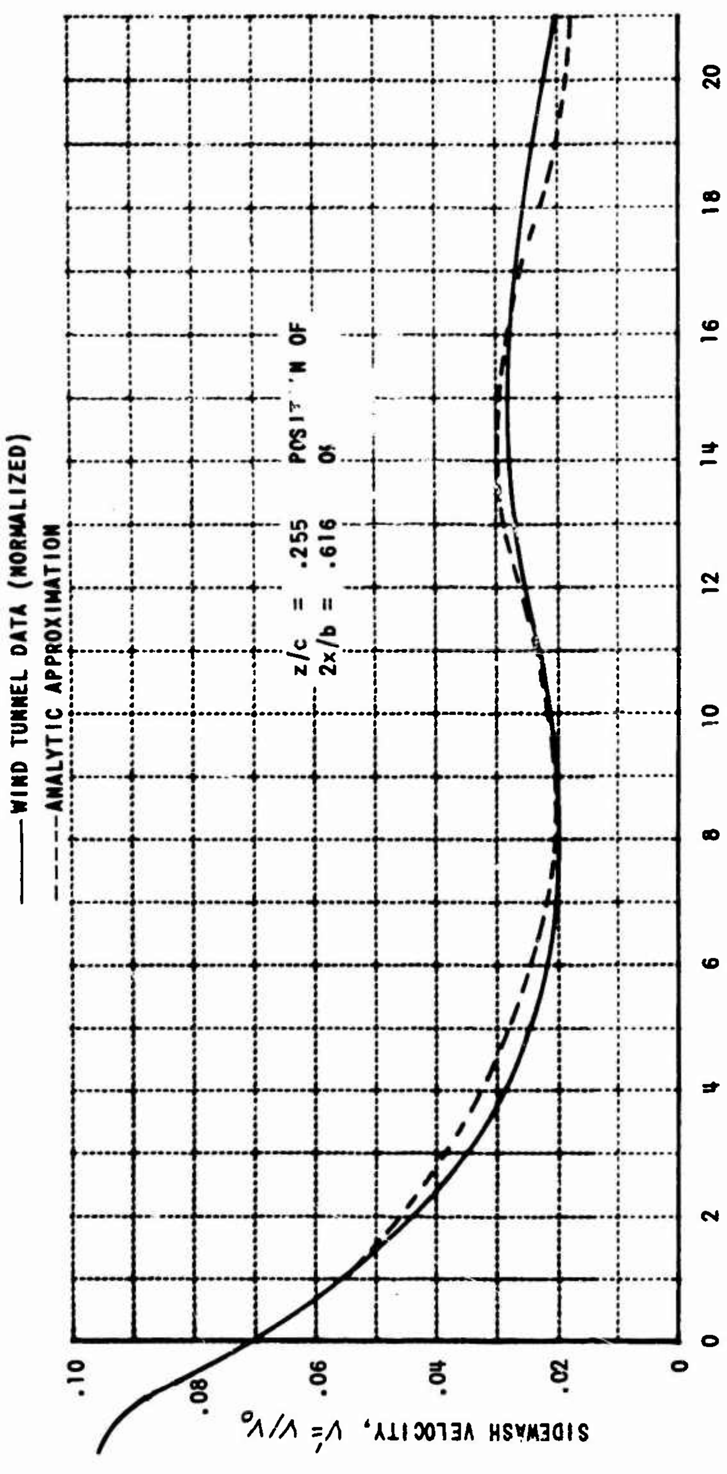


Figure A.2 X VARIATION OF SIDEWASH

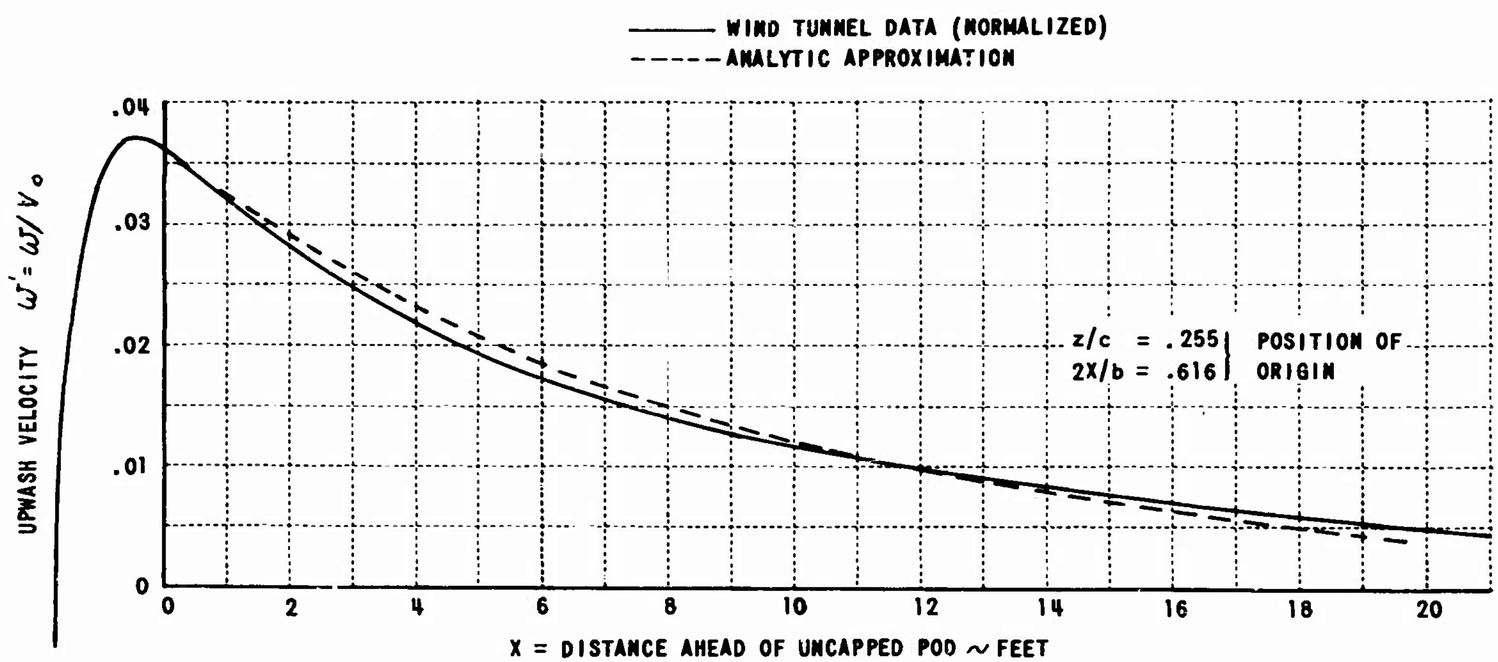


Figure A.3 X VARIATION OF UPWASH

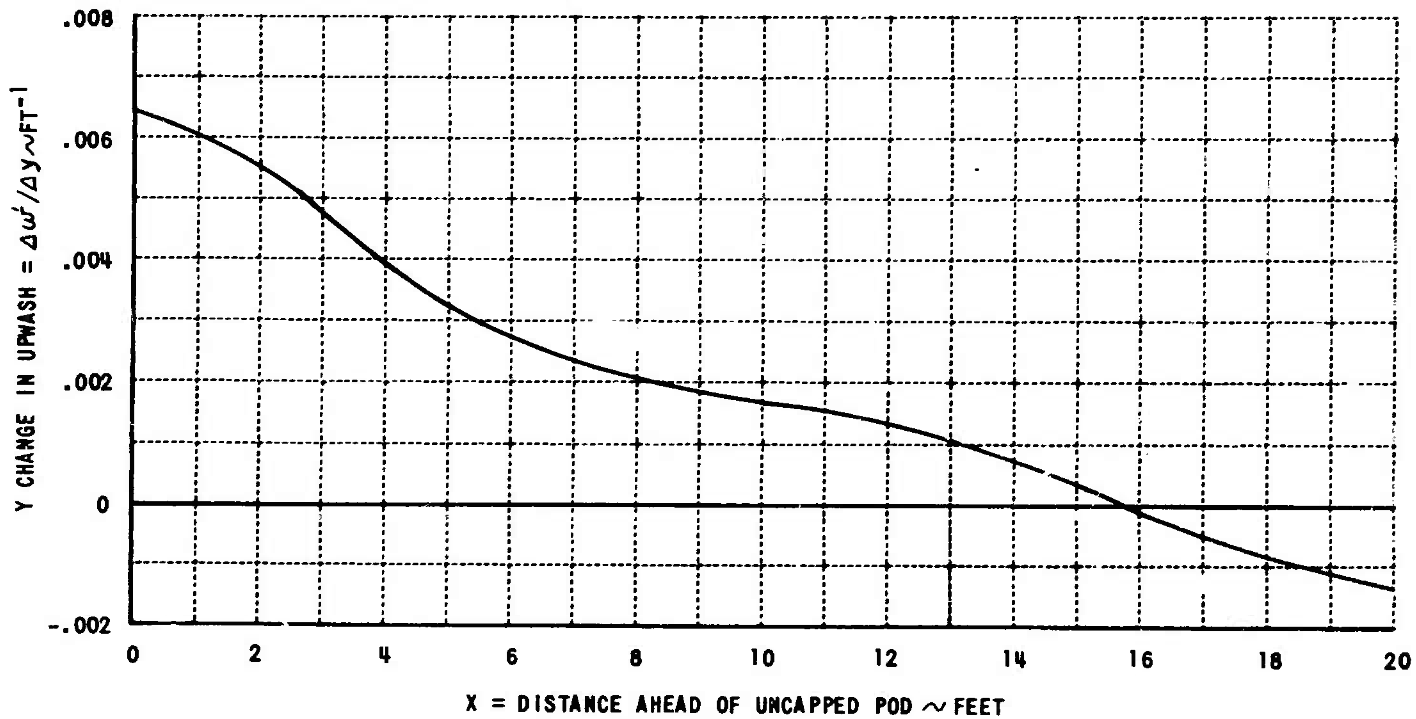


Figure A.4 X VARIATION OF $\Delta\omega'/\Delta y$

w' at a station $\Delta$ y outbound of y is obtained from

$$w' (\text{at } y + \Delta y) = w' (\text{at } y) + \quad y (\Delta w'/\Delta y)$$

A similar variation was computed for sidewash but, for the purposes of this analysis, it is negligible. The variation of sidewash and upwash with $\Delta$ z is conservatively neglected, i.e., the larger wash velocities occuring at the higher (nearer the wing) locations are used. (The missile, after launch, tends to fall into the weaker wash fields.)

It must be emphasized that the above flow field description is valid only for non maneuvering aircraft. Flow field perturbations due to maneuvers can vary markedly from the above (e.g., tripling the angle of attack could nearly double the upwash).

## A.3 OTHER CONSIDERATIONS

### A.3.1 Space-time Transformation

In the preceding section, the flow field about the missile-carrying aircraft has been defined in terms of the geometric coordinates x, y, and z. Unfortunately, the computer program described in Appendix D computes missile coordinates as a function of time. Unless one knows where the missile is in space at any given time, it is not possible to define, in a direct manner, the direction of the flow field at any given time. To resolve this computer problem, an iterative computational procedure, involving a set of space-time transfer equations was derived to obtain flow field wash velocities as a function of time. Because this subroutine is required only because of the particular manner in which the flight path is computed (in the program described in Appendix D), details of this routine are not recorded here. Mention is made of its existence, however, for the sake of completeness.

### A.3.2 Effects of Finite Missile Length and Width

Because the strength and direction of the flow field around the carrier aircraft varies with x, y, and z position, any body of finite length, $\Delta$ x, and width, $\Delta$ y, will be subjected to a varying flow field along its length or width. If the velocity gradients are large with respect to body dimensions, the flow

along the body or across the wing or tail could induce unsymmetrical forces and moments on the missile. (See Figure A.5.)

To account for these induced forces and moments, an analysis was made in which separate but interrelated forces were computed on the missile at the wing, the tail, and the body. These forces were made to vary with the "x" position of the missile (i.e., distance forward of the launch point). A subroutine was added to the simulation program (Appendix D) to account for this phenomenon.

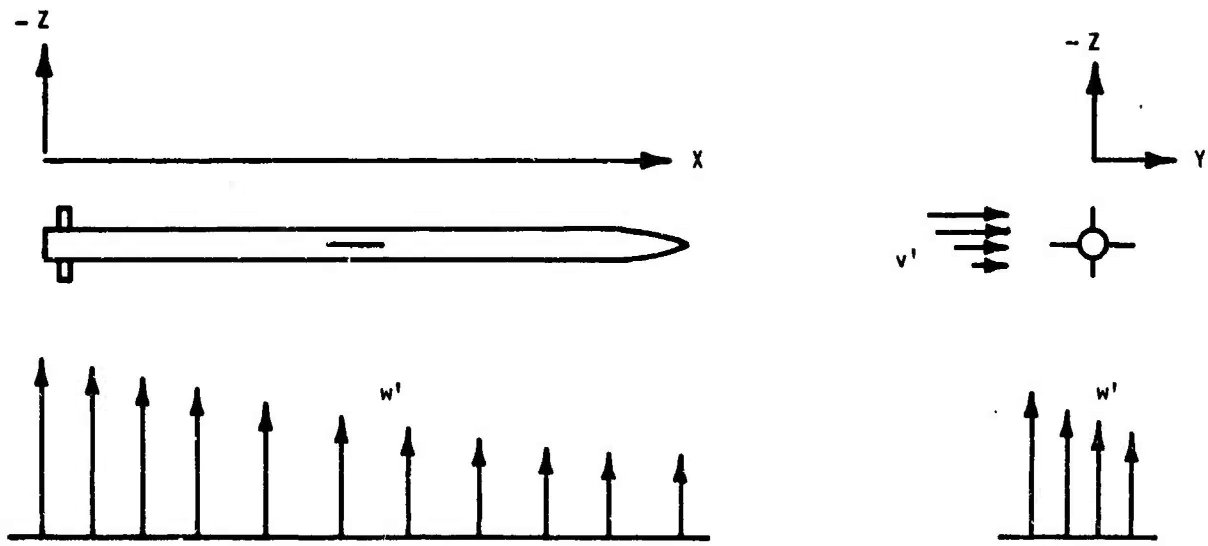


Figure A.5 VARIATION OF WASH VELOCITIES ALONG AND ACROSS MISSILE

## APPENDIX B

## DETERMINATION OF OPTIMUM LIFT TO DRAG RATIO FOR HIGH DRAG, SUBSONIC, AIR VEHICLES

### B.1 STATEMENT OF THE PROBLEM

For a missile having a relatively large body and small wings, most of the missile drag is created by the body. If this missile is required to cruise, subsonically, at a constant velocity, then, to obtain maximum range per pounds of fuel used, the wing size should be so chosen that the ratio of lift to drag is a maximum. As will be shown, the "usual" method of optimizing wing area (e.g. see Reference 5, page 465) does not apply. A method unique to this large drag design is derived in its stead.

### B.2 SOLUTION OF THE PROBLEM

Lift and drag on the missile are expressed in terms of conventional aerodynamic coefficients.

$$L = W = 1/2 \rho V^2 C_L S_w \qquad (B.1)$$

$$D = 1/2 \rho V^2 C_D S_w \qquad (B.2)$$

where

$L$ = lift pounds

$D$ = drag pounds

$W$ = weight pounds

$\rho$ = air density slugs/ft$^3$

$S_w$ = wing area ft$^2$

$C_L$ = missile lift coefficient

$C_D$ = missile drag coefficient
$= C_{Do} + C_{Di}$

$C_{Do}$ = missile profile drag coefficient
$= (C_{Db} + C_{Dbw}) + C_{Dw}$

$C_{Di}$ = induced drag coefficient

$C_{Db}$ = profile drag coefficient of body

$C_{Dbw}$ = interference drag (coeff) between body and wing

$C_{Dw}$ = profile drag coefficient of wing

$q$ $= 1/2 \rho V^2$ = dynamic pressure pounds/ft$^2$

Body drag is usually given in terms of body cross sectional area, $S_b$, rather than wing area, $S_w$. Hence,

$$(C_{Db} + C_{Dbw}) = (C_{Db}' + C_{Dbw}') \; S_b/S_w \qquad (B.3)$$

where the primes refer to body cross sectional area for reference.

The ratio of drag to lift, D/L, can now be determined from Equations (B. 1), (B. 2), and (B. 3).

$$\frac{D}{L} = \frac{C_D}{C_L} = \frac{(C_{Db}' + C_{Dbw}') \; S_b/S_w + C_{Dw} + C_{Di}}{C_L} \qquad (B.4)$$

$$\text{Now } C_{Di} = \frac{C_L^{\,2}}{\pi \; AR \; e} \qquad \text{Ref. 6, Sect VII. 4} \qquad (B.5)$$

where AR = wing aspect ratio

e = Oswald efficiency factor = .8 to .95

also $S_w$ = $W/q \; C_L$ (from Equation (B. 1)) (B. 6)

Substituting Equations (B. 5) and B. 6) into Equation (B. 4), one obtains

$$\frac{C_D}{C_L} = \frac{(C_{Db}' + C_{Dbw}') \; S_b}{W/q} + \frac{C_{Dw}}{C_L} + \frac{C_L}{\pi \; AR \; e} \qquad (B.7)$$

To obtain a minimum value of $C_D/C_L$, the above equation is differentiated with respect to $C_L$. For a given size body, a given weight, and a given elocity and altitude, the first term of the equation is invariant with $C_L$, hence

$$\frac{d\,(C_D/C_L)}{d\,C_L} = -\frac{C_{Dw}}{C_L^{\,2}} + \frac{1}{\pi \; AR \; e} = 0$$

$$C_{L\,opt} = (C_{Dw} \, \pi \; AR \; e)^{1/2} \qquad (B.8)$$

= value of $C_L$ that gives $(D/L)_{min}$

or $(L/D)_{max}$

If Equation (B.8) is substituted back into Equation (B.7), the expression for minimum D/L is obtained.

$$\frac{C_D}{C_{L\ min}} = \frac{(C'_{Db} + C'_{Dbw})\, q}{W/S_b} + \frac{C_{Dw}}{\pi\ AR\ e}^{1/2} + \frac{C_{Dw}}{\pi\ AR\ e}^{1/2}$$

$$\frac{C_D}{C_{L\ min}} = \frac{(C'_{Db} + C'_{Dbw})\, q}{W/S_b} + 2\,\frac{C_{Dw}}{\pi\ AR\ e}^{1/2} \qquad \text{(B.9)}$$

The above equations show that (L/D) max will occur when the last two terms are equal, that is, when the induced drag of the wing is equal to the profile drag of the wing. In the usual form of this equation, for cruise airplanes, (L/D) max occurs when the induced drag of the lifting surfaces equals the profile drag of the entire airplane.

Equation (B.9) is solved for some typical values of missile coefficients. The results are plotted in Figure B.1.

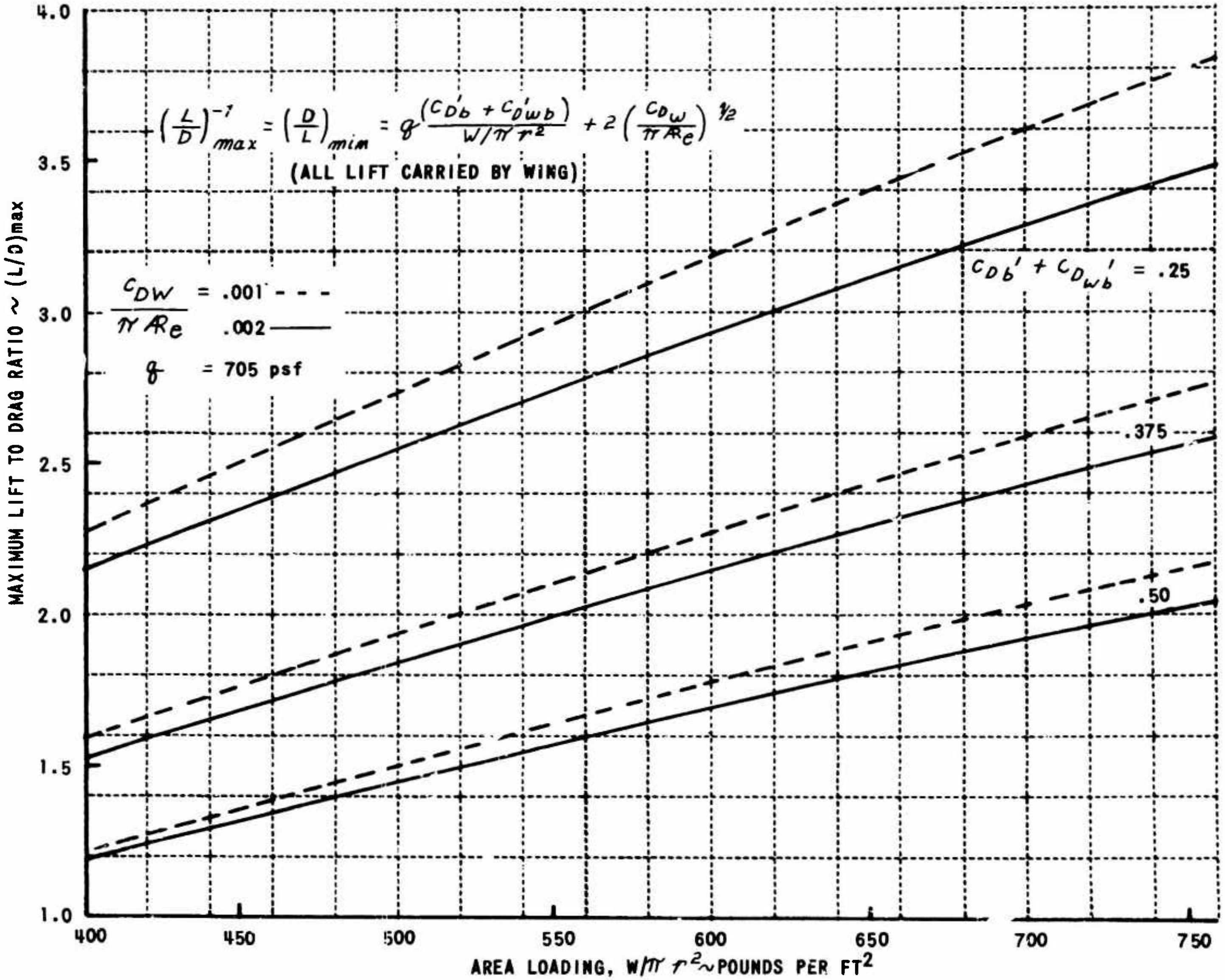


Figure B.1 VARIATION OF MISSILE $(L/D)_{max}$ WITH MISSILE WEIGHT AND PROFILE DRAG OF WING AND BODY

# APPENDIX C
## DESIGN OF ROCKET MOTORS

### C. 1 SUSTAINER MOTOR

The sustainer is designed to produce a thrust sufficient to just cancel vehicle drag during cruise. From Section 3.2.2 (b), the drag of the winged missile is shown to be relatively constant, i.e., 13.9 to 14.0 pounds. Rocket thrust and propellant requirements are determined using the 13.9 pound value. Motors for other configurations are sized to their respective needs.

Rocket Thurst, $F = C_F P_c A_t$ (Ref. 7, page 450)

where $C_F$ = thrust coefficient

$P_c$ = chamber pressure lbs/in$^2$

$A_t$ = nozzle throat area in$^2$

$A_e$ = nozzle exhaust area in$^2$

$P_e$ = exhaust pressure lbs/in$^2$

Let $P_c = 1000$ psi and $P_e = 14.7$ psi (sea level), then $P_c/P_e = 68$

From Ref. 7, page 451, Figure 10.14, for the noted pressure ratio and with an optimum expansion, $C_F = 1.54$ and $A_e/A_t = 7.6$

$$F = 13.9 = 1.54 \times 1000 \times A_t$$

$$\text{Hence } A_t = 9.02 \times 10^{-3} \text{ in}^2 \text{ and } A_e = 6.85 \times 10^{-2} \text{ in}^2$$

$$r_t = \text{throat radius} = 0.054 \text{ in and } r_e = 0.148 \text{ in}$$

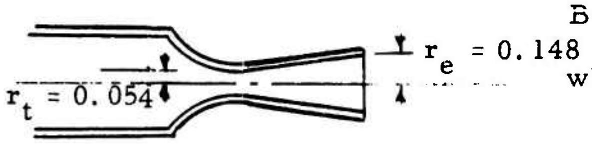


Burning rate $= \dot{w} = F/I_{sp}$

where $I_{sp}$ = specific impulse of propellant

= 242 sec (see Ref. 11)

$$\dot{w} = 13.9/242 = 0.0575 \text{ lb/sec}$$

Total fuel needed for 70 sec $= W_f = 0.0575 \times 70 = 4.03$ lbs

If propellant is housed in a cylinder 2.45 in. in diameter, then area of propellant face $= \pi\,(1.275)^2 = 5.11$ in$^2$. If the propellant has a density of 0.063 lb/in$^3$ then burning rate $\dot{w} = 0.0575 = 0.063 \times 5.11 \times \Delta X$ and $\Delta X =$ 0.178 in/sec.

The booster motor should supply sufficient thrust so that at burnout the missile is about 50 to 100 feet ahead of the launch tube.

Let range = 75 feet = $1/2\ a\ t^2$

then a = acceleration = 100 ft/sec$^2$ = 3.1 "g"

If missile weight = 26.0 pounds, then thrust = 3.1 x 26.0 = 80.6 lbs

As before, $F = C_F\ P_c\ A_t$

$80.6 = 1.54 \times 1000 \times A_t$

$A_t = 5.23 \times 10^{-2}\ in^2$ and $A_e = 0.398\ in^2$

$r_t = 0.129$ in. and $r_e = 0.357$ in

Burning rate, $\dot{w} = \dfrac{F}{I_{sp}} = \dfrac{80.6}{235} = 0.343$ lb/sec

As before, $\Delta X = .343/(0.63 \times 5.11) = 1.07$ in/sec and propellant weight = $\dot{w}\ t = 0.343 \times 1.25 = 0.42$ lbs

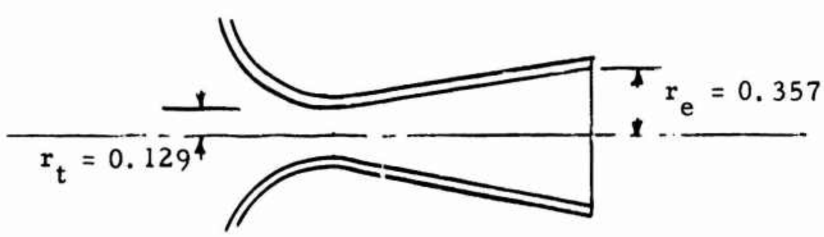

# APPENDIX D
# DESCRIPTION OF SIMULATION PROGRAM

## D.1 PROGRAM STRUCTURE AND FEATURES

The flight path and control system of the penetration aid missile studied in this report was simulated on a digital computer program. The major features of this program are:

(1) The motion of the missile through the air-space is represented by "conventional" six-degree-of-freedom linearized equations of motion (e.g., see Ref. 12, Chapter 4). Missile positions and velocities are obtained relative to the launching aircraft.

(2) Missile force and moments resulting from the flow field surrounding the launching aircraft can be computed and applied as a separate input.

(3) Arbitrary control inputs from rudder, aileron, elevator and rocket motor thrust can be applied. These can be either open loop (time dependent) or closed loop (dependent upon some function of missile motion).

(4) Random disturbances in the form of vertical or lateral gusts can be computed and applied. The mathematical model used for these disturbances closely fits measured gust data for altitudes up to 1000 feet. The only input required is the specification on the RMS gust velocity.

(5) The missile lateral and longitudinal equations are solved independently. However, in the computation of the missile position in three dimensional space, information from both solutions is utilized. Small angle assumptions, for pitch angle, angle of attack and sideslip are used in this computation.

The program is written in a general manner to allow for an arbitrary vehicle configuration. To specify a particular vehicle (in this case, a penetration aid missile), the geometric, inertial and aerodynamic characteristics

of that vehicle are read into the program at the beginning of the run. These characteristics can be specified as a function of time, Mach number, altitude or other convenient variable. The initial conditions at launch can also be specified at will.

The integration step size (specified in seconds) is arbitrary--within reasonable limits imposed by accuracy requirements in computing the vehicle trajectory. The number of steps taken--that is, the total flight time divided by the step size--can be any number up to 1300. With some modifications to the existing storage (to increase the number of available storage locations), this 1300 number can be increased.

Any computed variable can be printed out in tabulated form and/or plotted on a variable-time coordinate chart. Figures 7.2 through 7.7 are replications of such computer plots.

This particular program was not written with economy of computer time in mind. However, the computing time for a run of 1300 steps was, typically, 0.06 hours including compiling time for the main portion of the program.